Master's thesis

NTNU
Norwegian University of Science and Technology
Faculty of Natural Sciences
Department of Biotechnology and Food Science

Monica Frøystad

Weed to Feed

From Seaweed to Sustainable Microbial Feedstocks

Master's thesis in Biotechnology
Supervisor: Fernando Pérez-García
Co-supervisor: Trygve Brautaset
May 2023

NTNU
Norwegian University of
Science and Technology

Monica Frøystad

Weed to Feed

From Seaweed to Sustainable Microbial Feedstocks

Master's thesis in Biotechnology
Supervisor: Fernando Pérez-García
Co-supervisor: Trygve Brautaset
May 2023

Norwegian University of Science and Technology
Faculty of Natural Sciences
Department of Biotechnology and Food Science

NTNU
Norwegian University of
Science and Technology

Abstract

More sustainable solutions are required in industry to preserve resources that the world population already relies heavily on, such as arable land. In this work seaweed has been investigated as a potential feedstock for microbial production of the vitamin riboflavin. The bacterium *Corynebacterium glutamicum* has been genetically engineered to utilize non-native carbon sources from the seaweeds *Laminaria hyperborea* and *Palmaria palmata*. New strains have been successfully cultivated in CgXII minimal media containing mannitol or galactose as sole carbon source and growth rates of 0.25 ± 0.02 h^{-1} and 0.34 ± 0.01 h^{-1} were achieved, respectively. New strains have also been successfully cultivated in seaweed-based media. No growth could be observed for cultivation in minimal medium with laminarin as sole carbon source. An uncharacterized native galactose import system in *C. glutamicum* has been investigated, with results indicating that either PTS^G or PTS^F is able to import galactose. Production capability for the blue pigment phycocyanobilin has been tested both in wild type and in galactose utilizing strains, but no blue colour could be observed for either. Riboflavin has been successfully produced with galactose as sole carbon source. Two in-parallel fed-batch fermentations with a galactose-utilizing riboflavin producer cultivated in seaweed hydrolysate (50 %) from *P. palmata* yielded riboflavin titer, yield and volumetric productivity of 1139.4 ± 58.6 mg/L, 106.2 ± 5.5 mg/g and 25.3 ± 1.3 mg/L h, respectively.

Sammendrag

Nye og mer bærekraftige løsninger kreves i industriell sammenheng for å konservere ressurser som verdensbefolkningen allerede er svært avhengig av, som for eksempel dyrkbar jord. I løpet av dette prosjektet har tare blitt undersøkt som en potensiell kandidat for føde i mikrobielle prosesser for produksjon av vitaminet riboflavin. Bakterien *Corynebacterium glutamicum* har blitt genetisk konstruert for å benytte karbonkilder fra tareartene *Laminaria hyperborea* og *Palmaria palmata* som den i utgangspunktet ikke kan benytte. Nye bakteriestammer har vist vekst i CgXII minimalt medium med mannitol eller galaktose som eneste karbonkilde, og oppnådde vekstrater på henholdsvis 0.25 ± 0.02 t^{-1} og 0.34 ± 0.01 t^{-1}. Stammene viste også vekst i tarebaserte medier. Kultivering i minimalt medium med laminarin som eneste karbonkilde ga ingen vekst. Et ukarakterisert, iboende importsystem for galaktose ble undersøkt i *C. glutamicum* og resultater tyder på at enten PTS^G eller PTS^F har evnen til å importere galaktose. Evnen til å produsere det blå pigmentet phycocyanobilin ble testet i både villtype *C. glutamicum* og i en bakteriestamme som kunne benytte galaktose, men ingen blåfarge ble observert hos noen av dem. Riboflavin har blitt produsert med galaktose som eneste karbonkilde. To parallelle «fed-batch» fermenteringer med en stamme som kan benytte galaktose og produsere riboflavin, kultivert i tarehydrolysat (50 %) fra *P. palmata,* ga endelig konsentrasjon, utbytte og volumetrisk produktivitet for riboflavin på henholdsvis 1139.4 ± 58.6 mg/L, 106.2 ± 5.5 mg/g og 25.3 ± 1.3 mg/L t.

Preface

These past two years have been by far the most fun, and the most educational, out of all my years as a student at NTNU. There is no book that quite captures the magic of biotechnology, or that can describe the incredible feeling of accomplishment when something actually works in the lab as it was hypothesized to work. On the other hand, lab life can be a real trudge when cloning or transformations fail time after time, for no obvious reason. In times like this it is important to be surrounded by supportive colleagues, and I feel that I have been very lucky in this regard. I would like to give a shout out to Rosa and Ingunn, who have been the most inclusive, supportive, and understanding lab mates I could ask for. This past year would not have been as fun without you!

The greatest support of all throughout my master's thesis has been my supervisor Fernando, who always pushes me to challenge myself when I hesitate and believe in myself when I am uncertain. The first two semesters of my master thesis were very challenging for me in other aspects of my life, and I don't think I would have made it without the patience, understanding and support of Fernando who let me do my own thing in my own time.

I dedicate this master's thesis to Fernando, without whose concept and groundwork it would never exist. Thank you for giving me such a cool project to work on and for trusting me to make your ideas reality.

"Be brave"

Monica Frøystad

Trondheim, May 2023

Table of Contents

1 Introduction

1.1 Background

Food is a precious commodity in many parts of the world today. As the world population continues to rise, the quest for sustainable solutions in all fields of science becomes more important and more urgent. Still, high-energy resources such as glucose and sucrose are being used to feed microbial producers in industrial settings.[1] Although glucose is a convenient choice because it is the preferred carbon source for industrially important organisms such as *Escherichia coli, Bacillus subtilis* and *Corynebacterium glutamicum*, it is a high-energy substrate that can also be used in the food industry.[2-5] Alternative feedstocks for microbial production of medicines, protein, vitamins and other products can help relieve the strain on food availability in the world today. In this regard, molecular genetics is a powerful tool that enables the engineering of new microbial strains able to utilize a wider range of substrates. Moving towards more sustainable microbial feed is the main aim of this thesis project, focusing on seaweed as a substrate for microbial growth and production of industrially important or valuable molecules such as riboflavin or phycocyanobilin. Seaweed requires no arable land and no freshwater for production and is in this way a sustainable alternative feedstock for microbial processes.

1.2 Seaweed

Seaweed is an abundant marine resource and in tropical parts of the world it is already being farmed intensively.[6] There, seaweed is mainly exploited for the extraction of useful biopolymers such as carrageenan, alginates and agar.[6-8] Seaweed also grows well in temperate climates, with some species such as *Laminaria hyperborea* growing along European coasts all the way from northern Norway to Portugal.[9, 10] *L. hyperborea* has been harvested in Norway for many years, amongst other by the Norwegian company Alginor, and is also harvested in France and Ireland.[11, 12] Another notable species that is harvested in Europe is *Palmaria palmata*, also known as red dulse.[13] This species is commonly used for food and is cultivated in amongst others Ireland, France and Spain.[13-15]

Seaweeds, or macroalgae, are full of carbohydrates that can be metabolized by microbes for industrial purposes.[16] The composition of carbohydrates varies seasonally for each species.[16] *L. hyperborea*, or brown kelp, has higher content of storage carbohydrates during the summer and autumn months than in the winter.[16] The dry weight of *L. hyperborea* harvested during the summer and autumn can consist of up to 25 % mannitol and 25 % of laminarin, the latter being a glucose-based polymer.[16] In *P. palmata*, most of the carbon is stored is the 1-linked galactose floridoside which is a compatible solute vital for osmoregulation in several species of red seaweed.[17, 18] Floridoside accounts for up to 24 % of the dry weight of *P. palmata* in high light conditions and along with the galactose-based polymers carrageenan and agar, accounts for the high galactose content in extracts of this species.[17, 19, 20]

In addition to carbohydrates, hydrolysates of seaweeds also contain growth inhibitors such as furfural, which is formed from xylose in the high-temperature acidic conditions used to produce the hydrolysates.[21, 22] These can negatively impact growth of microbes that

cannot detoxify these substances, leading to inefficient processes. This has made seaweed hydrolysate far from the first choice for microbial feedstocks, especially for the big industrial producers *E. coli* and *B. subtilis* which cannot detoxify furfural.[23, 24] The advantage of using *C. glutamicum* in this instance is that it can detoxify furfural and even grow in furfural concentrations as high as 20 mM.[25] However, furfural can negatively impact the growth of *C. glutamicum* and should be minimized to maintain high growth rates.[25] Furfural could be present in seaweed hydrolysate from red seaweed such as *P. palmata*, which is rich in the furfural-precursor D-xylose.[17, 22] Xylose is in this case stored in the polymer xylan, which can be degraded by acid hydrolysis at high temperatures.[26] Finally, furfural has been detected in small concentrations, at around 0.42 mM, in brown seaweed hydrolysate from *L. hyperborea*.[21]

1.3 *Corynebacterium glutamicum*

Corynebacterium glutamicum is a Gram-positive facultative anaerobic bacterium found in various places in nature, including soil where it was first isolated.[2, 27] It is small and non-motile, making it easily identifiable in the microscope as seen in Figure 1. It has previously been described as a club-like rod and forms a typical V-shape with other cells.[28] In this work observations were made that cells under high metabolic stress, i.e. containing many genetic inserts, clung together in clusters and appeared bloated as shown in Figure 1.

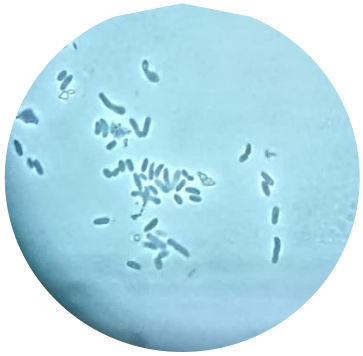

Figure 1: An image of *C. glutamicum* as seen in a common tabletop light microscope with an oil immersion objective lens (100x) with a total of 1000x magnification. Image taken by the author.

C. glutamicum breaks down and thrives on many different carbon sources such as sugars, sugar alcohols, organic acids, and amino acids. Glucose, fructose and sucrose are its preferred carbon sources.[2, 5] *C. glutamicum* is Generally Recognized As Safe (GRAS) and its genome is fully sequenced and annotated, making it suitable for metabolic engineering.[29-31] *C. glutamicum* has been used for industrial applications for several decades, for instance in the production of amino acids like L-lysine and L-glutamate, as well as other added-value compounds.[32, 33]

A typical characteristic of *C. glutamicum* is that is can utilize several different carbon sources in parallel.[34] This is because it lacks a complex carbon catabolite repression system which in other bacteria such as *E. coli* and *B. subtilis* enables only one carbon source to be used at any given time.[4, 34] This makes *C. glutamicum* especially interesting for growing on novel substrates that contain many different carbon sources, such as seaweed.[16, 17]

1.3.1 PTS systems in *C. glutamicum*

C. glutamicum has well-characterized phosphotransferase systems (PTS) in place with selective enzymes that import different sugars.[35] All PTSs in *C. glutamicum* use energy

from phosphoenolpyruvate (PEP) via PEP kinase encoded by the gene *ptsI*, and a phosphocarrier protein (HPr) encoded by *ptsH*.[35] The selectivity for each sugar is due to permeases that are named "type II" enzymes, which include subunits A, B and C (EIIABC). These proteins are located at the membrane and can be permeable to one or several different molecules.[35] There are four characterized EII proteins in *C. glutamicum*, three of which import glucose (PTS^G), fructose (PTS^F) and sucrose (PTS^S) respectively.[36-38] The substrate of the fourth EII is still not confirmed, but it may import ascorbate (vitamin C).[36-38] Although *C. glutamicum* also has PTS-independent import systems for glucose, the PTS^G is the main pathway for uptake and phosphorylation of glucose.[39]

1.3.2 Galactose utilization

Galactose is an aldohexose that can be found amongst others in seaweed such as red dulse.[17] *C. glutamicum* cannot use galactose as a carbon source natively, but introduction of galactose utilizing genes from *E. coli* or *Lactococcus cremoris* can confer this ability.[34, 40-42] One way galactose utilization in *E. coli* is achieved is through a galactose utilization operon and an additional gene, *galP*, which encodes a symporter for β-D-galactose and protons.[43] The operon *galMKTE* includes four genes which collectively convert β-D-galactose into UDP-glucose as seen in Figure 2.[43] Galactose utilization in *L. cremoris* is achieved by similar genes as described here for *E. coli*.[42] *GalM* encodes an epimerase which converts β-D-galactose to α-D-galactose.[43] *GalK* encodes a galactokinase, which phosphorylates α-D-galactose. *GalT* encodes uridylyltranferase, converting galactose-1-P and UDP-glucose into UDP-galactose and glucose-1-P. Finally, *galE* encodes an epimerase which converts UDP-galactose into UDP-glucose.[43] UDP-glucose can then be utilized in a number of different metabolic pathways in *C. glutamicum*.[43]

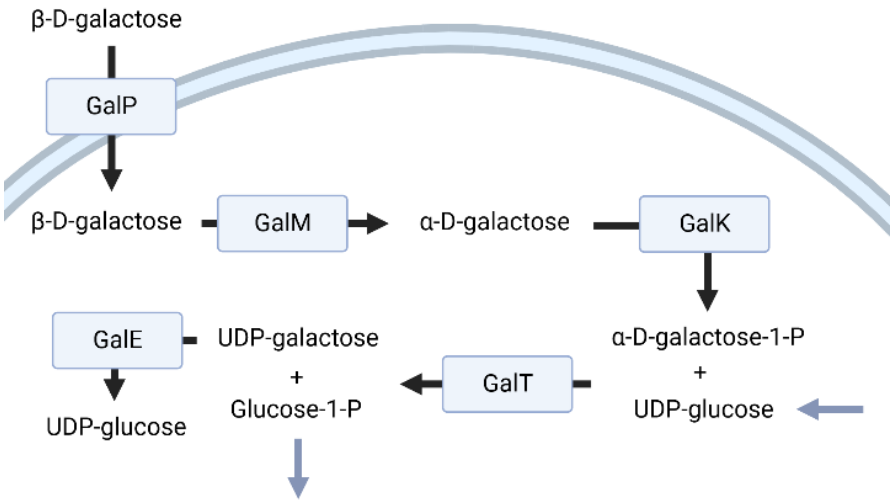

Figure 2: A simplified illustration of the pathway for the utilization of galactose using the operon *galMKTE* and the galactose symporter gene *galP* in *E. coli.*[43] Gene products are shown in blue boxes and their activities are indicated by black arrows. Blue arrows indicate a substrate entering or leaving the pathway. UDP is short for uridine diphosphate and P is short for phosphate. Created with BioRender.com

Galactose is similar in structure to glucose, being its C-4 epimer, and the two sugars differ only in the orientation of the hydroxyl group and hydrogen attached to C-4. While glucose is imported by one of the three characterized PTS systems in *C. glutamicum,* there is no characterized import system for galactose in this bacterium. Figure 3 shows the Haworth formula for D-galactose compared to the formulae of the three sugars imported by PTS, D-glucose, D-fructose and sucrose.

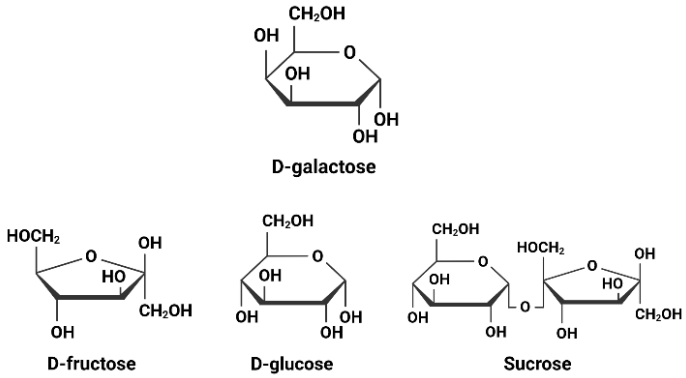

Figure 3: Haworth formulae of D-galactose alongside the three sugars imported by PTS systems in *C. glutamicum*; D-fructose, D-glucose, and sucrose, imported by PTS^F, PTS^G and PTS^S, respectively.[36-38] Created with BioRender.com

1.3.3 Mannitol utilization

Mannitol is a sugar alcohol found in amongst other things plants and seaweed, and is commonly used as a sweetener.[44] Mannitol is not a native carbon source for *C. glutamicum*.[45] However, *C. glutamicum* does have a native gene called *mtlD*, which encodes a dehydrogenase that converts arabitol or mannitol 1-phosphate to fructose 6-phosphate.[45] The *mtlD* gene is involved in arabitol utilization and will not be expressed in the absence of arabitol.[45] It has been demonstrated that overexpression of *mtlD* in a restriction deficient *C. glutamicum* strain by deletion of a repressor gene *atlR* enables growth on mannitol alone.[45] The same strain with normal expression of *atlR* could only utilize mannitol alone following growth on arabitol.[45]

To enable growth on mannitol as the sole carbon source for this work, mannitol utilizing genes from *B. subtilis* were introduced. In *B. subtilis* there is a PTS responsible for import and conversion of mannitol into fructose-6-phosphate which has been introduced successfully into *C. glutamicum* before.[21] The genes include *mtlD*, *mtlA* and *mtlF* which together execute the same function as in *B. subtilis,* shown in Figure 4. The genes *mtlA* and *mtlF* encode the EIICB and EIIA subunits of enzyme II in the mannitol-specific PTS, respectively.[46] The resulting EII protein (PTS^M) imports and phosphorylates mannitol.[46] The gene *mtlD* encodes a dehydrogenase which converts mannitol-1-phosphate into fructose-6-phosphate, which can be used in central metabolism such as glycolysis.[46] Some studies have shown that the native MtlD in *C. glutamicum* plays a role in converting mannitol to fructose, which is excreted from the cell and taken up again by the PTS^F.[45, 47]

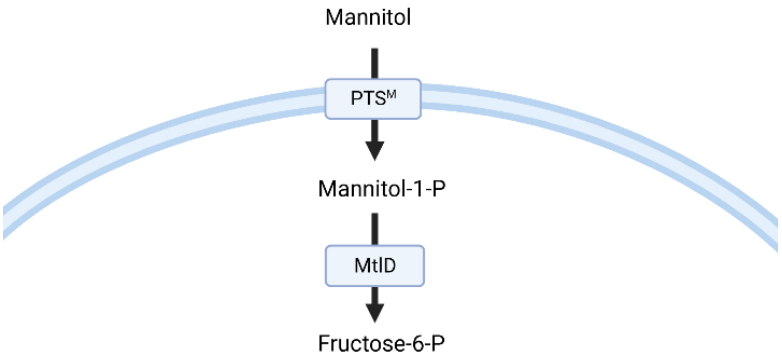

Figure 4: A simplified illustration of the mannitol specific PTS pathway in *B. subtilis,* showing the gene products for *mtlAF* (PTS^M or mannitol-specific EII) and *mtlD* (MtlD; mannitol-1-P-5-

dehydrogenase) and their activities, indicated by black arrows.[46] P is short for phosphate. Created with BioRender.com

1.3.4 Laminarin utilization

Laminarin is an abundant polysaccharide in the seaweed *L. hyperborea*.[16] Much like cellulose is the most abundant biopolymer on land, laminarin is the most common storage polymer in a great variety of marine organisms, including diatoms and macroalgae.[48, 49] It is a β-1,3 glucan composed mainly of D-glucose monomers, but may also contain some D-mannitol substituents.[48, 50, 51] *C. glutamicum* cannot metabolize laminarin natively, but some microbes produce enzymes called laminarinases which can break down laminarin into glucose residues and oligomers by breaking glycosidic linkages.[52] One example is the bacterium *Flavobacterium commune* isolated from rotting seaweed, which can use laminarin as a sole carbon source.[52, 53] The genetic sequence for the laminarinase gene from *F. commune* could potentially enable laminarin utilization in *C. glutamicum*. The resulting D-glucose could then be utilized in central metabolism.[35]

Laminarin from different sources have different ratios of β-1,3- and β-1,6-linkages, and laminarinases have different specificities. For example, laminarin in *Laminaria digitata* has a ratio of 7:1 for β-1,3-linkages and β-1,6-linkages, respectively.[54] The laminarinase from *F. commune* is an endo-β-1,3-glucanase, meaning that it cleaves β-1,3-linkages anywhere in the polymer to release oligosaccharides or monomers of glucose.[52] With seven times as many β-1,3-linkages as β-1,6-linkages, both oligomers and monomers of glucose would result with the *F. commune* laminarinase on laminarin from *L. digitata.*

1.3.5 Phycocyanobilin production

Phycocyanobilin (PCB) is a blue pigment which acts as a chromophore in photosystems in algae and cyanobacteria.[55] Blue pigments such as PCB are rare in nature compared to green, red and yellow pigments, possibly because the molecular machinery required to absorb red light, and emit blue light, is more complicated than absorbing blue light.[56] In addition, some of the organisms that appear blue use "tricks of the light", i.e. taking advantage of light scattering or diffraction, and do not actually produce any blue pigment.[56] The rarity of blue pigments makes phycocyanobilin one of only few eligible candidates for natural blue food colorants.[56, 57]

Apart from industrial applications, PCB also exhibits antioxidant, anti-inflammatory and anti-cancer effects that can be exploited for medical purposes.[58-60] PCB has been shown to have anti-inflammatory effects in mice with edema, in part due to its antioxidant properties and partly because of its ability to downregulate proinflammatory cytokines.[59, 60] PCB also has anti-cancer effects as demonstrated in mice xenotransplanted with cancerous human cells.[58]

The pathway for the production of PCB can require few reaction steps, such as in the cyanobacterium *Synechococcus* sp. as shown in Figure 5.[61, 62] Here PCB production from heme requires only two enzymes, each encoded by a single gene. The *ho1* gene encodes a heme oxygenase, an enzyme which converts heme to biliverdin.[61] The other gene, *pcyA*, encodes a phycocyanobilin oxidoreductase which converts biliverdin to phycocyanobilin (PCB).[62]

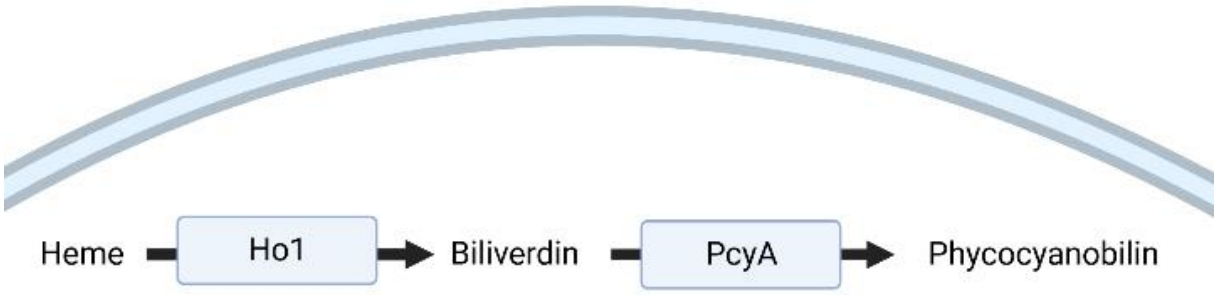

Figure 5: A simple illustration of an intracellular pathway for the biosynthesis of phycocyanobilin (PCB) from heme in a two-step pathway from *Synechococcus sp.*[61, 62] The heme oxygenase Ho1 converts heme to biliverdin, while the oxidoreductase PcyA converts biliverdin to PCB. Created with BioRender.com.

1.3.6 Riboflavin production

Riboflavin, or vitamin B_2, is a water soluble vitamin which is essential for the human body[63]. It is water-soluble and is supplied in the diet through foods such as eggs, dairy products and organ meats.[64, 65] Riboflavin is the precursor for both flavin mononucleotide (FMN) and flavin adenine dinucleotide (FAD), which act as coenzymes for various enzymes and act in redox reactions.[66] Riboflavin is light sensitive and will degrade to lumichrome when exposed to light at neutral pH, which in culture media can be observed as loss of yellow colour.[67-69]

Industrially, riboflavin is produced in large scales mainly by the bacterium *B. subtilis* and the yeast *Ashbya gossypii*.[70] Around 70 % of industrially produced riboflavin is used as feed for domestic animals, and the rest for food and pharmaceuticals.[70, 71] Previously, chemical synthesis of riboflavin was the main production strategy, but today microbial fermentation has replaced chemical synthesis as a more cost-effective process.[70]

The biosynthesis of riboflavin is a native function in *C. glutamicum* and is achieved by a biosynthetic operon for riboflavin. Overexpression of the operon *ribGCAH* in *C. glutamicum* has already been demonstrated to increase riboflavin production.[21] Riboflavin can be synthesized from GTP and ribulose 5-phosphate, which are derived from purine metabolism and the pentose phosphate pathway, respectively.[31] The biosynthesis of riboflavin requires the gene products RibG, RibC, RibA and RibM from the riboflavin biosynthetic operon and is achieved by a series of complicated reactions.[31] A simplified illustration of the pathways are shown in Figure 6. Intermediates are not shown.

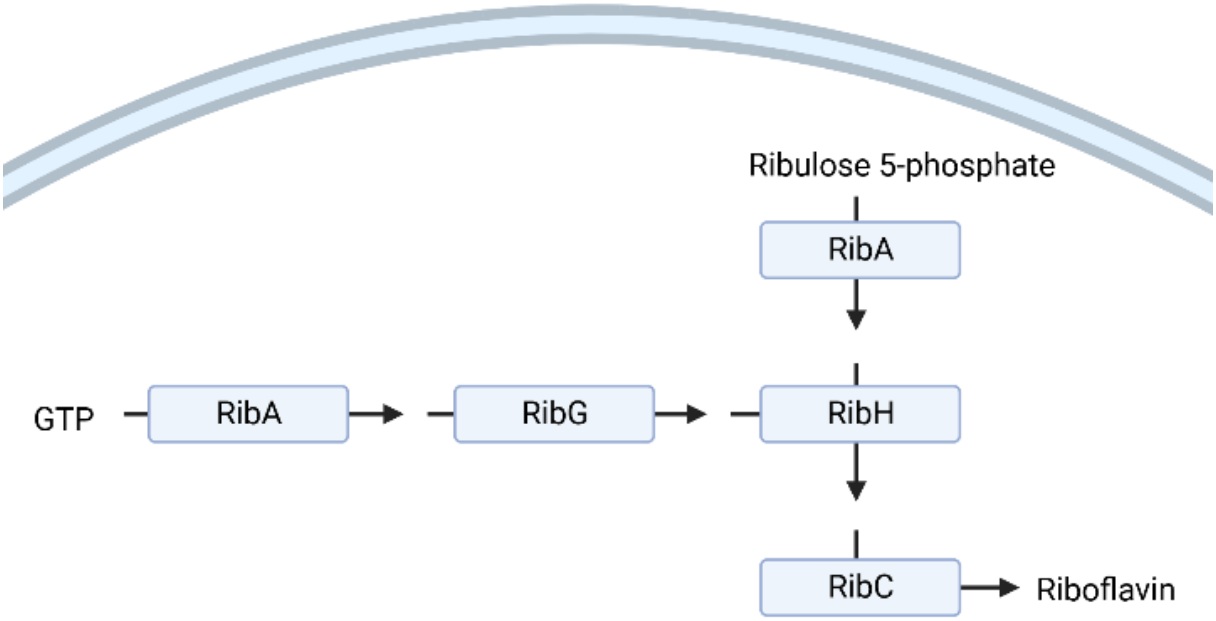

Figure 6: A simplified illustration of the pathway of riboflavin production from GTP and ribulose 5-phosphate by the native biosynthetic operon *ribGCAH* in *C. glutamicum.*[31] Gene products are shown in blue boxes. Intermediates are not shown. Created with BioRender.com.

1.4 Thesis project

In this thesis project, carbohydrates from red and brown seaweed were made accessible to *C. glutamicum* by introducing genes from bacteria that could natively utilize these carbohydrates. New strains that could utilize galactose were constructed with genes from *E. coli* and cultivated in red seaweed hydrolysate media. A potential native route for galactose import was investigated in *C. glutamicum*. Production capability for phycocyanobilin and riboflavin, respectively, were attempted in combination with galactose utilization. Riboflavin production was achieved in red seaweed hydrolysate medium and upscaled to lab-scale fermenters to achieve competitive titers of riboflavin. New strains that were capable of mannitol utilization were cultivated with mannitol as sole carbon source and tested in brown seaweed hydrolysate. Finally, strains that should have been able to utilize laminarin from brown seaweed were constructed and tested with laminarin as sole carbon source.

2 Materials and methods

2.1 Introduction to materials and methods

In this thesis project, new strains of *C. glutamicum* have been constructed by transforming plasmid vectors into competent cells of *C. glutamicum* using electroporation. Genes from bacterial gDNA or from synthetic DNA sequences have been cloned and inserted into plasmid vectors using the molecular cloning technique Gibson assembly. For some genes, specific base changes were made in cloning primers to establish distinct translational initiation rates for these genes. Strains were then tested in growth experiments with various media and conditions in flasks or in a BioLector. Finally, up-scaling was performed in lab-scale fermenters.

In this section materials and methods will be presented, respectively, for strain construction, growth experiments and fermenter processes. The text will follow the workflow used in the lab and there will be a brief introduction to each technique. Protocols will appear as you would see them in the lab.

2.2 Strain construction

Constructing novel bacterial strains may require many different techniques from the field of molecular genetics. The process of strain construction via genetic cloning requires knowledge and understanding of both genetics, for designing primers *in silico*, and of molecular biology and metabolism, for the selection of genes which might function as expected in the desired host. All techniques used for strain construction in this work will be presented in this section, with a brief introduction to each technique.

2.2.1 Recipes for media, buffers and sugar solutions

All media, buffers and sugar solutions used for strain construction will be presented here along with their respective uses. All complex media, buffers and sugar solutions were made with deionized water and sterilized by autoclavation at 121°C for 20 minutes unless stated otherwise. All stock solutions were sterilized by autoclavation (20 minutes, 121°C) or by filtration. All sterilization by filtration was performed with filters with 0.2 µm pores.

Strains were cultivated in complex media as precultures for e.g. growth experiments, plasmid extraction or for making competent cells. Complex media are nutritionally rich and ensure that cells have all the nutrients they need for normal cell growth. Table 1 shows recipes for the complex media 2x yeast-tryptone (2-YT), lysogeny broth (Lennox) (LB-Lennox), brain-heart infusion (BHI), BHI with sorbitol (BHIS), as well as sorbitol.

Table 1: Recipes for the complex media 2x yeast-tryptone (2-YT), lysogeny broth (LB-Lennox), brain-heart infusion (BHI), BHI with sorbitol (BHIS) and the sugar alcohol sorbitol. All were made with deionized water and sterilized by autoclavation.

2-YT	**LB-Lennox**	**BHI**	**BHIS**	**Sorbitol[2]**
16 g/L tryptone	10 g/L tryptone	37 g/L BHI broth[1]	37 g/L BHI broth[1]	455 g/L
10 g/L yeast extract	5 g/L yeast extract	Deionized water	Add 1:4 sorbitol to BHI	Deionized water
5 g/L NaCl	5 g/L NaCl		Deionized water	
Deionized water	Deionized water			

1. Millipore BHI from Sigma-Aldrich
2. Heat to dissolve

Antibiotics were used in precultures and in culture media to ensure that strains retained their plasmid vectors. It should be noted that the concentration of antibiotic in the final medium was always the same, see recipe for agar plates below. Type of antibiotic(s) depended on the antibiotic resistance of plasmid vector(s) in the strain to be cultivated, see Table 4. Antibiotic stocks for kanamycin (50 g/L) and spectinomycin (100 g/L) were made with deionized water and filtered to sterilize. Tetracycline stock (10 g/L) was made with ethanol (70 %) and filtered to sterilize. Glycerol solutions of 89 % and 86 % (w/v), respectively, were made with deionized water from a stock of 99.5 % glycerol and sterilized by autoclavation.

Agar plates were used to cultivate strains on solid medium. They were made in petri dishes with either LB, 2-YT or BHI using the same recipes as in Table 1. Antibiotic was added if needed. The following protocol was used to make agar plates.

- Mix the components of the complex medium
- Add bacteriological agar to a concentration of 15 g/L
- **NB!** Leave stirring magnet in bottle if adding antibiotics before plating
- Autoclave at 121°C for 20 minutes
- When the agar solution is sufficiently cooled to around 60°C, add antibiotic or skip to next step. Kanamycin (50 g/L) is added to a concentration of 0.025 g/L (0.5 µL/mL). Spectinomycin (100 g/L) is added to a concentration of 0.1 g/L (1 µL / mL). Tetracycline (10 g/L) is added to a concentration of 0.005 g/L (0.5 µL/mL). Mix well
- Pour agar solution into petri dishes in sterile conditions and leave to set for around 15 minutes depending on the size and thickness of the plates

A 10x Tris acetate EDTA (TAE) buffer was prepared as running buffer for gel electrophoresis, see section 2.2.4.1. The 10 x TAE buffer was diluted 1:10 to obtain 1x TAE buffer. The following recipe was used for a final volume of 1 L.

- To 800 mL of deionized water, add:
  - 48.5 g tris base
  - 11.4 mL glacial acetic acid
  - 20 mL EDTA (0.5 M) (pH 8)
- Reach final volume with deionized water

Part of strain construction consisted of making competent cells of *E. coli* and *C. glutamicum* that could be transformed with plasmid vectors, see section 2.2.7 and 2.2.12. Competent cells require buffers that increase transformation rates and maintain cell viability after electroporation.[72] Table 2 shows recipes for buffers RF1 and RF2 used for washing and storing of *E. coli* competent cells, respectively, as described by Hanahan et al.[72] Recipes for electroporation buffers EPB1 and EPB2 are included, which were used to wash and store *C. glutamicum* competent cells, respectively, as described by Eggeling et al.[5] All buffers were autoclaved before use and stored at 4°C.

Table 2: Recipes for buffers EPB1, EPB2, RF1 and RF2, used to wash and store competent cells of *C. glutamicum* (EPB) and *E. coli* (RF).[5, 72] All buffers were autoclaved before use and stored at 4°C.

EPB1	**EPB2**	**RF1**	**RF2**
5.05 g/L HEPES	0.075 g/L HEPES	12 g/L RbCl	1.2 g/L RbCl
45.75 mL/L glycerol (89 %)	8.563 mL/L glycerol (89 %)	7.1 g/L $MnCl_2 \cdot 4H_2O$	2.1 g/L MOPS
pH to 7.2 with NaOH	pH to 7.2 with NaOH	30 mL/L potassium acetate (1M)	
Deionized water to reach 800 mL	Deionized water to reach 50 mL	15.2 g/L $CaCl_2 \cdot 2H_2O$	3.04 g/L $CaCl_2 \cdot 2H_2O$
		142 mL/L glycerol (86 %)	142 mL/L glycerol (86 %)
		Adjust pH to 5.8 with HCl	Adjust pH to 6.4 with NaOH
		Deionized water to reach 100 mL	Deionized water to reach 50 mL

2.2.2 Primers and primer design

Primer design is the cornerstone of gene cloning. In this work Gibson assembly was used to insert genes into plasmid vectors, meaning that primers had to be designed correctly to clone the desired gene and generate vector overlaps. Using this cloning technique, appropriate vector design also includes ensuring that the cloned genes can be inserted into the plasmid after the plasmid is cut with a predetermined restriction enzyme.

Primer design was especially important in this work as the goal for some of the strains was to vary the expression level of certain genes. This was achieved by a single base edit in the ribosomal binding site (RBS) and in the start codon, here resulting in four distinct translational initiation rates for the same gene. The design concept is visualized in Figure 7, which shows four different primers for the same genes, in this case *mtlAF* (see section 1.3.3). Within this design, the highest expression rate achieved by *C. glutamicum* is with the sequence GAAAGGAGGCCCTTCAG as RBS and ATG as start codon.[73] The lowest rate is achieved by GAAAGGTGGCCCTTCAG as RBS and GTG as start codon. The constructions "AG" and "TA" have intermediate translational initiation rates, see Figure 7.

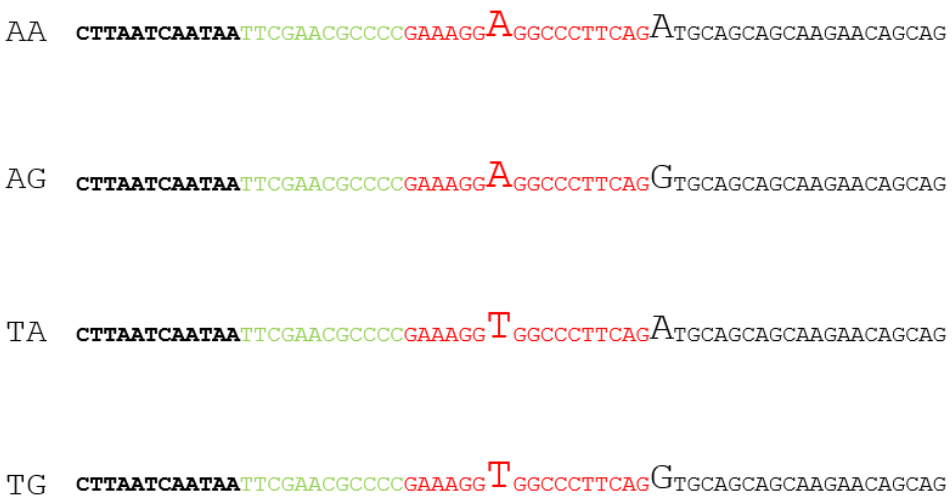

Figure 7: An image showing primer sequences for the genes *mtlAF* (see section 1.3.3) with single base changes in the ribosomal binding site (RBS) and in the start codon of the gene. Base changes are shown in large letters. Bold: overlapping region. Green: linker sequence. Red: RBS.

Primer design was performed *in silico* in this work using either CloneManager or Benchling, and primers were tested *in silico* using CloneManager to check whether they would bind to the template sequence in a PCR reaction. Here the full size of the fragment as well as the optimal annealing temperature of the primers were noted. CloneManager was also used to simulate Gibson assembly to check if it would work *in vitro*.

All primers used in this work were purchased from Sigma-Aldrich or Invitrogen and can be found in Table 3. Where synthetic sequences were used as template, the sequences were ordered from and synthesized by Integrated DNA Technologies (IDT). Primers were resuspended with deionized water according to the number of nanomoles in the tube. Resuspension volume in µL = 10 x nmol. Primers were incubated for 10 minutes at room temperature, mixed well and further diluted 1:10 to reach 10 pmol for the stock solution.

Table 3: A list of primers used in this work along with their names, DNA sequences in the (5′ - 3′) direction as well as their associated vector or gene, and source of template DNA. Bold: overlapping region. Red: ribosomal binding site with spacer. Green: link sequence. Single base changes are bold in their respective colours.

Vector	**Primer name**	**Primer sequence (5′ - 3′)**
pVWEx1 and pEKEx3	Ex1Fw	CATCATAACGGTTCTGGC
pVWEx1 and pEKEx3	Ex1Rv	ATCTTCTCTCATCCGCCA
pVWEx6	Ex6Fw	ATGCCGCTTCGCCTTCGTTG
pVWEx6	Ex6Rv	CGACGGCCAGTGAATTCGAG
Gene (template)	**Primer name**	**Primer sequence (5′ -> 3′)**
galMKTE (*E. coli)*	galEc_Fw	**GCATGCCTGCAGGTCGACTCTAGAG**GAAAGGAGGCCCTTCAGATGAGAGTTCTGGTTACCGG
galMKTE (*E. coli)*	galEc_Rv	**CGAGCTCGGTACCCGGGGATC**TTACTCAGCAATAAACTG
galMKTE (*E. coli*)	galEc_Rv2	**TTACTCAGCAATAAACTG**
galMKTE (*E. coli*)	galEc_Rv3	**TTACTCAGCAATAAACTGATATTCC**
galMKTE (*Lactococcus cremoris*)	galCre_Fw	**GCATGCCTGCAGGTCGACTCTAGAG**GAAAGGAGGCCCTTCAGATGGAAATTACAACAAAAG
galMKTE (*L. cremoris*)	galCre_Rv	**CGAGCTCGGTACCCGGGGATC**TCAGTAGCCTTTTGGATGAC

galP (*E. coli*)	galPFw_AA	**CGGAATATCAGTTTATTGCTGAGTAA**TTCGAACGCCCCGAAAGG**A**GGCCCTTCAG**A**TGCCTGACGCTAAAAAACAGGGGC
galP (*E. coli*)	galPFw_AG	**CGGAATATCAGTTTATTGCTGAGTAA**TTCGAACGCCCCGAAAGG**A**GGCCCTTCAG**G**TGCCTGACGCTAAAAAACAGGGGC
galP (*E. coli*)	galPFw_TA	**CGGAATATCAGTTTATTGCTGAGTAA**TTCGAACGCCCCGAAAGG**T**GGCCCTTCAG**A**TGCCTGACGCTAAAAAACAGGGGC
galP (*E. coli*)	galPFw_TG	**CGGAATATCAGTTTATTGCTGAGTAA**TTCGAACGCCCCGAAAGG**T**GGCCCTTCAG**G**TGCCTGACGCTAAAAAACAGGGGC
galP (*E. coli*)	galPRv	**AATTCGAGCTCGGTACCCGGGGATC**TTAATCGTGAGCGCCTATTTCGCG
LamFc (*F. commune*)	Lam-Fc_Fw1	**GGAATTCGAGCTCGGTACCCGGG**GAAAGGAGGCCCTTCAGATGAATAAATTTTTAATTATAC
(for assembly with 1577SP from *cgl1577*)	Lam-Fc_Fw2	**GGATTAATGACACCCGCAACAGCA**ATGAATAAATTTTTAATTATAC
(for assembly with 1577SP and display from *cgl1577*)	Lam-Fc_Fw3	**CTCACCTCAAGTGGTGGTGTGGCT**ATGAATAAATTTTTAATTATAC
	Lam-Fc_Rv	**CTGCAGGTCGACTCTAGAGGATC**TTACTGATAAACCTTGATATAATC
Cgl1577 SP (*C. glutamicum*)	1577SP_Fw	**GGAATTCGAGCTCGGTACCCGGG**GAAAGGAGGCCCTTCAGATGGCTCAGCGAAAACTGGC
Cgl1577 SP (*C. glutamicum*)	1577SP_Rv	**TGCTGTTGCGGGTGTCATTAATC**
Cgl1577 SP and display (*C. glutamicum*)	1577SP_Rv2	**AGCCACACCACCACTTGAGG**
mtlD (*B. subtilis*)	mtlD_Fw	**GCATGCCTGCAGGTCGACTCTAGAG**GAAAGGAGGCCCTTCAGATGATCGCCTTACATTTCGG
mtlD (*B. subtilis*)	mtlD_Rv	GGGGCGTTCGAATTATTGATTAAGTTTCTTTAAAATG
mtlAF (*B. subtilis*)	mtlFw_AA	**CTTAATCAATAA**TTCGAACGCCCCGAAAGG**A**GGCCCTTCAG**A**TGCAGCAGCAAGAACAGCAG
	mtlFw_AG	**CTTAATCAATAA**TTCGAACGCCCCGAAAGG**A**GGCCCTTCAG**G**TGCAGCAGCAAGAACAGCAG
	mtlFw_TA	**CTTAATCAATAA**TTCGAACGCCCCGAAAGG**T**GGCCCTTCAG**A**TGCAGCAGCAAGAACAGCAG
	mtlFw_TG	**CTTAATCAATAA**TTCGAACGCCCCGAAAGG**T**GGCCCTTCAG**G**TGCAGCAGCAAGAACAGCAG
	mtlAF_Rv	**AATTCGAGCTCGGTACCCGGGGATC**TCAGTTCACCTCGTTGAAAATGG
LamFc (*F. commune*)	LamFc_Fw	**GCATGCCTGCAGGTCGACTCTAGAG**GAAAGGAGGCCCTTCAGATGAATAAATTTTTAATTATAC
	LamFc_Rv	**AATTCGAGCTCGGTACCCGGGGATC**TTACTGATAAACCTTGATATAATC
ho1 (synthetic DNA)	ho1_Fw	**GCATGCCTGCAGGTCGACTCTAGAG**GAAAGGAGGCCCTTCAGATGTCCGTGAACCTGGCATCC
	ho1_Rv1	**GAATTCGAGCTCGGTACCCGGGGATC**CTAGCCTTCGGAGGTTGCCAGG
ho1-pcyA (synthetic DNA)	ho1_Rv2	**GGGACAGATCGGTCACTGCCAT**CTGAAGGGCCTCCTTTCGGGGCGTTCGAACTAGCCTTCGGAGGTTGCCAGG
	pcyA_Fw	**CCTGGCAACCTCCGAAGGCTAG**TTCGAACGCCCCGAAAGGAGGCCCTTCAGATGGCAGTGACCGATCTGTCC
	pcyA_Rv	**GAATTCGAGCTCGGTACCCGGGGATC**TTACTGGATCACATCGAACAGC

2.2.3 Vectors and strains of *C. glutamicum*

During this work new strains of *C. glutamicum* have been constructed using plasmid vectors. There are several established expression vectors for the metabolic engineering of *C. glutamicum*. The vector pVWEx1 is a low copy number vector that has been used for the successful overexpression of various genes from different organisms.[74, 75] The pEKEx3 vector is a high copy number vector that has been used to enable *C. glutamicum* to utilize lactate as sole carbon source.[76] pECXT-pSyn is a medium copy number vector containing the constitutively active promoter pSyn.[77] The pVWEx6 vector is a medium to high copy number vector that was attempted for strain construction in this work, but did not yield any strains.[77]

Table 4 lists all strains and plasmid vectors used in this work, their abbreviated names and which organism genes originate from. All strains constructed in this work were made using the workflow described in the next section, and are made from wildtype *C. glutamicum* ATCC 13032 unless otherwise stated.[78] It should be noted that the *C. glutamicum* Δ*ptsF*Δ*ptsG* strain is yet unpublished but was kindly provided by Professor Wendisch at Bielefeld University.

Table 4: All plasmid vectors and strains of *C. glutamicum* used in this work along with a description and source, as well as the origin of each gene. Strains have been given shorthand names, also listed here. ^{R} = resistance. The *C. glutamicum* Δ*ptsF*Δ*ptsG* strain is yet unpublished but was kindly provided by Professor Wendisch at Bielefeld University.

Plasmid name	**Description**	**Origin of cloned genes**	**Source**
pVWEx1	Kanamycin^{R}, *C. glutamicum/E. coli* shuttle plasmid (P_{tac}, *lacI*, pHM1519 $OriV_{Cg}$). Overexpression of genes.		Peters-Wendisch et al. (2001)[74]
pVWEX6	Kanamycin^{R}, *C. glutamicum/E. coli* shuttle plasmid (P_{syn}, *lacI*, pHM1519 $OriV_{Cg}$). Overexpression of genes.		Henke et al. (2021)[77]
pEKEx3	Spectinomycin^{R}, *C. glutamicum/E. coli* shuttle plasmid (P_{tac}, *lacI*, pBL1 $OriV_{Cg}$). Overexpression of genes.		Stansen et al. (2005)[76]
pECXT-Psyn-*ribGCAH*	Tetracycline^{R}, *C. glutamicum/E. coli* shuttle plasmid. (P_{syn}, pGA1 $OriV_{Cg}$). Overexpressing the biosynthetic operon for riboflavin from *C. glutamicum*.	*C. glutamicum*	Pérez-García et al. (2022)[21]
Strain name			
E. coli	DH5α strain: Δ*lac*U169 (φ80*lacZ* ΔM15), *sup*E44, *hsd*R17, *rec*A1, *end*A1, *gyr*A96, *thi*-1, *rel*A1.[72]		Hanahan (1983)[72]
C. glutamicum	Wildtype strain ATCC 13032[78]		Abe et al. (1967)[78]
C. glutamicum Δ*ptsF*Δ*ptsG*	Wildtype strain ATCC 13032: Δ*ptsF*Δ*ptsG*		Prof. Wendisch, Bielefeld
Cgx1	*C. glutamicum* (pVWEx1)		Pérez-García et al. (2016)[75]
CgM-AA	*C. glutamicum* (pVWEx1-*mtlD*-(AA)*mtlAF*)	*B. subtilis 168*	This work
CgM-AG	*C. glutamicum* (pVWEx1-*mtlD*-(AG)*mtlAF*)	*B. subtilis 168*	This work
CgM-TA	*C. glutamicum* (pVWEx1-*mtlD*-(TA)*mtlAF*)	*B. subtilis 168*	This work
CgM-TG	*C. glutamicum* (pVWEx1-*mtlD*-(TG)*mtlAF*)	*B. subtilis 168*	This work

CgG	*C. glutamicum* (pVWEx1-*galMKTE*)	*E. coli*	This work
CgG-AA	*C. glutamicum* (pVWEx1-*galMKTE*-(*AA*)*galP*)	*E. coli*	This work
CgG-AG	*C. glutamicum* (pVWEx1-*galMKTE*-(*AG*)*galP*)	*E. coli*	This work
CgG-TA	*C. glutamicum* (pVWEx1-*galMKTE*-(*TA*)*galP*)	*E. coli*	This work
CgG-TG	*C. glutamicum* (pVWEx1-*galMKTE*-(*TG*)*galP*)	*E. coli*	This work
Cgx1Δ	*C. glutamicum ΔptsGΔptsF* (pVWEx1)		This work
CgGΔ	*C. glutamicum ΔptsGΔptsF* (pVWEx1-*galMKTE*)	*E. coli*	This work
CgG-TGΔ	*C. glutamicum ΔptsGΔptsF* (pVWEx1-*galMKTE*-*(TG)galP*)	*E. coli*	This work
CgG-Rib	*C. glutamicum* (pVWEx1-*galMKTE*-(*TG*)*galP*)(pECXT-pSyn-*ribGCAH*)	*E. coli, C. glutamicum*	This work
Cgx3	*C. glutamicum* (pEKEx3)		This work
CgHO	*C. glutamicum* (pEKEx3-*ho1*)	*Synechocystis* sp.	This work
CgPCB	*C. glutamicum* (pEKEx3-*ho1-pcyA*)	*Synechocystis* sp.	This work
CgGx3	*C. glutamicum* (pVWEx1-*galMKTE*-(*TG*)*galP*) (pEKEx3)	*E. coli*	This work
CgG-HO	*C. glutamicum* (pVWEx1-*galMKTE*-(*TG*)*galP*) (pEKEx3-*ho1*)	*E. coli, Synechocystis* sp.	This work
CgG-PCB	*C. glutamicum* (pVWEx1-*galMKTE*-(*TG*)*galP*) (pEKEx3-*ho1-pcyA*)	*E. coli, Synechocystis* sp.	This work
CgLam	*C. glutamicum* (pVWEx1-*LamFc*)	*F. commune*	This work

2.2.4 Molecular cloning

Gene cloning was achieved using appropriate primers and a template in a three-step PCR reaction. High temperature (98°C) in the first step encourages denaturation of double stranded DNA into single strands.[79] As the temperature is lowered in step two (55°C), primers anneal to the template DNA. The final step is the elongation step (72°C), where the primer DNA elongates to create sequences complementary to the template. This three-step reaction is repeated 35 times to create a large number of PCR products, or gene copies.[79] In this work all cloning was achieved using thermocyclers and the CloneAmp HiFi PCR Premix Protocol-At-A-Glance from Takara Bio (previously Clontech Laboratories), specifically the protocol for less than 100 ng template DNA.[80] Genes or operons were cloned from gDNA or synthetic DNA. Extraction of gDNA from the desired organism was achieved using the Monarch gDNA purification kit from New England Biolabs (NEB). Synthetic sequences were designed *in silico* from the genetic sequence of *Synechocystis* sp. and synthesized by Integrated DNA Technologies (IDT). An overview of all genes cloned in this work can be found in Table 3.

2.2.4.1 Gel electrophoresis

Gel electrophoresis is a separation method which separates DNA molecules based on size, or number of base pairs (bp). The method exploits the fact that the phosphate backbone of DNA is negatively charged, causing DNA molecules to migrate towards a positively charged electrode (anode) and away from a negatively charged electrode (cathode) when subjected to an electric field. The separation itself is aided by an agarose gel in which big fragments migrate slower than small fragments due to pores in the gel matrix.[81] The approximate size of the DNA molecules following migration can be determined by

comparison with an established standard, in this case a GeneRuler 1 kb Plus DNA ladder from Thermo Scientific.

Agarose gel electrophoresis was used to compare the size of DNA fragments to *in silico* predictions, as well as to ensure that each gene was cloned in its entirety. Samples were run on GelRed gels with 0.8 % (w/v) agarose using a PowerPac Basic power supply and cell, lid and electrodes from Bio-Rad.

- In a flask, mix:
  - 3.2 g agarose (or to a concentration of 8 g/L)
  - 400 mL 1x Tris Acetate-EDTA (TAE) buffer
  - 20 µL GelRed Nucleid Acid Gel Stain (or to a concentration of 0.005 % (w/v))
- Heat in microwave for 5 minutes at 700 watts
- Keep solution at 60 degrees until use
- Pour a thin layer of the solution into an appropriate mold and place a rack at the top of the gel to make wells. Leave to set for 10-30 minutes
- Mix 3 µL of the PCR sample and 2 µL of loading buffer (New England Biolabs)
- Load 3 µL of GeneRuler 1 kb Plus ladder (0.5 µg/µL, Thermo Scientific) in the first well
- Load sample(s) in wells
- Load 3 µL of GeneRuler 1 kb Plus ladder (0.5 µg/µL, Thermo Scientific) in the final well
- Run the gel in an electrophoresis machine at 100 Volts and 400 milliamp (mA) for 30 or 37 minutes for small or big gels respectively. Make sure samples are loaded on the same side of the gel as the negatively charged electrode
- Illuminate the gel with UV light to see DNA bands and compare to ladder

When DNA bands showed the expected size, the remaining PCR product was purified with QIAGEN QIAquick PCR purification kit.[82] For the DNA elution step 30 µL of deionized water was used rather than elution buffer.

2.2.4.2 Preculture

Methods like plasmid extraction, glycerol stocks and growth experiments required precultures. All precultures in this work were made with the appropriate antibiotic always in the same concentration. Kanamycin (50 g/L) was added to a concentration of 0.025 g/L (0.5 µL/mL). Spectinomycin (100 g/L) was added to a concentration of 0.1 g/L (1 µL / mL). Tetracycline (10 g/L) was added to a concentration of 0.005 g/L (0.5 µL/mL). The incubation temperature was set to the optimum of the bacterial species in use. For plasmid extraction *E. coli* was used and the incubation temperature set to 37°C. For *C. glutamicum* the optimal growth temperature is 30°C. Precultures were made using the following protocol.

- In 5 mL complex medium, add 2.5 µL kanamycin or tetracycline / 5 µL spectinomycin
- Inoculate with living bacterial cells

- Incubate overnight in a shaking incubator at the optimal temperature for the bacterial species used. Rpm will vary among incubators, but the culture should stay in the bottom of the tube or flask and should be properly aired

2.2.5 Plasmid extraction and digestion

Plasmid extraction is a method to extract plasmid vectors from hosts such as *E. coli* and is typically performed using a kit. In this work the ZR Plasmid Miniprep – Classic kit from Zymo Research was used, which is specialized for extracting and purifying plasmid DNA from precultures of *E. coli*. The protocol in the kit was followed exactly except the elution step, where 30 µL MQ water was used to elute the plasmid DNA. In the context of strain construction, plasmid extraction was performed in parallel to gene cloning. Plasmids that were extracted and purified were either empty vectors, i.e., only a vector backbone such as pVWEx1, or vectors which already contained cloned genes.

Primers for gene cloning were designed with a cut site for a specific restriction enzyme in mind, e.g. EcoRI or BamHI. In this work the enzymes BamHI-HF and EcoRI-HF from New England Biolabs (NEB) were used along with the NEB rCutSmart Buffer. Extracted vectors were digested, i.e., cut, and purified before genes could be inserted with Gibson assembly. Digested vectors were purified with QIAGEN QIAquick PCR purification kit. Vector digestion was performed using the following protocol.

- Combine 600-1000 ng vector, 1 µL restriction enzyme, 5 µL 10x CutSmart Buffer and deionized water to reach a final volume of 50 µL
- Incubate for 2 hours in 37°C water bath or at the optimum temperature of the restriction enzyme
- Run gel electrophoresis to check that the vector was cut properly. There should be only one band and it should be the correct size
- Purify the digested vector with QIAGEN QIAquick PCR purification kit and elute with 30 µL deionized water

2.2.6 Gibson assembly

Gibson assembly is used to combine purified genes and purified, digested vector through complementary primer design as explained in section 2.2.2. For Gibson assembly the DNA-Assembly protocol by Gibson et al. was used, which includes a recipe for Gibson assembly master mix, an excel sheet for reaction calculations and a protocol for the assembly reaction itself.[83] Assembly Master-Mix (A-MM) was made using the following recipe.

- For 1.2 mL A-MM (80 reactions) mix the following components on ice:
  - 320 µL 5x isothermal reaction buffer (IRB) (NEB)
  - 0.64 µL T5 Exonuclease (NEB; 10 U/µL)
  - 20 µL Phusion® High-Fidelity DNA polymerase (NEB; 2 U/µL)
  - 160 µL Taq DNA Ligase (NEB; 40 U/µL)
  - 700 µL MilliQ water
- Aliquot 15 µL of the A-MM into PCR tubes and freeze at -20°C

The Gibson reaction itself requires the DNA concentration of the purified PCR product(s) and the digested vector, which were determined using a NanoDrop One from Thermo Scientific. Calculations were made for how many nanograms (ng) of vector and PCR

product should be added in the Gibson A-MM. Equation (1-1) was used with vector quantity being set to 100 ng.

- Determine DNA concentration (ng/µL) for purified PCR products and digested vector (e.g. NanoDrop)
- Calculate how many ng of vector and PCR product should be added to the Gibson A-MM using equation (1-1). Vector quantity should be set to maximum 100 ng

$$\boldsymbol{Insert\ quantity\ (ng) = vector\ quantity\ (ng) \times \frac{insert\ size\ (bp)}{vector\ size\ (bp)}} \qquad \textbf{(1-1)}$$

- Calculate the necessary volume for each PCR product and vector using the respective DNA concentrations and the insert quantity from equation (1-1)
- Add the calculated volumes to a 15 µL aliquot of A-MM
- Incubate for 1 hour at 50°C in a thermocycler

2.2.7 Competent cells of *E. coli*

Competent cells are chemically induced to be more receptive to double stranded DNA through making the plasma membrane more permeable.[84] This is necessary for high success rates when transforming *E. coli* with plasmid vectors. Competent cells of *E. coli* were made using the following protocol.[84]

- Inoculate 5 mL of LB and incubate O/N at 37°C
- Inoculate 2 x 50 mL of LB with the preculture
- Incubate at 37°C, 2-3 hours until OD at 600 nm is 0.2–0.4
- Put in falcon tubes
- Incubate on ice for 10 min
- Centrifuge at 4000 rpm, 20 min, 4°C
- Resuspend the pellet with 30 ml of RF1-buffer
- Join everything in one falcon
- Centrifuge at 4000 rpm, 7 min, 4°C
- Resuspend the pellet with 8 mL of RF2-buffer
- Prepare aliquots of 100 µL and freeze at -80°C

2.2.8 Transformation in *E. coli*

Transformation is a method for introducing plasmid vectors into bacteria by allowing plasmid DNA to enter competent cells following perturbations such as heat shock.[84] The finished Gibson reaction mix was transformed directly into competent *E. coli* DH5α cells.[84] The competent cells were transformed with heat shock using the following protocol.[84]

- Thaw *E. coli* DH5α competent cells on ice
- Add 100 ng DNA or 10 µL of Gibson mix to the competent cells
- Incubate 15 minutes on ice
- 1.5 minute heat shock at 42°C in a thermomixer
- Incubate 1 minute on ice
- Add 500 µL of LB medium
- Incubate 1 hour at 37°C and 450 rpm in a thermomixer

- Plate in selective medium using two plates. Pipette 100 µL onto one plate, then centrifuge the rest for 3 minutes at 4000 rpm. Remove almost all supernatant, resuspend cells and pipette all remaining cells onto another plate
- Incubate over night at 37°C

2.2.9 Colony PCR

Colony PCR is a method to screen transformed *E. coli* colonies for the presence of an insert with the expected band size when analyzed on a gel. Colonies are picked directly from a transformation plate and inserts are amplified in a PCR reaction using vector primers, see Table 3, that will extend in the direction of the insert. Amplified fragments were analyzed using gel electrophoresis, see section 2.2.4.1.

Colony PCR was run using the GoTaq G2 DNA polymerase from Promega and the associated protocol.[85] Specifically, the 5x Green GoTaq Buffer was used and each reaction was halved to a total volume of 25 µL rather than 50 µL. Whole cells were used instead of template DNA. For this reason, the initial denaturation step in the PCR reaction was extended to 10 minutes. Denaturation and annealing were set to 1 minute each and the reaction was always set to run for 35 cycles.

2.2.9.1 Glycerol stocks

Glycerol stocks are made to preserve live bacteria for long periods of time. Glycerol enters the cell and stabilizes the interior of the cell as well as the membrane by preventing hydrogen bonding between water molecules, hindering the formation of ice crystals, and enables cells to survive at freezing temperatures.[86] When positive transformants were identified by colony PCR, the colony was cultivated on a fresh plate and glycerol stocks were prepared. Those glycerol stocks were made using the following protocol.

- Make a preculture (5 mL) of the positive colony
- The next day, mix 630 µL preculture***** with 370 µL of glycerol (89 %) in a 1 mL cryotube kept on ice
- Label the tube with strain name, date and initials
- Freeze at –80°C

*****The remaining preculture can be used for plasmid extraction

2.2.10 Digestion test

Plasmids extracted from positive transformant *E. coli* colonies underwent another test to ensure that the fragment was indeed the desired insert. A digestion test can be used to this end, where the plasmid is simply digested by a restriction enzyme to give distinct, pre-determined bands. The band sizes from the digestion were predicted *in silico* with Benchling and enzymes that cut two-three times both inside and outside the insert were used to ensure that bands could be clearly distinguished from each other. The following protocol was used.

- Assemble the DNA sequences from the vector and inserts *in silico* (e.g. Benchling)
- Using the available DNA analysis tools, find an enzyme that cuts in 3-4 different places throughout the assembly. The enzyme should cut at least once inside the insert
- Run an *in silico* digestion with the appropriate enzyme and take note of the expected fragment sizes. Make sure fragments are big enough to be separated on an agarose gel

- Run the digestion, see section 2.2.5
- Run an agarose gel (0.8 % GelRed, 100 V, 400 mA, 30-37 mins) and inspect to see if gel bands match expected fragment sizes from the *in silico* digestion

2.2.11 Sequencing

All plasmid vectors constructed in this work have been verified by sequencing. Benchling was used to align template sequences with sequences from sequencing reactions to verify the presence of inserted genes. Sequencing data was acquired by extracting and sending plasmid vectors to Eurofins genomics for Sanger sequencing. Sequencing primers were purchased from Sigma-Aldrich or Invitrogen and can be found in Table A-1 in Appendix A. The following protocol from Eurofins was used to prepare samples for sequencing.

- Take 5 µL of the purified template DNA with either of the following concentrations in a microcentrifuge tube:

  - Purified plasmid DNA: 50-100 ng/µL
  - Purified PCR products:
    150-300 bp, 1 ng/µL
    300-1000 bp, 5 ng/µL
    1000-1500 bp, 10 ng/µL

- Add 2.5 µL primer with a concentration of 10 pmol/µL
- Add MQ water to reach 10 µL
- Label the tubes with barcodes and make a note of what primer is used in each tube

2.2.12 Competent cells of *C. glutamicum*

As for *E. coli*, competent cells of *C. glutamicum* are better suited for the uptake of DNA such as plasmid vectors. When a digestion test of a plasmid yields the expected band sizes and sequencing can verify the presence of the desired gene, the plasmid vector can be transformed into competent *C. glutamicum* cells. Competent *C. glutamicum* cells were prepared according to the following protocol as described by Eggeling et al.[5]

- Inoculate 5 mL of BHI and incubate overnight at 30°C
- Inoculate 4 x 25 mL of BHIS (1 mL from the overnight culture in each flask)
- Incubate at 30°C until OD at 600 nm reaches 0.6 (approx. 2-4 hours)
- Add 15 µL of ampicillin (5 mg/mL) in each flask
- Incubate at 30°C (1-1.5 hours)
- Distribute each culture evenly between two falcon tubes
- Centrifuge (7 minutes, 4000 rpm, 4°C). Remove supernatant
- Resuspend in 30 mL EPB1-buffer. Incubate on ice for five minutes. Centrifuge for 7 minutes at 4000 rpm and 4°C. Remove supernatant
- Repeat the previous step two more times
- Resuspend in 375 µL of EPB2-buffer
- Aliquot 150 µL in microcentrifuge tubes
- Freeze at -80°C

2.2.13 Transformation in *C. glutamicum*

Transformation of a plasmid into *C. glutamicum* was done by heat shock and electroporation as described by Eggeling et al.[5] Glycerol stocks of positives were made as

previously described in section 2.2.9.1. The following protocol was used to transform *C. glutamicum*.

- Thaw competent *C. glutamicum* cells on ice
- Put an electroporation cuvette on ice
- Put 1 mL of BHIS in a microcentrifuge tube and preheat at 46°C
- Mix 300-600 ng of vector DNA with the competent cells. **Note:** for low copy-number vectors use 800 ng of vector
- Transfer the mixture to the electroporation cuvette
- Do the electroporation (single pulse, 2.5 Kv, 25 Fv, 200 Ω)
- Mix preheated BHIS with the cell mixture
- Incubate for 6 minutes at 46°C
- Incubate 1 hour in a thermomixer (30°C, 450 rpm)
- Plate in selective medium: Pipette 100 µL onto a fresh plate. Centrifuge the rest (3 minutes, 5000 rpm). Remove almost all supernatant, then resuspend cells and plate onto a new plate. **Note:** for a low copy-number vector centrifuge immediately after incubation and plate on only one plate
- Incubate for 1-2 days at 30°C

2.3 Growth experiments

Experiments conducted in baffled shaking flasks or in a BioLector aimed to test the functionality of inserted genes, in this work consumption and production capabilities, or to identify best performing strains or conditions. In this section materials and methods used for growth experiments will be presented. Materials will be presented first and consist mainly of carbon sources, buffers and media. Methods used for growth experiments varied according to what equipment was used, i.e. whether experiments were conducted in baffled shaking flasks or a BioLector.

2.3.1 Materials for growth experiments

In this section materials used in growth experiments conducted in baffled shaking flasks and in a BioLector will be presented.

2.3.1.1 Recipes for stock solutions used in minimal media

Stocks of IPTG (1 M or 2.38 g/L), $MgSO_4 \cdot 7H_2O$ (250 g/L), $CaCl_2 \cdot 2H_2O$ (13.25 g/L) were made with deionized water and filtered to sterilize. Biotin (0.2 g/L) and protocatechuic acid (PCA) (30 g/L) solutions were both made with NaOH (1 M) and filtered to sterilize. Antibiotics, biotin, IPTG and PCA were stored at -20°C. Stocks of Mg and $CaCl_2$ were stored at 4°C.

A trace element solution was made using the following protocol.

- To ca. 80 mL deionized water, add:
  - 1.64 g $FeSO_4 \cdot 7H_2O$ or to a concentration of 16.4 g/L
  - 1 g $MnSO_4 \cdot H_2O$ or to a concentration of 10 g/L
  - 0.1 g $ZnSO_4 \cdot 7H_2O$ or to a concentration of 1 g/L
  - 0.031 g $CuSO_4 \cdot 5H_2O$ or to a concentration of 0.31 g/L
  - 0.002 g $NiCl_2 \cdot 6H_2O$ or to a concentration 0.02 g/L
- Adjust pH to 1 with HCl

- Reach 100 mL with deionized water
- Store at 4°C

2.3.1.2 CgXII buffer solution

CgXII is a common buffer commonly used for the cultivation of *C. glutamicum.*[5] It should be noted that the concentrations of components in this recipe refer to concentrations as they were in the total volume of the final minimal medium, of which the CgXII buffer was only 80 % or 50 % (v/v). In cases where 50 % CgXII was used, the same amount of each component was dissolved in 500 mL of water rather than 800 mL of water.

Example volume: 800 mL (1000 mL final minimal medium)

- Start with ca. 500 mL ion-free water. Leave room for components and pH adjustment.
- While stirring, add:

  - 10 g $(NH_4)_2SO_4$ **or** to a concentration of 10 g/L
  - 1 g KH_2PO_4 **or** to a concentration of 1 g/L
  - 1 g K_2HPO_4 **or** to a concentration of 1 g/L
  - 5 g UREA **or** to a concentration of 1 g/L
  - 42 g MOPS **or** to a concentration of 42 g/L
  - 1 mL $CaCl_2$ stock 1000x (13.25 g/L) **or** to a concentration of 1 mL/L
  - 1 mL $MgSO_4$ stock 1000x (250 g/L) **or** to a concentration of 1 mL/L

- Adjust pH to 7.00 with KOH
- Add ion-free water to reach 800 mL
- Autoclave at 121°C for 20 minutes

2.3.1.3 CgXII minimal medium

The components of the CgXII minimal medium are mostly the same for all experiments. Deviations from the recipe will be presented with the results for each growth experiment. In the following example, all antibiotics relevant to this work are listed. They were included or excluded depending on the antibiotic resistance of the plasmid vector that the strain in question possessed, see Table 4. IPTG was added when vector induction was needed.

Example volume: 1000 mL

- 800 mL 80 % CgXII buffer (80 % of the medium volume) or 500 mL 50 % CgXII buffer (50 % of the medium volume)
- Carbon source, e.g. to 1 % (w/v) of the final medium volume
- Sterile water to reach 200 mL. **Note:** carbon source + sterile water should make up 20 % of total volume of the medium
- 1 mL trace elements (to a final concentration of 1 mL/L)
- 1 mL biotin (0.2 g/L) (to a final concentration of 1 mL/L)
- 1 mL PCA (30 g/L) (to a final concentration of 1 mL/L)

  When needed:
- 500 µL kanamycin stock (50 g/L) or to a final concentration of 0.5 mL/L
- 500 µL tetracycline stock (10 g/L) or to a final concentration of 0.5 mL/L
- 1 mL spectinomycin stock (100 g/L) or to a final concentration of 1 mL/L
- 1 mL of IPTG (1 M) or to a final concentration of 1 mL/L

2.3.1.4 Seaweed hydolysate

The brown seaweed hydrolysate from *L. hyperborea* used in this thesis was kindly provided by Alginor. Before use the hydrolysate underwent enzymatic treatment with a cellulase enzyme blend from Sigma-Aldrich (product no. SAE0020). Not yet published HPLC analyses kindly provided by Fernando Pérez-García prior to this work, of brown SWH after cellulase treatment revealed a glucose concentration of 3.5 ± 0.0 g/L and a mannitol concentration of 6.8 ± 0.1 g/L. The method that was used for the HPLC analysis can be found in section 2.5.2.

Fresh red seaweed biomass of the species *P. palmata* was provided by Alginor and kept frozen at -20 °C. Red seaweed hydrolysate was made from frozen biomass following this protocol.

- Thaw 500 g of frozen *P. palmata* biomass
- Blend the seaweed with 1 L of hot (100 °C) deionized water
- Carefully add 2% (w/v) H_2SO_4 and be wary of excessive foaming
- Distribute 600 mL each in two 2 L bottles
- Autoclave at 121°C for 1 hour
- Cool solution to < 30°C and adjust pH to 5 with KOH
- Put the solution in a 5 L shake flask
- Add 1 mL cellulase enzyme blend (Sigma-Aldrich, product no. SAE0020) per 100 mL hydrolysate solution
- Incubate at 50°C and 200 rpm over night
- Ultracentrifuge the hydrolysate at maximum speed at 4°C for 30 minutes
- Avoiding the pellet and debris, pour the supernatant carefully into a beaker
- Adjust pH to 7 with KOH
- Autoclave for 20 minutes at 121°C
- Store in the dark at 4°C*****

*****Acid treatment can be repeated with 1% (w/v) H_2SO_4 to increase polymer degradation. In this case the pH must be adjusted again to pH 7 with KOH.

Unpublished HPLC analyses kindly provided by Fernando Pérez-García of red SWH after an additional cellulase treatment (see * in recipe for red SWH) showed a glucose concentration of 4.4 ± 0.7 g/L and a galactose concentration of 14 ± 1.2 g/L. The method that was used for HPLC can be found in section 2.5.2.

2.3.1.5 CgXII seaweed hydrolysate medium

In this work, both brown and red SWH have been used as carbon sources in growth experiments. The medium recipe was the same for each SWH, and carbohydrate concentrations presented in the previous section were used to calculate yield (g/g) in these experiments. For more detail see section 2.3.2.1.

The recipe used to make minimal media with 10, 20, 50 and 100 % (v/v) SWH was the same as for regular growth experiments, except a 50 % CgXII buffer was used instead of the standard 80 % CgXII buffer. SWH was added to 10, 20, 50 % (v/v) concentrations, for instance 10 mL / 100 mL medium for 10 % (v/v). In media with 100 % (v/v) SWH, only IPTG and antibiotic was added to the hydrolysate.

2.3.2 Method for flask experiments

The procedure for experiments conducted in shaking flasks was always the same, but experimental design in terms of strains, antibiotics, carbon source etc. varied. The

conditions and any deviations from the following protocol are stated in the results section for each growth experiment. Samples were collected from culture media and OD was measured at 600 nm in a spectrophotometer every two hours for 8-12 hours, or until the exponential growth phase was finished. It should be noted here that cells were washed with the same CgXII buffer used for the media, in this work either 50 % or 80 % CgXII. All flask experiments were conducted at 30°C and 175 rpm.

- Make precultures (25 or 50 mL) for each strain in the experiment. Incubate at optimum temperature overnight in a shaking incubator
- Measure OD at 600 nm of each preculture and calculate how much preculture is needed to reach an OD at 600 nm of 1 in 25 mL of minimal medium
- Transfer the calculated amount into falcon tubes
- Centrifuge falcon tubes for 10 minutes at 4200 rpm and 20°C
- While the centrifuge is running, prepare minimal medium
- Transfer 1 mL of finished minimal media to a microcentrifuge tube and freeze at -20°C
- Discard the supernatant from the falcon tubes and resuspend cells
- Add 25 mL CgXII buffer in each falcon tube and centrifuge for 7 minutes at 4200 rpm and 20°C
- Put 25 mL of CgXII minimal media in baffled flasks
- Remove supernatant from falcon tubes and resuspend cells
- Mix resuspended cells with CgXII minimal media in flasks
- Measure OD at 600 nm for each flask and take a note of the time
- Incubate flasks for 26-28 hours in a shaking incubator at optimal temperature Measure OD at 600 nm every two hours for the first eight hours, then at 24 hours and finally at 26 or 28 hours. To prepare samples for HPLC include the following steps
- After the final OD measurement, put 1 mL from each culture in microcentrifuge tubes and centrifuge for 10 minutes at > 11,000 G
- Transfer supernatant into fresh tubes and store at -20°C

2.3.2.1 Calculations for growth rate, biomass accumulation and biomass yield

The OD measurements at each time interval as well as the final OD measurements were analyzed using Excel. An example is shown in Figure 8, where the strain CgG-TG (here called "TG") was cultivated in minimal CgXII medium with 1 % (w/v) galactose and 0.1 mM IPTG. The OD measurements in the exponential growth phase were analyzed using an exponential trendline to fit the data. The R^2 value was maximized for the growth curve of each replicate. It should be noted here that not all growth curves had a perfect exponential fit like the example in Figure 8, in which case an attempt was made to maximize the R^2 value while still retaining at least 4 data points for analysis. The growth rate was found directly by displaying the equation for the exponential trendline, where the exponent of the exponential constant "e" equaled the growth rate. The average and standard deviation for the three replicates of each strain in each condition was found by using the functions "AVERAGE" and "STDEV" in Excel.

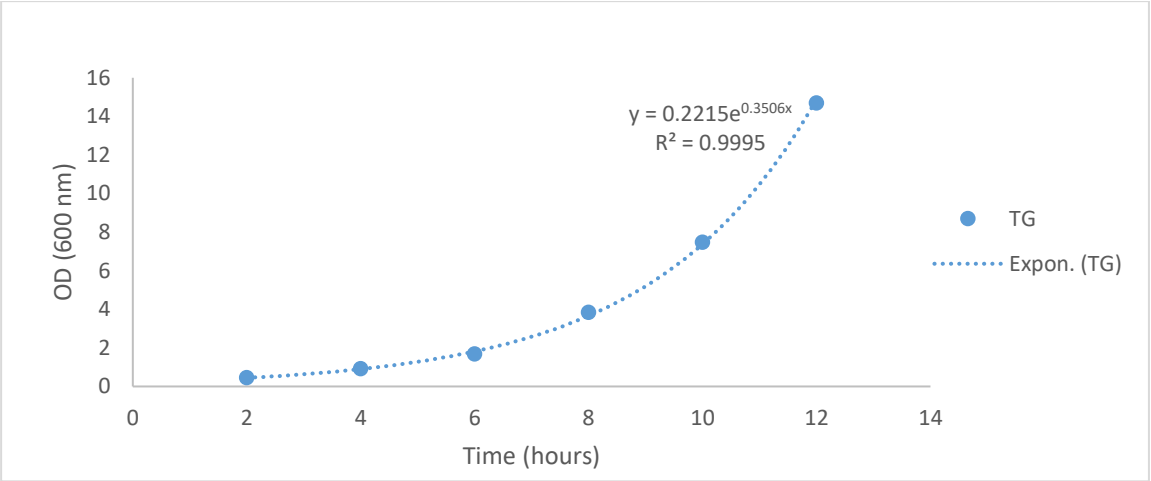

Figure 8: Example of an exponential growth curve with OD at 600 nm plotted against time (hours) for one replicate of CgG-TG (here "TG") in galactose (1 %) and 0.1 mM IPTG. In the equation for the exponential trendline, the exponent to the constant "e" is the growth rate, in this case 0.3506 h^{-1}. The R^2 value should be as high as possible, i.e. the fit of the data to the exponential trendline should be maximized.

The final OD measurements were used to find the final biomass accumulation and the biomass yield for each strain in each condition. The "AVERAGE" and "STDEV" functions in Excel were used to find the average final OD and standard deviation, respectively, for the replicates of each strain in each condition. The average value was multiplied by a correlation factor specific for *C. glutamicum* to give the final biomass value, as optical density (OD) in sample at 600 nm is a relative unit of measurement. The value of the correlation factor was found experimentally by Pérez-García et al. and is 0.343, meaning that an OD at 600 nm of 0.343 corresponds to 1 g/L cell dry weight.[21] The yield was calculated from the biomass by dividing by the amount (g) of carbon source available in the medium. E.g. in experiments where 1 % (w/v) of carbon source is used, the biomass value was divided by 10 (g/L) to find the yield (g/g). In experiments where SWH was used, the amount of available carbon source was calculated as the amount of carbohydrate in the hydrolysate that *C. glutamicum* could metabolize. In brown SWH, the amount of glucose (3.5 ± 0.0 g/L) and mannitol (6.8 ± 0.1 g/L) together gave ca. 10.3 g/L of available carbon source. In red SWH, glucose (4.4 ± 0.7 g/L) and galactose (14 ± 1.2 g/L) accounted for approximately 18.4 g/L of available carbon source.

2.3.3 Method for BioLector experiments

In this thesis project, all BioLector experiments were conducted at 30°C and 1,100 rpm. In experiments where red or brown SWH was used as carbon source, cells were washed with 50 % CgXII buffer instead of the standard 80 % CgXII. This is because cells should be washed with the same CgXII that is in the medium that they will be cultivated in. Biomass was measured automatically in the BioLector every 10 minutes. Samples were collected from culture media and OD was measured at 600 nm in a spectrophotometer at the end of the experiment. Growth rate (h^{-1}), biomass (g/L) and biomass yield (g/g) were calculated in the exact same way as for flask experiments, see the previous section.

- Make precultures (25 mL) for each strain. Incubate at optimum temperature overnight in a shaking incubator
- Measure OD at 600 nm of each preculture and calculate how much preculture is needed to reach an OD of 1 in 1 mL of minimal medium

- Transfer the calculated volume to each of 3 microcentrifuge tubes per condition for each strain
- Centrifuge the tubes for 1 minute at max rpm. Discard supernatant. Use a pipette to remove any leftover supernatant
- Put 1 mL of CgXII (80 % or 50 %) in each microcentrifuge tube. Resuspend cells by pipetting
- Centrifuge for 1 minute at max rpm. Discard supernatant. Use a pipette to remove any leftover supernatant
- Add 1 mL of media to each tube. Resuspend cells by pipetting
- Unwrap 48 well FlowerPlate (m2p labs) and put it on aluminum foil to protect the bottom of the plate from fats or other spots. Pipette 1 mL from each epi into its own well
- Run the BioLector at optimum temperature and at 1,100 rpm for 24 hours or until a plateau is reached
- Measure the final OD at 600 nm for each well. To prepare samples for HPLC, also include the following steps
- Put 1 mL from each well in microcentrifuge tubes and centrifuge for 10 minutes at > 13,000 rpm
- Transfer supernatant into fresh tubes and store at -20°C

2.4 Fed-batch fermentation

Fed-batch fermentations were run in lab-scale fermenters and required additional materials compared to growth experiments in flasks or in a BioLector. Fermenters are convenient for upscaling production of industrially interesting molecules such as riboflavin, which was produced in this work.

2.4.1 Materials for fed-batch fermentation

For cultivation in fermenters a 50 % CgXII without MOPS was used, which can be made following the recipe in section 2.3.1.2 and excluding the MOPS. CgXII minimal medium was prepared for fermenters as for flasks, see section 2.3.1.3. No PCA was used for the fermentations. A fermenter system requires acid and base to automatically adjust the pH. For this purpose, a 10 % (w/v) phosphoric acid solution and a 4 mM KOH solution were made with deionized water. Antifoam 204 from Sigma-Aldrich was used in drop-size volumes to alleviate foaming in the medium when necessary.

2.4.2 Method for fermentation in lab-scale fermenters

In this work 2 L baffled glass fermenters from Applikon Biotechnology were used for fed-batch fermentations. The fermenters were autoclaved before use. The working volume was 700 mL and the reactor was inoculated at an OD600 of 3 from overnight cultures. The temperature was maintained at 30°C by a heating jacket wrapped around the fermenter wall. The relative dissolved oxygen saturation (rDOS) was monitored in each fermenter with 12 mm polarographic DO_2 sensors from AppliSens. The rDOS was set *in silico* to 30 % and maintained automatically by the stirring frequency (rpm), with rpm set to increase if rDOS drops below the setpoint and to decrease if rDOS exceeds its setpoint. Two four-blade Rushton impellers were attached to the rotor in each fermenter. The impellers had outer diameters of 45 mm and were kept submerged in the medium to ensure efficient oxygen supply. The pH was set to 7 *in silico* in each fermenter and maintained automatically by pumping of phosphoric acid (10 %) or KOH (4 mM) to decrease or increase the pH, respectively. Bottles containing phosphoric acid and KOH were attached to the

reactor system via pumps in the Applikon tower. The pH was monitored with 12 mm pH sensors (AppliSens). A constant rate of aeration at 0.75 ml/min was supplied from the bottom of the fermenter with an L-type sparger.

Samples for OD600 measurements and HPLC were collected manually with Super Safe Samplers from Infors HT. The batch medium contained 50 % (v/v) RSWH while the feed medium contained 100 % (v/v) RSWH. Feeding was started manually after the OD600 measurements showed a stationary growth phase and was conducted at 1.75 mL/min until all the feed (140 mL) had been added. The fermenters were stopped at 45 hours as the increase of rDOS to 60-80% during the final hours of the process indicated the completion of the fermentation processes as the cultures ceased to consume oxygen at high rates.

Samples were collected from culture media and OD at 600 nm was measured in a spectrophotometer every two hours until the exponential growth phase had finished in both reactors. HPLC samples were prepared according to section 2.5.2 and analyzed as described in section 2.5.2.1. The relative dissolved oxygen saturation (rDOS) (%) was automatically measured every 10 minutes and exported to Excel for analysis at the end of the processes.

2.4.2.1 Analysis of relative dissolved oxygen saturation (%) data

Data points for rDOS (%) were analyzed separately for the two fermenters. The data points were averaged in groups of three, i.e. for every half hour of data, and then combined with datapoints for the same half hour for the other fermenter to obtain an average rDOS % every half hour for both fermenters. When plotted, this yielded a line fluctuating around the setpoint in the process at 30 % rDOS, see Figure 16.

2.5 High-performance liquid chromatography

High-performance liquid chromatography (HPLC) is a method for the quantification of a diverse array of compounds, including carbohydrates, amino acids and vitamins.[87] The method exploits the electrostatic interaction of molecules in a mixture (mobile phase) with a solid substrate in a column (the stationary phase), yielding different flow rates and elution times for different molecules.[87]

HPLC was used to measure the concentration of carbohydrates and vitamins in this work. Each of the compounds that were quantified have different requirements for sample preparation, buffers and columns, which will be presented here. Carbohydrate or riboflavin standards of known concentration were necessary in HPLC analysis as the resulting chromatograms yielded only relative quantities of each molecule. Standards were used to calculate the exact concentration of the molecule in question in each sample. Materials and methods for HPLC will be presented here.

2.5.1 Materials for HPLC

This subsection contains recipes for buffers and solutions used either in the preparation of standards or samples for HPLC, or as buffer for running the HPLC itself (mobile phase).

For preparation of samples containing riboflavin, a trichloroacetic acid solution (15 %) and a tripotassium phosphate (2 M) solution were made with deionized water and filtered (0.2 µm pores). To use as mobile phase for the detection of riboflavin, an ammonium acetate buffer (5 mM) was made with acetic acid and deionized water, adjusted to pH 6 and filtered (0.2 µm pores).

For the quantification of mannitol and galactose only, a H_2SO_4 buffer (5 mM) was needed and prepared with deionized water and filtered in a 0.2 µm pore filter.

2.5.2 Methods for HPLC

The sugars galactose, glucose and mannitol, as well as the vitamin riboflavin, were quantified using HPLC. Samples were extracted from culture medium, centrifuged for 10 minutes at 13,300 rpm and 1 mL of supernatant was transferred to fresh microcentrifuge tubes and stored at 4°C until use.

Samples for analysis of carbohydrates were prepared by 1:10 dilution of supernatants with deionized water in HPLC vials. When SWH was used in the culture media, a dilution of 1:20 was used instead. Quantification of carbohydrates was conducted in a 1290 Infinity system from Agilent Technologies with a 300 mm × 7.7 mm Hi-Plex H column (Agilent Technologies) and detected by a refractive index detector (Shodex RI-101, ECOM, Czech Republic). The column was prewarmed to 45°C, samples kept at 4°C, and a 5 mM H_2SO_4 buffer was used as a mobile phase with a flow rate of 0.6 mL/min.

In samples where simultaneous detection of glucose and galactose or mannitol was necessary, a 300 mm × 7.7 mm Hi-Plex Pb column (Agilent Technologies) was used with deionized water as mobile phase and a flow rate of 0.5 mL/min. The column was prewarmed at 70°C and samples were kept at 4°C. Standards for the detection of galactose, glucose and mannitol were made in with deionized water in dilution series of 1 %, 0.5 %, 0.25 %, 0.125 % and 0.0625 % (w/v). Standards were then diluted 1:10 with deionized water in HPLC vials prior to analysis.

The vitamin riboflavin (B_2) was quantified using an e2695 Separations Module from Waters, with a 75 mm × 4.6 mm Symmetry C18 Column 3.5 µm column (Waters). Detection was achieved using a fluorescence detector (2475 FLR Detector, Waters) with an excitation wavelength of 370 nm and an emission wavelength of 520 nm. The temperature of the column was kept at 25°C while samples were kept at 4°C. A 5 mM ammonium acetate buffer with a pH of 6 (73 %) and pure methanol (27 %) were used as mobile phase with a isocratic flow rate (100 %) of 0.8 ml/min. Standards of riboflavin were made in a dilution series of 50 mg/L, 25 mg/L, 12.5 mg/L, 6.25 mg/L and 3.125 mg/L. Sample preparation for riboflavin quantification of samples and standards was done as described by Petteys and Frank (2011)[88].

- Transfer 500 µL of the sample to be quantified into a sterile microcentrifuge tube*****
- Add 1 mL of TCA (15%) and agitate samples for 1 minute
- Incubate in the dark at 25°C for 20 minutes
- Centrifuge at 8000 rpm for 20 minutes at 4°C
- Transfer 1 mL of the supernatant into a HPLC vial
- Add 150 µL K_3PO_4 (2 M) into the vial and vortex
- Keep at 4°C until use

*****Due to the high production of riboflavin in culture media and the high sensitivity of the quantification method, supernatants were diluted 1:10 before starting this protocol.

2.5.2.1 Analysis of HPLC data

The standards for each carbohydrate and for riboflavin were used to determine the retention time of the molecule and to calculate the concentration of the molecule in each sample. The retention time for each molecule was simply read off the chromatograms of the standards, as shown for standards of riboflavin in Figure 9. The peaks in Figure 9 are

also good examples of clear, sharp peaks that are ideal for calculating the concentration in samples containing riboflavin. Examples of suboptimal standard peaks are shown in Figure A-1 for galactose and in Figure A-5 for mannitol in Appendix C.

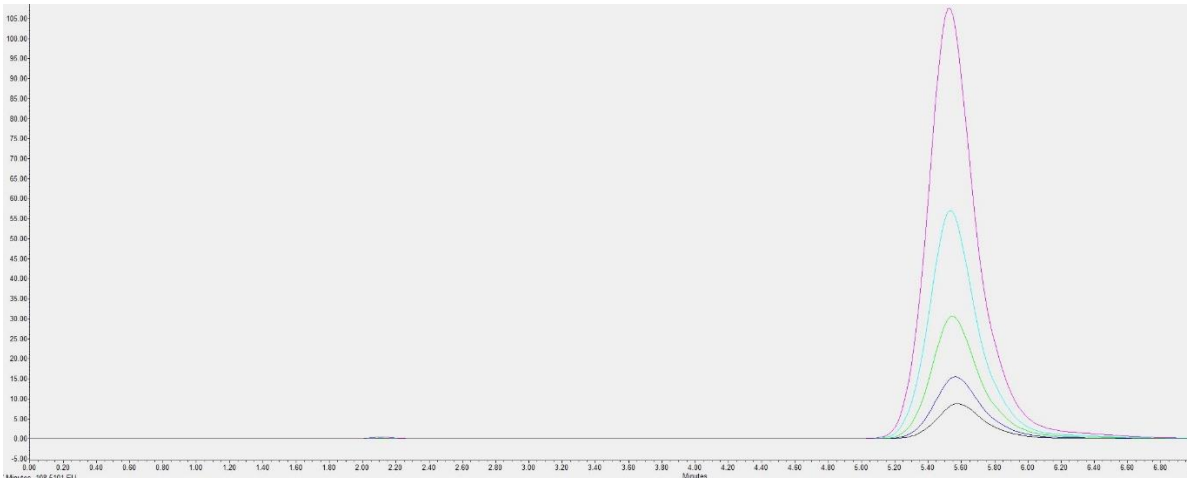

Figure 9: A comparison of chromatograms for standards of riboflavin with concentrations of 50 mg/L, 25 mg/L, 12.5 mg/L, 6.25 mg/L and 3.125 mg/L, from top (pink) to bottom (black). The samples were analyzed by HPLC. The retention time for riboflavin was 5.6 minutes.

Height of the peaks in each chromatogram were used rather than area due to broad shoulders in some standards, as seen in Figure A-1 for galactose. Using the height enabled the utilization of data despite some overlapping peaks or broad shoulders in non-overlapping peaks. The height of each standard peak was plotted in a scatter plot against the known concentration of each standard and fitted with a linear trendline as seen in Figure 10 for riboflavin.

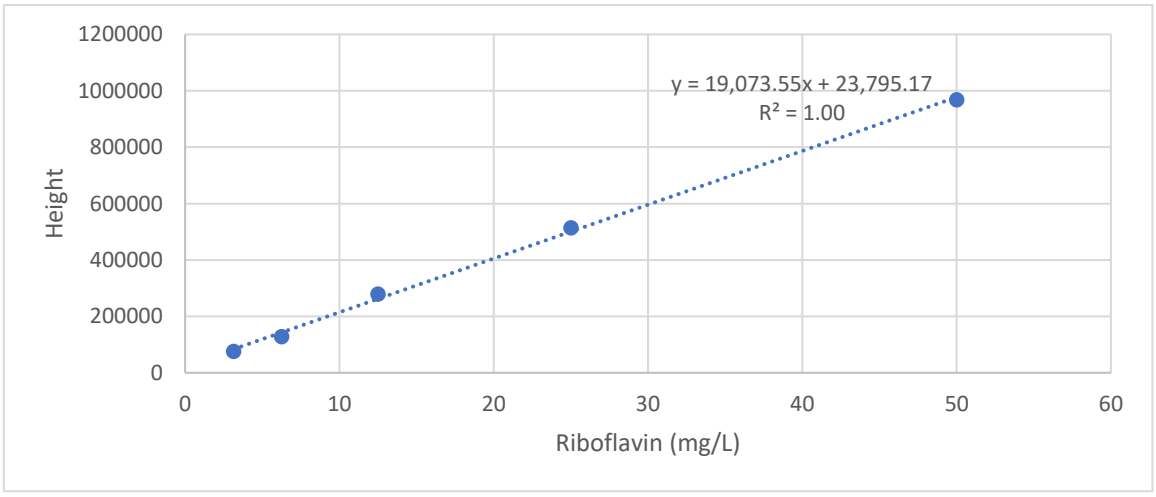

Figure 10: Scatter plot with height of chromatogram peaks plotted against standards with known concentrations of riboflavin (mg/L). A linear trendline was used with R^2 value and equation displayed. The rate of increase (x value) in the equation is used as a conversion factor from peak height to actual concentration in mg/L.

The rate of increase in the equation displayed in Figure 10 is used to convert height to concentration (mg/L) by dividing the height by this number. Dilutions are accounted for where necessary.

During fed-batch fermentations some precipitation of riboflavin was observed in samples taken at 28 hours for both fermenters. Precipitated riboflavin was not detected by the HPLC

and precipitation therefore manifested in HPLC data analyses as lower concentrations of riboflavin in these samples. As more riboflavin precipitated with time and increased concentration, this trend continued until the end of the fermentation. In an attempt to amend this trend, a precipitation factor was calculated based on the volumetric productivity (mg/L h) achieved up until precipitation was observed at 28 hours.

The riboflavin concentration after 26 hours was 650 mg/L, which was divided by 26 (hours) to get a volumetric productivity of 25 mg/L h. According to this value, the riboflavin concentration at 28 hours was expected to be at 700 mg/L, or 50 mg/L more than in the previous sample. However, the riboflavin concentration at 28 hours was 600 mg/L according to HPLC. Precipitation was observed in the culture media samples for both reactors. This means that approximately 100 mg/L of riboflavin precipitated in two hours, from 26 to 28 hours. This gives a precipitation factor of 100 mg/L / 700 mg/L = 0.143 mg/L 2h. This factor was divided by two to obtain a precipitation factor which accounts for precipitation every hour rather than every two hours. The final precipitation factor used for calculations was 0.0715 mg/L h. In other words, there was an assumed 7.5 % of riboflavin precipitation per hour.

To calculate the total precipitation (mg/L) in samples taken after 26 hours, equation (1-2) was used. Rib^{28h} is the concentration of riboflavin (mg/L) expected at 28 hours, as previously described. F^{prec} is the precipitation factor for riboflavin, 0.0715 mg/L h, and h is the number of hours that have passed after 26 hours, as precipitation occurred between 26 and 28 hours.

$$\boldsymbol{Rib^{28h} \times (F^{prec} \times h) = Total\ precipitation\ (mg/L)} \qquad \textbf{(1-2)}$$

The expected riboflavin concentration at 28 hours was used in this equation because both glucose and galactose had run out in the media earlier, at 24 hours. For this reason, it was assumed that the volumetric productivity did not increase after 26 hours. Even if the volumetric productivity increased after 26 hours, it could not be detected due to precipitation of riboflavin.

The resulting total precipitation was added to the concentration of riboflavin that was detected by the HPLC for each sample. See Appendix D for an example of how the total amount of riboflavin precipitation was calculated in samples taken after 26 hours.

For riboflavin production in fermenters, final titer (mg/L), yield (mg/g) and volumetric productivity (mg/L h) values were calculated. The final titer is the concentration of riboflavin (mg/L) in the final sample at the end of the fermentation. The yield was calculated by dividing the final titer by the concentration of available sugars (g/L) in the media. Finally, volumetric productivity was calculated by dividing the final titer by the number of hours the fermentation had been running.

3 Results

3.1 Introduction to results

In this section results for growth experiments, fermentations, and HPLC analyses will be presented. All gene sequences were confirmed by sequencing.

3.2 Utilization of galactose by *C. glutamicum*

The initial approach to enable galactose utilization in *C. glutamicum* was to introduce galactose utilizing genes from *E. coli* and from *L. cremoris*, respectively, and compare the strains in terms of growth rate, biomass accumulation and biomass yield. However, cloning genes from *L. cremoris* gDNA failed many times and was scrapped due to time limitations in the project. Instead, several different strains were made containing galactose utilizing genes from *E. coli*.

The strains CgG, CgG-AA, CgG-AG, CgG-TA and CgG-TG contain galactose-utilizing genes from *E. coli* inserted into the plasmid vector pVWEx1. CgG contains only the operon *galMKTE,* while the rest contain both the operon and a galactose importer gene, *galP*. The four strains containing the *galP* gene have different translational initiation rates of this gene due to specific base changes in the RBS and the start codon sequences, see section 2.2.2. See Table 4 for information and description of strains. Different initiation rates were tested to investigate whether, or to which extent, the membrane protein GalP would cause disruption in the cell membrane that may affect growth. CgG-AA has the highest translational initiation rate of the GalP protein, while CgG-TG has the lowest rate. CgG-AG and CgG-TA have intermediate translational initiation rates.

3.2.1 Proof of concept: galactose utilization in *C. glutamicum*

The galactose utilizing strains CgG, CgG-AA, CgG-AG, CgG-TA and CgG-TG, as well as the control Cgx1, were cultivated in CgXII minimal medium with 1 % (w/v) galactose and 0.1 mM IPTG in flasks. The aim of this experiment was to identify a best-performing strain among the different galactose utilizers. A summary of average growth rates (h^{-1}), biomass accumulation (g/L) and biomass yield (g/g) can be found in Table 5. No growth was observed for the control strain Cgx1. The highest growth rate was achieved by CgG-TG at 0.34 ± 0.01 h^{-1}. Highest biomass and yield were achieved by CgG-AA at 5.0 ± 0.1 g/L and 0.50 ± 0.01 g/g, respectively. Figure 11 illustrates the differences in growth rates between the five galactose utilizing strains.

Figure 12 shows the OD at 600 nm plotted against time for all six strains from 0 to 48 hours. The strains CgG, CgG-AG and CgG-TA were still growing after 24 hours, and still had not reached final OD at 48 hours. This illustrates their slow growth compared to the best performer CgG-TG, as well as CgG-AA which had the second highest growth rate at 0.21 ± 0.02 h^{-1}.

Table 6 shows the final galactose concentration (g/L) as quantified by HPLC in the supernatants of culture media for each strain. Samples for HPLC were collected immediately following the final OD measurement at 48 hours. No galactose was utilized by the control Cgx1. No galactose could be detected for strains CgG-AA and CgG-TG. Strains

CgG and CgG-AG utilized about half the galactose present in the medium, at 2.3 ± 0.4 g/L and 2.2 g/L, respectively, compared to the initial 3.8 g/L detected in the minimal medium prior to inoculation.

Table 5: Summary of average growth rate (h^{-1}), biomass (g/L) and biomass yield (g/g) with standard deviations for six galactose utilizing *C. glutamicum* strains cultivated in CgXII minimal medium with 1 % (w/v) galactose and 0.1 mM IPTG. The experiment was conducted in flasks.

	Growth rate (h^{-1})	**Biomass (g/L)**	**Yield (g/g)**
Cgx1	0.00	0.00	0.00
CgG	0.14 ± 0.02	2.0 ± 0.4	0.20 ± 0.04
CgG-AA	0.21 ± 0.02	5.0 ± 0.1	0.50 ± 0.01
CgG-AG	0.16 ± 0.03	2.2 ± 0.2	0.22 ± 0.02
CgG-TA	0.13 ± 0.01	2.1 ± 0.3	0.21 ± 0.03
CgG-TG	0.34 ± 0.01	4.8 ± 0.0	0.48 ± 0.00

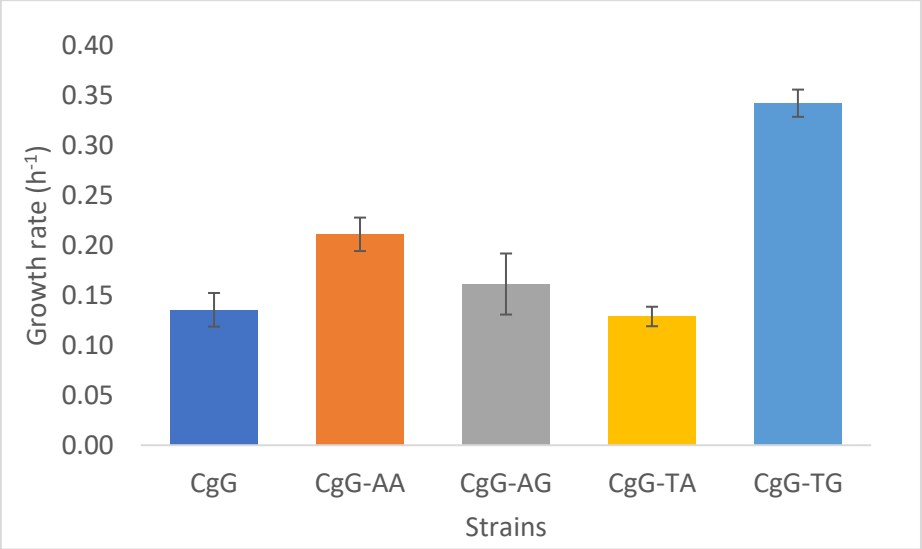

Figure 11: Average growth rates (h^{-1}) with standard deviations for CgG, CgG-AA, CgG-AG, CgG-AG, CgG-TA and CgG-TG cultivated in CgXII minimal medium with galactose (1 %)(w/v) and 0.1 mM IPTG for 48 hours in flasks. No growth was observed for Cgx1 and it has therefore been omitted from the figure.

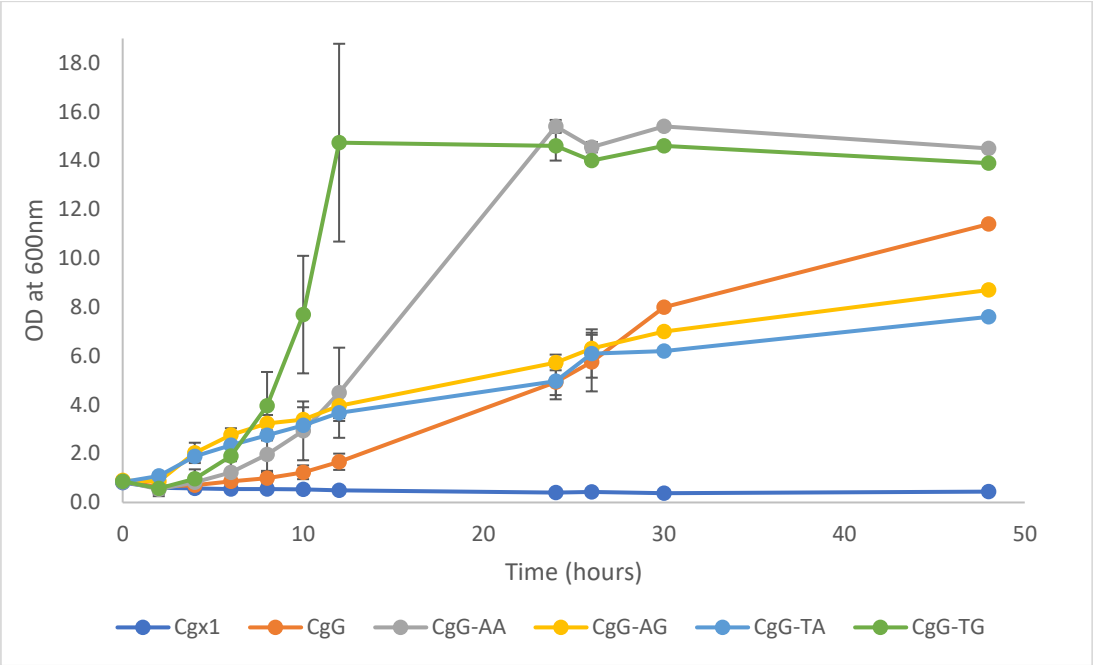

Figure 12: Average OD measurements at 600 nm with standard deviations from 0-48 hours for culture media from Cgx1, CgG, CgG-AA, CgG-AG, CgG-TA and CgG-TG cultivated in CgXII minimal medium with 1 % (w/v) galactose and 0.1 mM IPTG for 48 hours in flasks.

Table 6: Average concentration of galactose (g/L) in the supernatant of each replicate for strains Cgx1, CgG, CgG-AA, CgG-AG, CgG-TA and CgG-TG cultivated in 1 % (w/v) galactose and 0.1 mM IPTG. Samples were taken immediately after final OD was measured and the galactose concentration was quantified by HPLC. Standard deviations are shown, except for CgG-AG where there was only one replicate with a visible peak. A dashed line indicates no peaks were detected, as shown for CgG-AA in Figure A-2 in Appendix C.

	Galactose (g/L)
CgXII minimal medium	3.8
Cgx1	4.2 ± 0.1
CgG	2.3 ± 0.4
CgG-AA	-
CgG-AG	2.2
CgG-TA	1.3 ± 1.1
CgG-TG	-

3.2.2 Native galactose import in *C. glutamicum*

As shown in Table 5 and in Figure 11, the strain CgG grew and accumulated biomass in CgXII minimal medium with 1 % (w/v) galactose. This indicated that there is some native galactose import in *C. glutamicum.* In this section the two native PTS systems for glucose (PTS^G) and fructose (PTS^F) in *C. glutamicum* are investigated as potential importers of galactose.

3.2.2.1 Strain construction

Two similar approaches were attempted to investigate how *C. glutamicum* was able import galactose without the use of the GalP protein. The first approach was to use a deletion strain which lacked the gene *ptsH* which encodes the protein Hpr, see section 1.3.1. This

would disable all PTS systems. The pVWEx1 vector containing the *galMKTE* operon only and one containing the operon plus the *galP* gene would be transformed into the *ptsH* deletion strain, respectively. The latter would serve as a control. The strains would be tested in minimal CgXII medium containing 1 % (w/v) galactose. If the strain containing only the *galMKTE* operon grew in this medium it would prove that none of the PTS systems import galactose, and vice versa. However, transformations failed many times with this approach and due to time constraints the following approach was chosen instead.

A deletion strain lacking PTS systems for both glucose and fructose, *C. glutamicum ΔptsFΔptsG*, was used to check if PTS^G or PTS^F is responsible for native galactose import in *C. glutamicum*. The deletion strain was transformed with the two vectors from the first approach, one containing only the *galMKTE* operon and the other containing both the operon and the *galP* gene. This yielded the strains CgGΔ and CgG-TGΔ, respectively. Cultivation of the strain CgGΔ in minimal medium containing galactose as the only carbon source determined whether galactose was imported by one of the deleted PTS systems or not. The control strain Cgx1Δ was created by transforming the *ΔptsFΔptsG* deletion strain with an empty pVWEx1 vector (strains information and description in Table 4).

3.2.2.2 Results

The strains CgGΔ and CgG-TGΔ, as well as the control Cgx1Δ, were cultivated in CgXII minimal medium with 1 % (w/v) galactose in flasks. Average growth rates (h^{-1}), biomass accumulation (g/L) and biomass yields (g/g) are summarized in Table 7. No growth or biomass accumulation was observed for Cgx1Δ or CgGΔ, while CgG-TGΔ achieved a growth rate of 0.10 ± 0.01 h^{-1}. Average concentrations of galactose (g/L) in the culture media after the growth phase was completed, as well as in the medium prior to inoculation, are shown in Table 8. No galactose could be detected in the culture medium of CgG-TGΔ at the end of the experiment.

Table 7: Average growth rates (h^{-1}), biomass accumulation (g/L) and biomass yield (g/g) with standard deviations for Cgx1Δ, CgGΔ and CgG-TGΔ cultivated in CgXII minimal medium with 1 % (w/v) galactose for 24 hours in flasks.

	Growth rate (h^{-1})	**Biomass (g/L)**	**Yield (g/g)**
Cgx1Δ	0.00	0.00	0.00
CgGΔ	0.00	0.00	0.00
CgG-TGΔ	0.10 ± 0.01	4.6 ± 0.1	0.46 ± 0.01

Table 8: Average concentrations of galactose (g/L) from the culture media of strains Cgx1Δ, CgGΔ and CgG-TGΔ cultivated in 1 % galactose. Samples were taken immediately after final OD was measured and the galactose concentration was measured by HPLC. Standard deviations are shown. A dashed line indicates no peaks were detected, as shown in Figure A-3 in Appendix C.

	Galactose (g/L)
Minimal medium	3.6
Cgx1Δ	3.5 ± 0.2
CgGΔ	3.4 ± 0.4
CgG-TGΔ	-

3.2.3 Cultivation of *C. glutamicum* in red seaweed hydrolysate

Following the rapid growth of CgG-TG in minimal medium with galactose (1 %) (w/v), at 0.34 ± 0.01 h^{-1}, the strain was cultivated in different concentrations of red seaweed hydrolysate (RSWH). CgG-TG and the control Cgx1 were cultivated in CgxII minimal media with 10, 20, 50 and 100 % (v/v) RSWH in a BioLector. The experiment aimed to determine which concentration of RSWH was the optimal condition for CgG-TG and therefore which concentration to use for upscaling in fermenters. Average growth rates (h^{-1}), biomass accumulation (g/L) and biomass yields (g/g) with standard deviations for both strains are shown in Figure 13, Figure 14 and Figure 15, respectively. As shown in Figure 13, CgG-TG had higher growth rates than Cgx1 in 10, 20 and 50% RSWH, but not in 100 % RSWH. The highest growth rate was achieved in 50 % RSWH, with 0.11 ± 0.00 h^{-1}. Figure 14 and Figure 15 show that both biomass accumulation and yield was higher for CgG-TG than Cgx1 for all concentrations of RSWH, with highest biomass at 8.96 ± 0.22 g/L in 100 % RSWH and highest yield at 0.58 ± 0.02 g/g in 50 % RSWH. Concentrations of glucose (g/L) and galactose (g/L) in all four media, as well as for Cgx1 and CgG-TG cultivated in each of the media, can be found in Table 9. The table shows that glucose was depleted after cultivation of Cgx1 and CgG-TG in 10, 20 and 50 % RSWH, while galactose was only depleted for CgG-TG in all concentrations of RSWH. The detection of glucose and galactose for Cgx1 and CgG-TG in 100 % (v/v) RSWH by HPLC proved impossible due to broad peaks of unknown compounds as shown in Figure A-4 in Appendix C. These peaks obscured the areas of the retention times for glucose and galactose, which were 17.6 minutes and 20.1 minutes, respectively. The concentrations of glucose and galactose were sufficiently low to be obscured by these peaks, but the exact amount of glucose and galactose remaining in the media could not be determined from these samples.

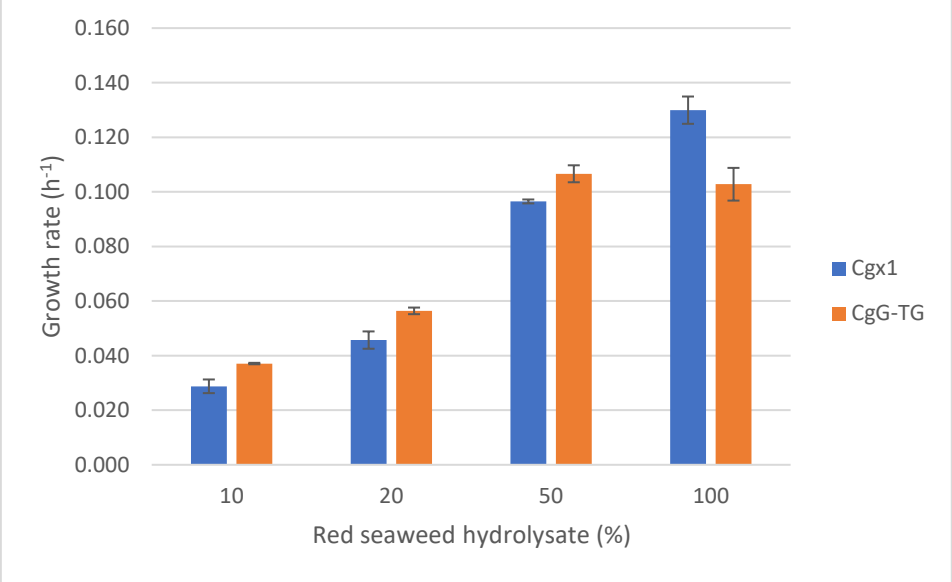

Figure 13: Average growth rates (h^{-1}) and standard deviations for Cgx1 and CgG-TG cultivated in CgXII minimal media with 10, 20, 50 and 100 % (v/v) RSWH.

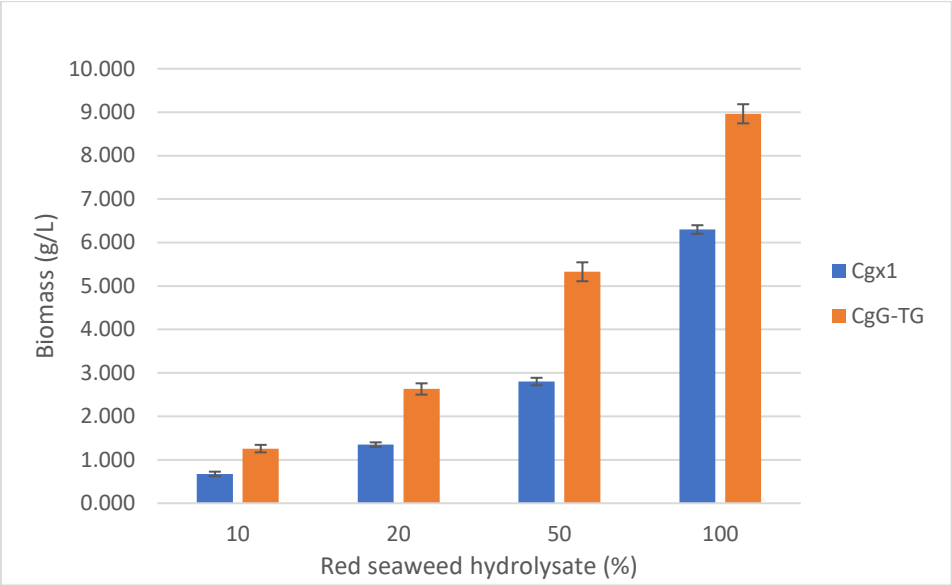

Figure 14: Average biomass accumulation (g/L) and standard deviations for Cgx1 and CgG-TG cultivated in CgXII minimal media with 10, 20, 50 and 100 % (v/v) RSWH.

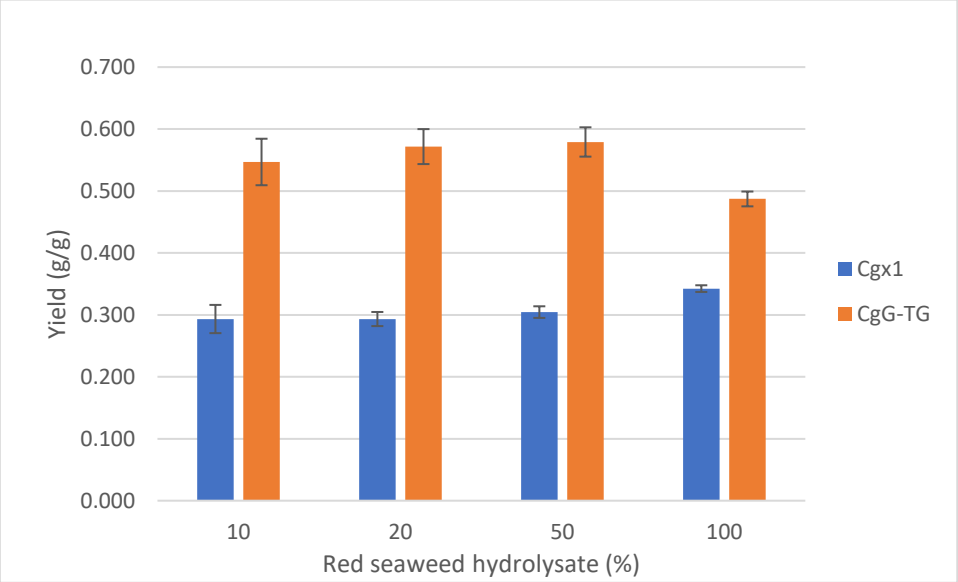

Figure 15: Average biomass yield (g/g) and standard deviations for Cgx1 and CgG-TG cultivated in CgXII minimal media with 10, 20, 50 and 100 % (v/v) RSWH.

Table 9: Average glucose (g/L) and galactose (g/L) concentrations in CgXII minimal media, as well as in culture media for Cgx1 and CgG-TG at the end of the growth experiment. The media contained 10, 20, 50 or 100 % (v/v) of RSWH. "-" means that the sugar was not detected, see Figure A-4 in Appendix C. Samples were collected at the end of the experiment and analyzed using HPLC.

	Glucose			Galactose		
RSWH (%)	**Medium**	**Cgx1**	**CgG-TG**	**Medium**	**Cgx1**	**CgG-TG**
10	0.72	0.00	0.00	0.81	0.85 ± 0.18	0.00
20	1.20	0.00	0.00	1.37	1.75 ± 0.12	0.00
50	3.41	0.00	0.00	4.02	4.02 ± 0.43	0.00
100	9.64	-	-	8.56	8.91 ± 0.56	-

3.2.4 Overproduction of riboflavin with galactose as sole carbon source

The high growth rate accomplished by the CgG-TG strain with galactose as the sole carbon source made it interesting to test the feasibility of galactose as a growth substrate for production of various molecules. Increased production capability of riboflavin in CgG-TG was achieved by transformation of an additional plasmid, pECXT-Psyn-*ribGCAH*, yielding the strain CgG-Rib. The pECXT-Psyn-*ribGCAH* plasmid has been shown to successfully induce overexpression of riboflavin in *C. glutamicum* by Pérez-García et al.[21]

CgG-Rib was cultivated in CgXII minimal media with 1 % (w/v) glucose, 1 % (w/v) galactose, and 1 % glucose plus 1 % galactose, respectively. The experiment was conducted in shaking flasks. The average growth rate (h^{-1}), biomass accumulation (g/L) and biomass yield (g/g) can be found in Table 10. The highest growth rate at 0.13 ± 0.00 h^{-1} and highest biomass at 4.7 ± 0.7 g/L were achieved in medium containing both glucose and galactose. The biomass and yield were the same for glucose and galactose, at 3.1 ± 0.2 g/L biomass and yield of 0.31 ± 0.02 g/g. Table 11 shows average concentrations of glucose (g/L) and galactose (g/L) in each of the three media before inoculation and after the growth phase was completed. All glucose and galactose was utilized for all replicates in all three media. Table 12 shows final concentration (mg/L) of riboflavin from samples collected after the growth phase was completed for CgG-Ribo in each of the three media. The highest concentration of riboflavin, at 638.38 ± 43.74 mg/L, was achieved in medium containing both glucose and galactose. A riboflavin concentration of 456.54 ± 13.83 mg/L was achieved with galactose as sole carbon source.

Table 10: A summary of average growth rate (h^{-1}), biomass accumulation (g/L) and biomass yield (g/g) and standard deviations for CgG-Rib cultivated in CgXII minimal media with 1 % glucose, 1 % galactose and 1 % glucose + 1 % galactose, respectively.

Medium	Growth rate (h^{-1})	Biomass (g/L)	Yield (g/g)
Glucose (1 %)	0.12 ± 0.00	3.1 ± 0.2	0.31 ± 0.02
Galactose (1 %)	0.09 ± 0.00	3.1 ± 0.2	0.31 ± 0.02
Galactose (1 %) + glucose (1 %)	0.13 ± 0.00	4.7 ± 0.7	0.23 ± 0.04

Table 11: Average glucose (g/L) and galactose (g/L) concentrations and standard deviations in minimal media containing glucose (1 %), galactose (1 %) or galactose (1 %) plus glucose (1 %), as well as in culture media for CgG-Rib cultivated in each of three media, respectively. Samples were collected after the growth phase was completed and analyzed using HPLC.

Media prior to inoculation	Glucose (g/L)	Galactose (g/L)
Glucose (1 %)	9.34	0.00
Galactose (1 %)	0.00	8.02
Glucose (1 %) + galactose (1 %)	8.58	7.96
Culture media		
Glucose (1 %)	0.00	0.00
Galactose (1 %)	0.00	0.00
Glucose (1 %) + galactose (1 %)	0.00	0.00

Table 12: Final concentration of riboflavin (mg/L) with standard deviations for samples from culture media following cultivation of CgG-Rib in CgXII minimal media with glucose (1 %), galactose (1 %) and glucose (1 %) plus galactose (1 %), respectively. Samples were collected after the growth phase was completed and were analyzed using HPLC.

Culture medium	Riboflavin (mg/L)
Glucose (1 %)	546.06 ± 22.02
Galactose (1 %)	456.54 ± 13.83
Glucose (1 %) + galactose (1 %)	638.38 ± 43.74

CgG-Rib was also cultivated in CgXII minimal media with 1 % (w/v) glucose, 1 % (w/v) galactose, 1 % glucose + 1 % galactose and 50 % (v/v) red SWH, respectively, in a BioLector. No growth could be observed in galactose (1 %), and for this reason both galactose, and galactose plus glucose, have been discarded and the data will not be presented here. Instead, CgG-Rib cultivated in 50 % (v/v) RSWH will be presented with cultivation in 1 % (w/v) glucose as control. The average growth rate (h^{-1}), biomass accumulation (g/L) and biomass yield (g/g) can be found in Table 13. Highest growth rate, biomass and yield for CgG-Rib were achieved in 50 % RSWH with 0.08 ± 0.01 h^{-1}, 5.04 ± 0.17 g/L and 0.55 ± 0.02 g/g, respectively. Average concentrations of glucose (g/L) and galactose (g/L) in both media before inoculation and after the growth phase was completed can be found in Table 14. HPLC analyses showed that galactose was present in the galactose (1%) medium and the galactose (1 %) plus glucose (1%) medium prior to inoculation, at concentrations of 8.6 g/L and 10.0 g/L, respectively. The 50 % RSWH medium contained 1.85 g/L glucose and 1.94 g/L galactose prior to inoculation, but both sugars were depleted after the growth phase was completed. In the culture medium for CgG-Rib cultivated in glucose, 3.38 ± 0.39 g/L of glucose remained. Table 15 shows final concentrations (mg/L) of riboflavin from samples collected after the growth phase was completed. In 50 % RSWH a final concentration of 388.65 ± 27.50 mg/L was achieved.

Table 13: A summary of average growth rate (h^{-1}), biomass accumulation (g/L) and biomass yield (g/g) and standard deviations for CgG-Rib cultivated in CgXII minimal media with 1 % glucose and 50 % (v/v) RSWH.

Medium	Growth rate (h^{-1})	Biomass (g/L)	Yield (g/g)
Glucose (1 %)	0.03 ± 0.00	2.18 ± 0.14	0.22 ± 0.01
RSWH (50 %)	0.08 ± 0.01	5.04 ± 0.17	0.55 ± 0.02

Table 14: Average glucose (g/L) and galactose (g/L) concentrations and standard deviations in minimal media containing glucose (1 %) or RSWH (50 %) and for CgG-Rib cultivated in each medium. Samples were collected after the growth phase was completed and analyzed by HPLC.

Medium	Glucose (g/L)	Galactose (g/L)
Glucose (1 %)	9.61	0.00
RSWH (50 %)	1.85	1.94
Culture medium		
Glucose (1 %)	3.38 ± 0.39	0.00
RSWH (50 %)	0	0.00

Table 15: Final riboflavin concentration (mg/L) with standard deviations in culture media following cultivation of CgG-Rib in CgXII minimal media with glucose (1 %) and RSWH (50 %), respectively. Samples were collected after the growth phase was completed and were analyzed using HPLC.

Medium	Riboflavin (mg/L)
Glucose (1 %)	525.35 ± 34.33
RSWH (50 %)	388.65 ± 27.50

3.2.5 Overproduction of riboflavin from red seaweed hydrolysate

As production of riboflavin could be observed when CgG-Rib was cultivated in 50 % red SWH the production was scaled up in fermenters (2 L). Two fed-batch fermentations were conducted in parallel with CgG-Rib cultivated in 50 % (v/v) RSWH. The initial working volume was 700 mL, with single feeding phase at 20 hours consisting of 140 mL of RSWH (100 %) (v/v). The fermentations were conducted over 45 hours, as shown in Figure 16. The figure includes plotted lines for biomass (g/L), galactose (g/L), glucose (g/L), riboflavin (mg/L), feed (mL) and relative dissolved oxygen saturation (rDOS) (%) during the fermentations. A growth rate of 0.12 ± 0.01 h^{-1} was achieved prior to feeding. A biomass accumulation of 5.4 ± 0.1 g/L and yield of 0.5 ± 0.01 g/g were achieved at the end of the process. Glucose and galactose were completely depleted in the fermenters immediately prior to, and following, the feeding at 20 hours. The final titer, yield and volumetric productivity for riboflavin were 1139.4 ± 58.6 mg/L, 106.2 ± 5.5 mg/g and 25.3 ± 1.3 mg/L h, respectively. Precipitation of riboflavin could be detected in samples taken after 26 hours, and a precipitation factor of 0.0715 mg/ L h was calculated to account for precipitation in the riboflavin concentration of these sample, see section 2.5.2.1 and Appendix D for more detail. The average rDOS mostly remained between 20 and 40 % until growth finished and it stabilized at 60-80 %.

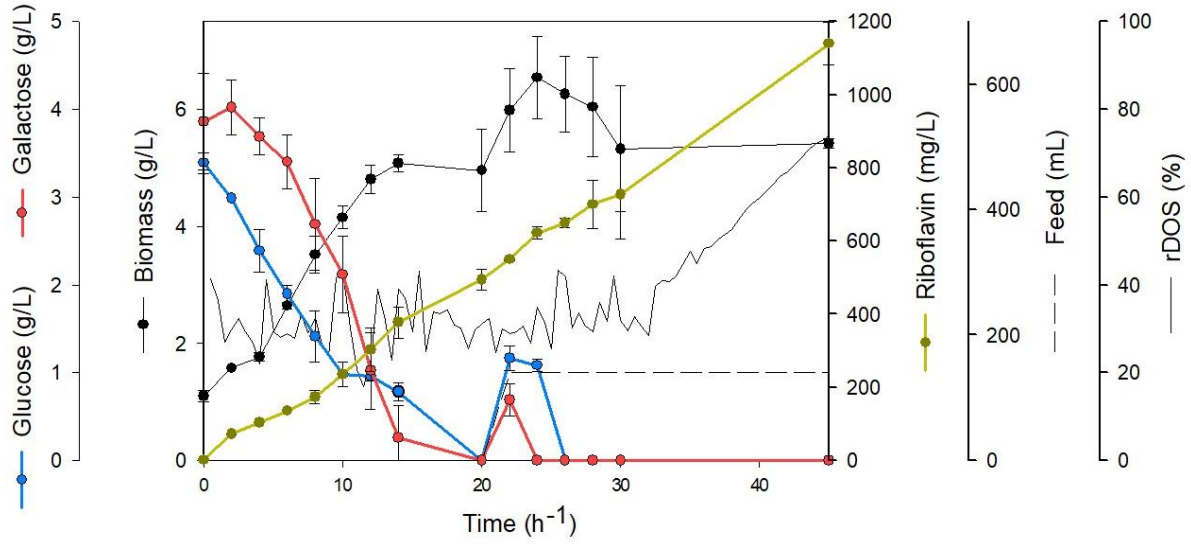

Figure 16: Values and standard deviations for biomass (g/L) (black dots), glucose (g/L) (blue dots), galactose (g/L) (red dots), riboflavin (mg/L) (yellow dots), relative dissolved oxygen saturation (rDOS) (%) (black line), as well as feed volume (mL) (dashed black line), over time for two in-parallel fed-batch fermentations with CgG-Ribo cultivated in 50 % (v/v) RSWH. The feed consisted of pure RSWH (100 % (v/v)).

3.2.6 Production of phycocyanobilin

New strains were constructed which in addition to the plasmid from CgG-TG had vectors containing the genes necessary to produce the blue pigment phycocyanobilin (PCB). The genes *ho1* and *ho1-pcyA* were cloned into the plasmid vector pEKEX3. Transformation in *C. glutamicum* yielded the strains CgG-HO and CgG-PCB which should have been producing biliverdin and PCB, respectively, with heme as substrate. The strain CgGx3 contained only the empty pEKEx3 vector in addition to the galactose utilizing genes from CgG-TG and was used as control. In addition, the vectors containing the genes *ho1* and *ho1-pcyA* were also transformed into wildtype *C. glutamicum*, resulting in the strains CgHO and CgPCB, respectively. This was to enable testing and comparison of PCB production capability in *C. glutamicum* with glucose and galactose as sole carbon sources. A final control strain was constructed, Cgx3, which contained only the empty pEKEx3 vector. See the complete list of strains in Table 4.

All four producer strains, CgHO, CgPCB, CgG-HO and CgG-PCB, as well as the controls Cgx3 and CgGx3, were cultivated in CgXII minimal medium with 1 % (w/v) glucose. The resulting average growth rates (h^{-1}), biomass (g/L) and biomass yields (g/g) for each strain are summarized in Table 16. The highest growth rates were observed for CgG-HO and CgG-PCB, both at 0.24 h^{-1}. The highest biomass and yield were observed for CgG-HO, at 5.3 ± 0.2 g/L and 0.53 ± 0.02 g/g. However, no green or blue colour could be observed in pellets or supernatants of producer strains.

Table 16: Summary of average growth rate (h^{-1}), biomass (g/L) and biomass yield (g/g) with standard deviations for strains Cgx3, CgHO, CgPCB, CgGx3, CgG-HO and CgG-PCB cultivated in CgXII minimal medium with 1 % (w/v) glucose.

	Growth rate (h^{-1})	**Biomass (g/L)**	**Yield (g/g)**
Cgx3	0.07 ± 0.01	3.5 ± 0.1	0.35 ± 0.01
CgHO	0.08 ± 0.00	4.5 ± 0.1	0.45 ± 0.01
CgPCB	0.09 ± 0.01	4.7 ± 0.1	0.47 ± 0.01
CgGx3	0.10 ± 0.01	2.9 ± 0.1	0.29 ± 0.01
CgG-HO	0.24 ± 0.01	5.3 ± 0.2	0.53 ± 0.02
CgG-PCB	0.24 ± 0.00	5.1 ± 0.1	0.51 ± 0.01

The strains CgGx3, CgG-HO and CgG-PCB were then cultivated in CgXII minimal medium with 1 % (w/v) galactose. CgGx3 was also cultivated in CgXII minimal medium with 1 % (w/v) glucose as an extra control. The resulting average growth rate (h^{-1}), biomass (g/L) and biomass yield (g/g) for each strain are summarized in Table 17. The highest growth rate was achieved by CgG-PCB at 0.23 ± 0.01 h^{-1}. No green or blue colour could be observed in pellets or supernatants of the producer strains CgG-HO and CgG-PCB.

Table 17: Summary of average growth rate (h^{-1}), biomass (g/L) and biomass yield (g/g) with standard deviations for strains CgGx3, CgG-HO and CgG-PCB cultivated in CgXII minimal medium with 1 % galactose. The control CgGx3 was also cultivated in minimal CgXII medium with 1 % glucose and is marked with "(glc)".

	Growth rate (h^{-1})	**Biomass (g/L)**	**Yield (g/g)**
CgGx3 (glc)	0.12 ± 0.05	2.4 ± 0.3	0.24 ± 0.03
CgGx3	0.09 ± 0.03	2.9 ± 0.1	0.29 ± 0.01
CgG-HO	0.21 ± 0.02	3.5 ± 0.2	0.35 ± 0.02
CgG-PCB	0.23 ± 0.01	3.7 ± 0.1	0.37 ± 0.01

3.3 Utilization of mannitol by *C. glutamicum*

In order to enable mannitol utilization in *C. glutamicum*, the genes *mtlD* and *mtlAF* were cloned into the plasmid vector pVWEx1. Differential primer design yielded four versions of the *mtlAF* gene, with different translational initiation rates of this gene due to specific base changes in the RBS and the start codon sequences as described in section 2.2.2. This was done to check whether the translational levels of the *mtlAF* gene products in the cell membrane would affect growth. Transformation in *C. glutamicum* wildtype yielded the strains CgM-AA, CgM-AG, CgM-TA and CgM-TG. See the list of strains in Table 4 for more strain information. CgM-AA has the highest translational initiation rate, while CgM-TG has the lowest rate. CgM-AG and CgM-TA have intermediate translational initiation rates.

3.3.1 Mannitol utilization in *C. glutamicum*

The four *C. glutamicum* strains capable of utilizing mannitol, CgM-AA, CgM-AG, CgM-TA and CgM-TG were cultivated in CgXII minimal medium with 1 % (w/v) mannitol and 0.1 mM IPTG in flasks. Cgx1 was used as control. Table 18 summarizes average growth rates (h^{-1}), biomass accumulation (g/L) and biomass yield (g/g) for all strains. The highest growth rate achieved was at 0.25 ± 0.02 h^{-1} for CgM-AA, but with the standard deviation overlapping the growth rate for CgM-AG, at 0.24 ± 0.02 h^{-1}. Figure 17 and Figure 18 illustrate the differences in average growth rate and biomass accumulation, respectively, for all mannitol utilizing strains. No growth was observed for Cgx1. All mannitol utilizing strains grew and accumulated biomass with mannitol as sole carbon source. A best-performing strain could not be determined from this experiment due to similar growth rates, biomass and biomass yields.

Table 18: Summary of average growth rate (h^{-1}), biomass accumulation (g/L) and biomass yield (g/g) with standard deviations for the strains CgM-AA, CgM-AG, CgM-TA and CgM-TG as well as control Cgx1 grown in CgXII minimal medium with 1 % (w/v) mannitol and 0.1 mM IPTG.

	Growth rate (h^{-1})	**Biomass (g/L)**	**Yield (g/g)**
Cgx1	0.00	0.00	0.00
CgM-AA	0.25 ± 0.02	4.25 ± 0.01	0.43 ± 0.00
CgM-AG	0.24 ± 0.02	4.49 ± 0.18	0.45 ± 0.02
CgM-TA	0.22 ± 0.01	3.90 ± 0.20	0.39 ± 0.02
CgM-TG	0.22 ± 0.01	4.38 ± 0.14	0.44 ± 0.01

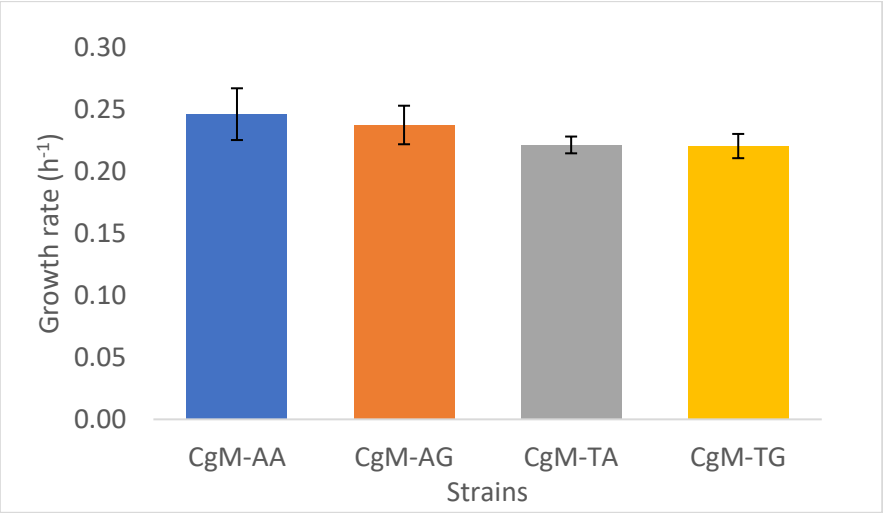

Figure 17: Average growth rates (h^{-1}) for mannitol utilizing strains CgM-AA, CgM-AG, CgM-TA and CgM-TG in 1 % (w/v) mannitol and 0.1 mM IPTG. Standard deviations are shown. No growth could be observed for Cgx1 and it was therefore omitted from the figure.

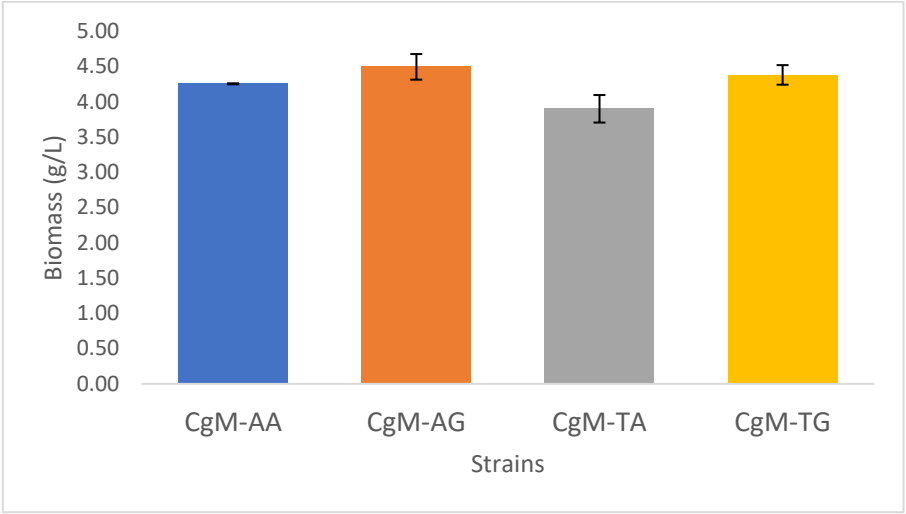

Figure 18: Average biomass accumulation (g/L) for mannitol utilizing strains CgM-AA, CgM-AG, CgM-TA and CgM-TG in 1 % (w/v) mannitol and 0.1 mM IPTG. Standard deviations are shown. No biomass accumulation from growth on mannitol could be observed for Cgx1 and it was therefore omitted from the figure.

In an attempt to optimize conditions for mannitol utilization, four different concentrations of IPTG were tested. The mannitol utilizing strains CgM-AA, CgM-AG, CgM-TA and CgM-TG were grown at different IPTG concentrations (0.1, 0.2, 0.4 and 0.7 mM) in CgXII minimal media with 0.2 % (w/v) mannitol. Cgx1 was used as control and the experiment was conducted in two rounds in a BioLector, as a single 48-well FlowerPlate (m2p labs) could not fit all conditions. All mannitol utilizing strains and Cgx1 were grown in 0.1 and 0.7 mM IPTG in one plate, and in 0.2 mM and 0.4 mM IPTG in another. Average growth rates (h^{-1}) and biomass accumulation (g/L) for each strain for all IPTG concentrations are illustrated in Figure 19 and Figure 20, respectively. Cgx1 has been omitted from both figures as no growth or biomass accumulation could be observed. Visual inspection of Figure 19 and Figure 20 reveal that the 0.2 mM and 0.4 mM IPTG conditions yielded consistently lower growth rates and biomass. Figure 21 shows the average mannitol concentration (g/L) in the supernatant for Cgx1, as well as the minimal media with 0.1 mM to 0.7 mM IPTG respectively, after the growth phase was completed. Samples were analysed by HPLC. No

mannitol could be detected for any of the mannitol utilizing strains at the end of the experiment. The chromatogram for CgM-AG is shown as an example in Figure A-6 in Appendix C.

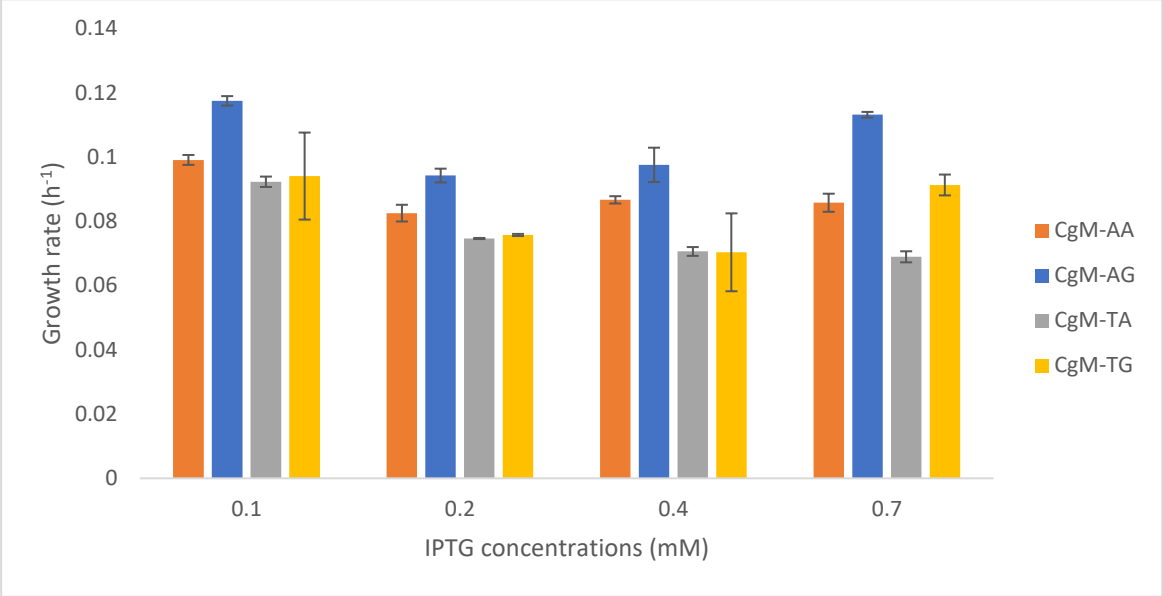

Figure 19: Average growth rates (h^{-1}) of strains CgM-AA, CgM-AG, CgM-TA and CgM-TG in CgXII minimal medium with 0.2 % (w/v) mannitol and IPTG concentrations of 0.1 mM, 0.2 mM, 0.4 mM and 0.7 mM, respectively. Standard deviations are shown. No growth was observed for the control, Cgx1, in the same media and it has therefore been omitted from the figure.

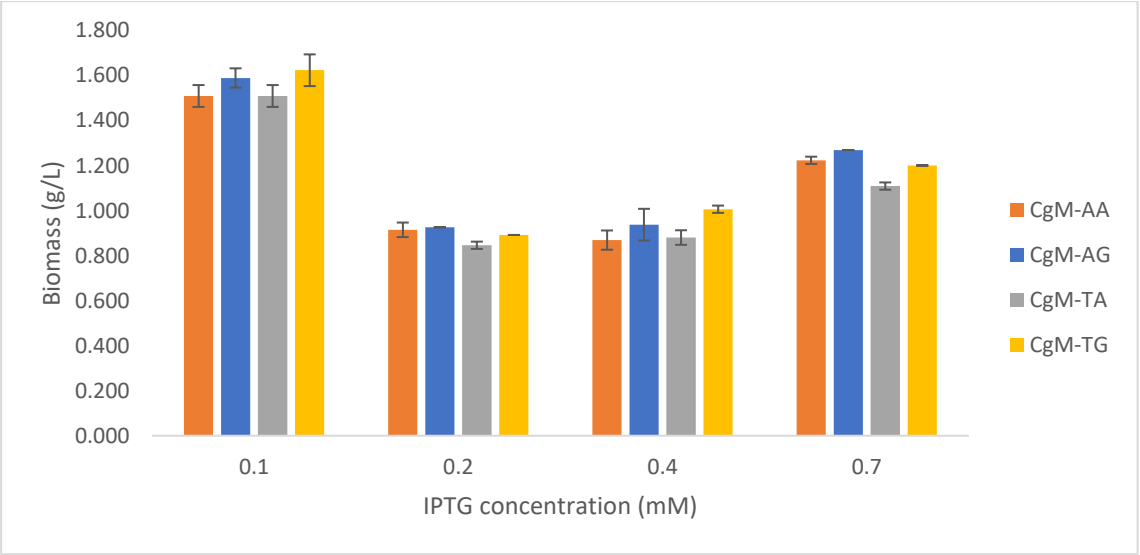

Figure 20: Average biomass accumulation (g/L) for strains CgM-AA, CgM-AG, CgM-TA and CgM-TG grown in CgXII minimal medium with 0.2 % (w/v) mannitol at IPTG concentrations from 0.1 mM to 0.7 mM. Standard deviations are shown. No biomass accumulation was observed for the control Cgx1 and it has therefore been omitted from the figure.

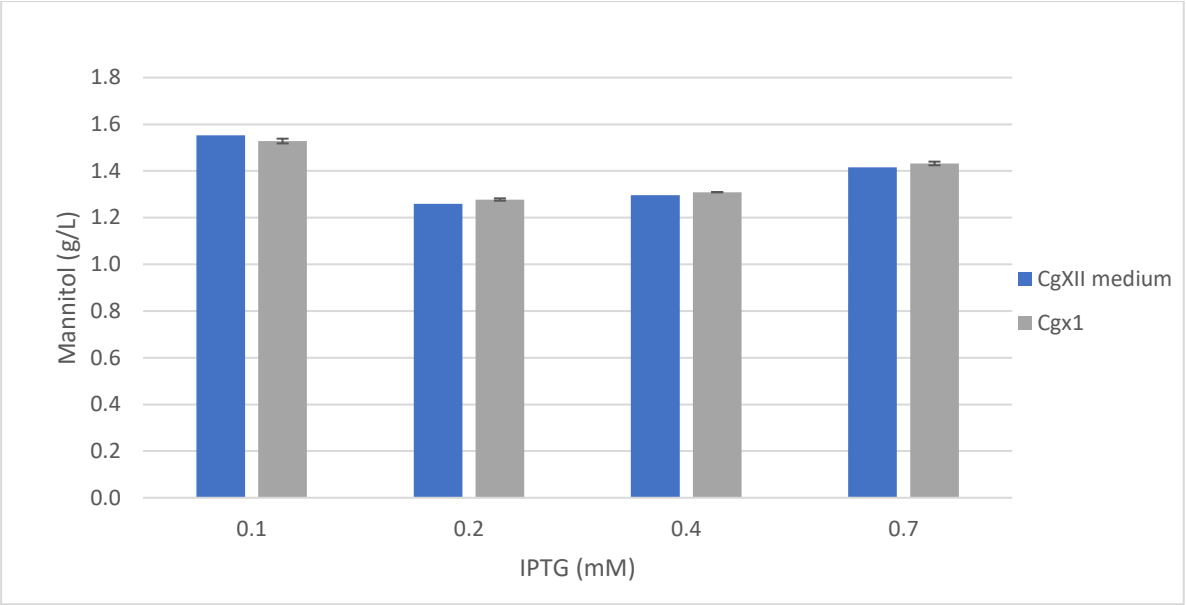

Figure 21: Average concentrations of mannitol (g/L) in the supernatant for Cgx1 cultivated in 0.2 % (w/v) mannitol and 0.1, 0.2, 0.4 and 0.7 mM IPTG, as well as in the minimal media prior to inoculation. Samples were taken immediately after final OD was measured and analyzed using HPLC. Standard deviations are shown for Cgx1. No peaks were detected for any of the mannitol utilizing strains, as exemplified by a replicate of CgM-AG in Figure A-6 in Appendix C.

The consistently lower growth rates and biomass in 0.2 mM and 0.4 mM IPTG conditions observed here due to the two conditions being run separately form 0.1 and 0.7 mM IPTG, lead to a repetition of the experiment with only two replicates for each strain in each condition. Mannitol utilizing strains and Cgx1 were cultivated in 0.2 % (w/v) mannitol and IPTG concentrations of 0.1, 0.2, 0.4 and 0.7 mM in a single FlowerPlate. Figure 22 and Figure 23 illustrate average growth rate (h^{-1}) and biomass accumulation (g/L) for each mannitol utilizing strain in each IPTG concentration, respectively. No growth or biomass accumulation could be observed for the control strain Cgx1 in any condition, and it has therefore been omitted from both figures. From Figure 22 it is evident that growth rates are more even than demonstrated in Figure 19, indicating that experimental differences affected growth rates for mannitol utilizing strains in 0.2 and 0.4 mM IPTG in the first run of the experiment. No best condition could be identified from this experiment due to similar growth rates for each strain across different IPTG concentrations. However, CgM-AA was determined to be the best-performing strain with the highest growth rate achieved at 0.24 ± 0.00 h^{-1} before conversion, and 0.11 ± 0.00 h^{-1} after conversion, in 0.2 mM IPTG.

Because there were only two replicates of each strain in each condition in this experiment, conversion factors for growth rate and biomass were calculated. They were calculated to 0.46 and 0.75, respectively. See Appendix B for calculations. All growth rates and biomass for all mannitol utilizing strains in all IPTG concentrations were multiplied by their respective conversion factors in order to approximate more statistically reliable values despite having only two replicates. The data presented in Figure 22 and Figure 23 have been calculated using these conversion factors.

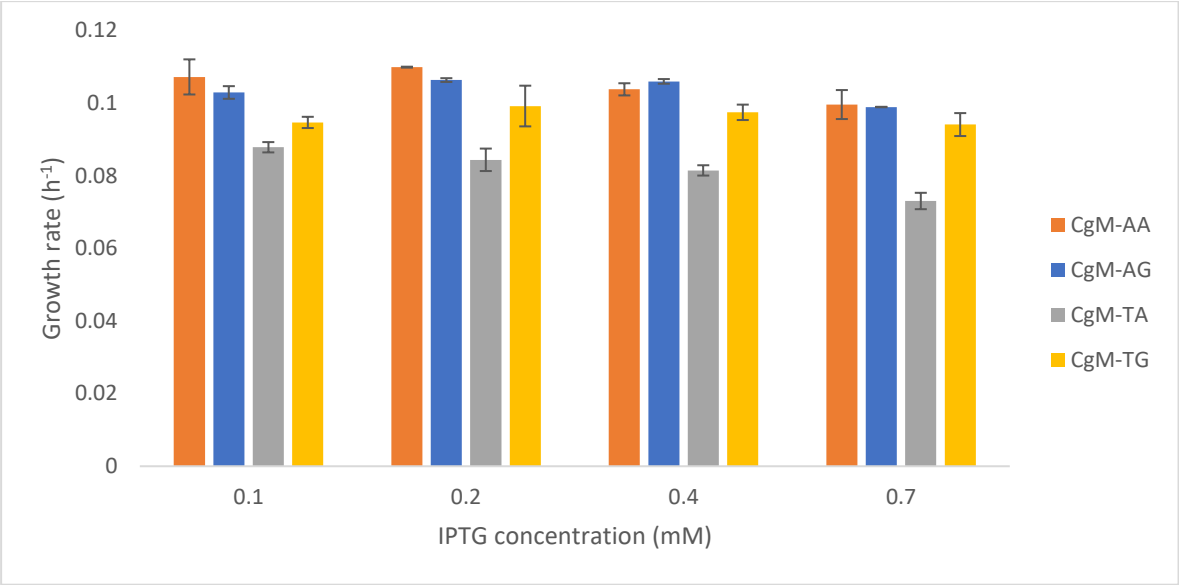

Figure 22: Average growth rates (h^{-1}) with standard deviations of strains CgM-AA, CgM-AG, CgM-TA and CgM-TG in CgXII minimal medium with 0.2 % (w/v) mannitol and IPTG concentrations of 0.1 mM, 0.2 mM, 0.4 mM and 0.7 mM, respectively. No growth was observed for Cgx1 in any medium and it has therefore been omitted from the figure. This experiment had only two replicates per strain per condition, and a conversion factor was used for calculations, see Appendix B.

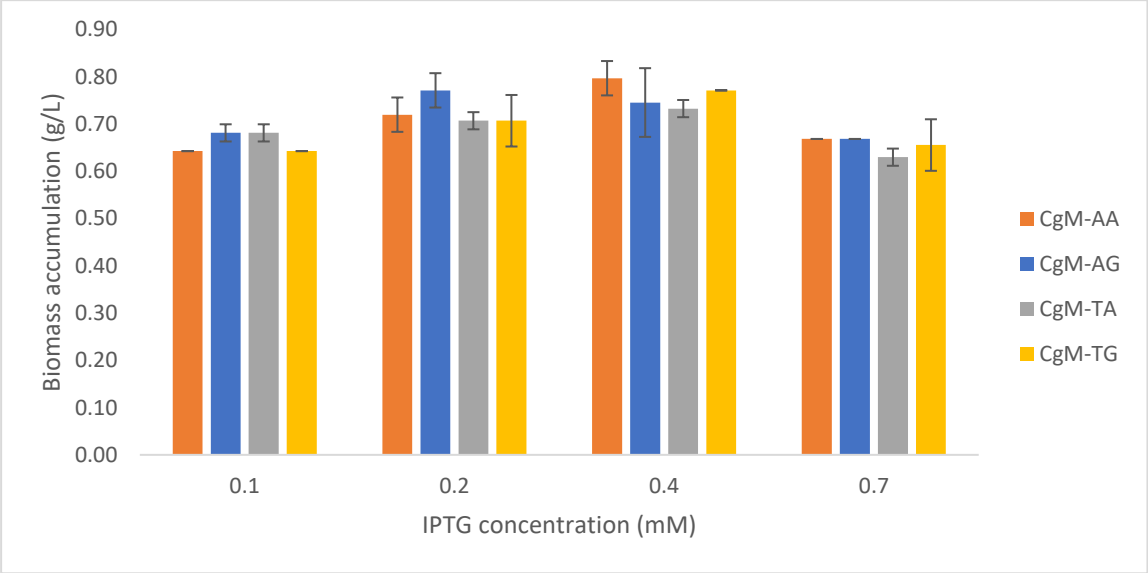

Figure 23: Average biomass (g/L) with standard deviations of strains CgM-AA, CgM-AG, CgM-TA and CgM-TG in CgXII minimal medium with 0.2 % (w/v) mannitol and IPTG concentrations of 0.1 mM, 0.2 mM, 0.4 mM and 0.7 mM, respectively. No biomass accumulation was observed for Cgx1 in any medium and it has therefore been omitted from the figure. This experiment had only two replicates per strain per condition and a conversion factor used for calculations, see Appendix B.

3.3.2 Cultivation of *C. glutamicum* in brown seaweed hydrolysate

Among the mannitol utilizing strains, CgM-AA was determined to be the best performing strain due to consistently high growth rates across all three experiments conducted with these strains, see the previous section. Due to similar performance across all IPTG concentrations, the cultivation of CgM-AA in brown SWH was performed with the standard 1 mM IPTG. CgM-AA was cultivated in CgXII minimal media with 50 % CgXII buffer and 10, 20, 50 and 100 % (v/v) brown seaweed hydrolysate (BSWH). Cgx1 was used as control. Average growth rates (h^{-1}), biomass accumulation (g/L) and biomass yields (g/g) are presented in Figure 24, Figure 25 and Figure 26, respectively. CgM-AA achieved the highest growth rate and biomass in 50 % BSWH at 0.15 ± 0.00 h^{-1} and 3.24 ± 0.17 g/L, respectively. CgM-AA had lower growth rates than control in 50 and 100 % BSWH. CgM-AA had higher biomass accumulation than Cgx1 in all BSWH concentrations except for 100 %. Biomass yield for both strains decreased with increasing concentration of BSWH. Concentrations of glucose (g/L) and mannitol (g/L) in the four different seaweed media, as well as in the culture media after the growth phase was completed, are presented in Table 19. There was no glucose left in 10 and 20 % BSWH media following the experiment, and glucose could not be detected in 50 and 100 % BSWH hydrolysate, see Figure A-7 and Figure A-8 in Appendix C. Mannitol had not been utilized by Cgx1, for which there was detected mannitol in all BSWH media at similar concentrations as in the media prior to inoculation, e.g. 1.11 ± 0.00 g/L mannitol for Cgx1 in 10 % BSWH compared to 1.24 g/L in the media prior to inoculation. For CgM-AA, there was no mannitol left in 10, 20 or 50 % BSWH. In 100 % BSWH there was 10.94 ± 0.62 g/L mannitol following the experiment, which was similar to the 100 % BSWH medium prior to inoculation at 10.53 g/L mannitol.

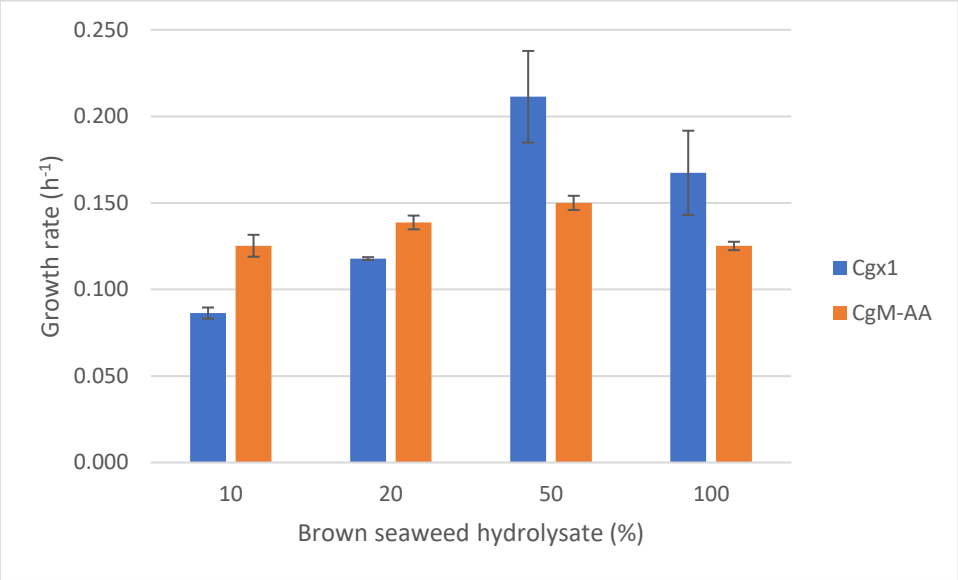

Figure 24: Average growth rates (h^{-1}) and standard deviations for Cgx1 and CgM-AA cultivated in 10, 20, 50 and 100 % (v/v) BSWH.

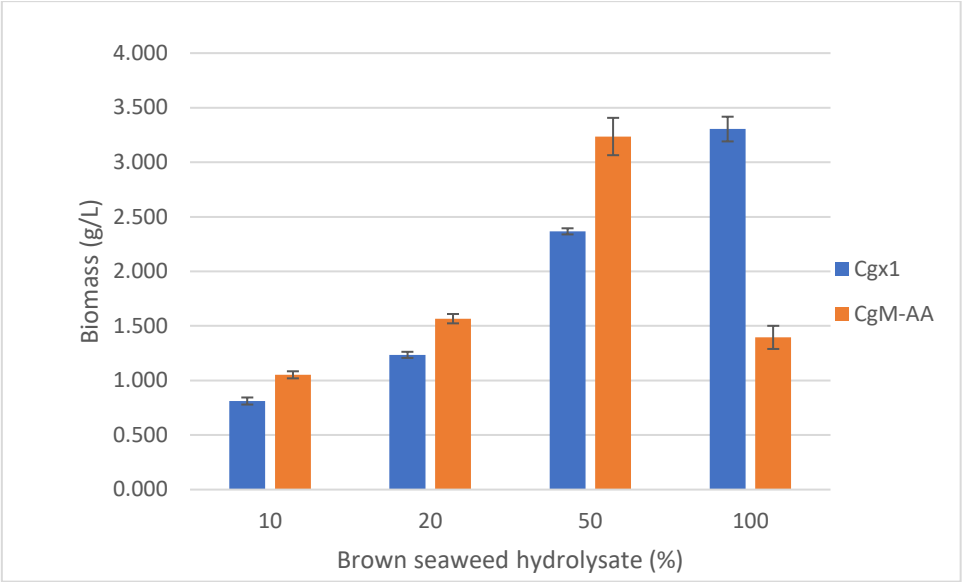

Figure 25: Average biomass accumulation (g/L) and standard deviations for Cgx1 and CgM-AA cultivated in 10, 20, 50 and 100 % (v/v) BSWH.

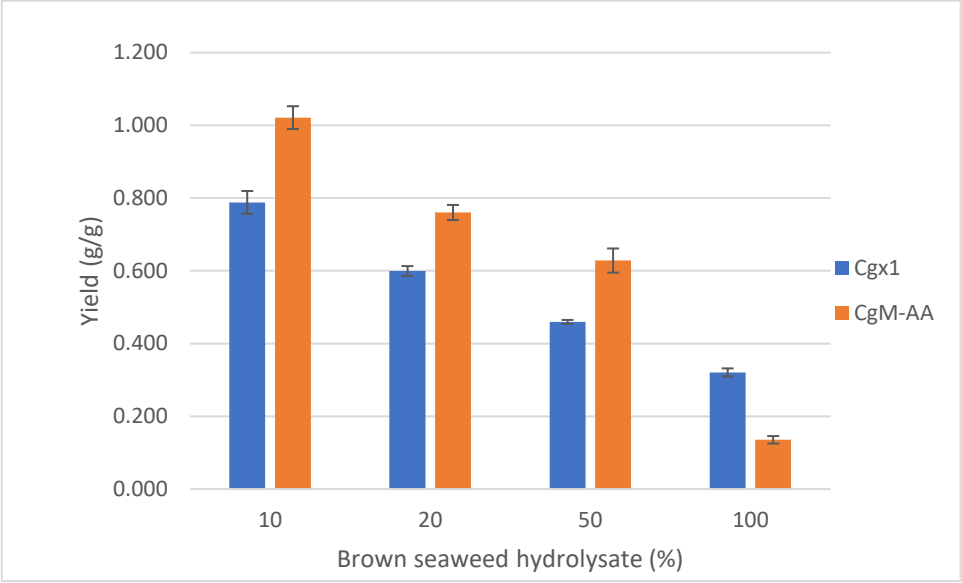

Figure 26: Average yield (g/g) and standard deviations for Cgx1 and CgM-AA cultivated in 10, 20, 50 and 100 % (v/v) BSWH.

Table 19: Concentrations of glucose (g/L) and mannitol (g/L) in seaweed media and in culture media following growth of Cgx1 and CgM-AA in 10, 20, 50 and 100 % (v/v) BSWH. "-" means no glucose could be detected, see Figure A-7 and Figure A-8 in Appendix C. *only one replicate, see Figure A-8 in Appendix C.

	Glucose (g/L)			Mannitol (g/L)		
BSWH (%)	**Medium**	**Cgx1**	**CgM-AA**	**Medium**	**Cgx1**	**CgM-AA**
10.00	0.95	0.00	0.00	1.24	1.11 ± 0.00	0.00
20.00	1.63	0.00	0.00	2.66	2.37 ± 0.04	0.00
50.00	8.38	-	-	6.56	6.48 ± 0.04	0.00
100.00	12.10	-	9.95*	10.53	13.19 ± 0.11	10.94 ± 0.62

3.4 Utilization of laminarin by *C. glutamicum*

In order to enable the utilization of laminarin in *C. glutamicum*, several approaches were attempted using the same laminarinase gene (*lamFc)* from *F. commune*. In the first approach, a native secretory signal peptide (SP) from *C. glutamicum*, specifically from a uncharacterized receptor gene *cgl1577*, was cloned with and without a display signal. The display signal should have enabled the display of the laminarinase enzyme on the cell surface. Using this design, three plasmid vectors would be designed using the pVWEx6 vector, one with only the *lamFc* gene, one with the gene plus the SP, and finally one containing the display signal as well as the gene and the SP, or pVWEx6-*LamFc*, pVWEx6-*LamFc-SP* and pVWEx6-*LamFc-SPD*, respectively. Several rounds of colony PCR of *E. coli* transformed with each of the plasmids (see section 2.2.8 and 2.2.9) yielded no positive transformants for either of the three plasmids. No bands appeared at all for the plasmids pVWEx6-*LamFc-SP* and pVWEx6-*LamFc-SPD*, while bands that were higher (above 1000 bp) than the expected fragment size (800 bp) appeared for pVWEx6-*LamFc*. Due to time limitations in the project, this approach was not pursued further.

Analysis of the *lamFc* gene with the online resource SignalP 5.0 lead to the discovery of a secretory signal, see Figure A-9 in Appendix E.[89] This existence of this secretory signal lead to another approach, where the *lamFc* gene was cloned into a pVWEx1 vector and transformed into wildtype *C. glutamicum*, yielding the strain CgLam. See Table 4 for more information regarding strains.

3.4.1 Results

The laminarin utilizing strain CgLam and the control, Cgx1, were cultivated in CgXII minimal media with 1 % (w/v) glucose and 1 % (w/v) laminarin, respectively, in a BioLector. At 21 hours, 0.1 % (w/v) glucose was added to the wells containing laminarin to check if CgLam could utilize laminarin following utilization of glucose. A summary of average growth rates (h^{-1}), biomass accumulation (g/L) and biomass yield (g/g) can be found in Table 20. CgLam achieved a growth rate of 0.22 ± 0.01 h^{-1} in medium containing glucose. No growth could be observed for Cgx1 or CgLam with laminarin as sole carbon source. Figure 27 shows the average growth curves for Cgx1 and CgLam in glucose and in laminarin, respectively, for 36 hours. A transient growth phase could be observed for CgLam cultivated in laminarin medium following glucose addition, between 21 to 30 hours.

Table 20: Average growth rate (h^{-1}), biomass (g/L) and biomass yield (g/g) with standard deviations for Cgx1 and CgLam cultivated in minimal CgXII medium with 1 % (w/v) glucose and 1 % (w/v) laminarin, respectively. Growth rates for replicates in laminarin after the addition of glucose are not included.

Carbon source	Strain	Growth rate (h^{-1})	Biomass (g/L)	Yield (g/g)
Glucose				
	Cgx1	0.18 ± 0.00	4.27 ± 0.06	0.43 ± 0.01
	CgLam	0.22 ± 0.01	4.29 ± 0.34	0.43 ± 0.03
Laminarin				
	Cgx1	0.00	0.00	0.00
	CgLam	0.00	0.00	0.00

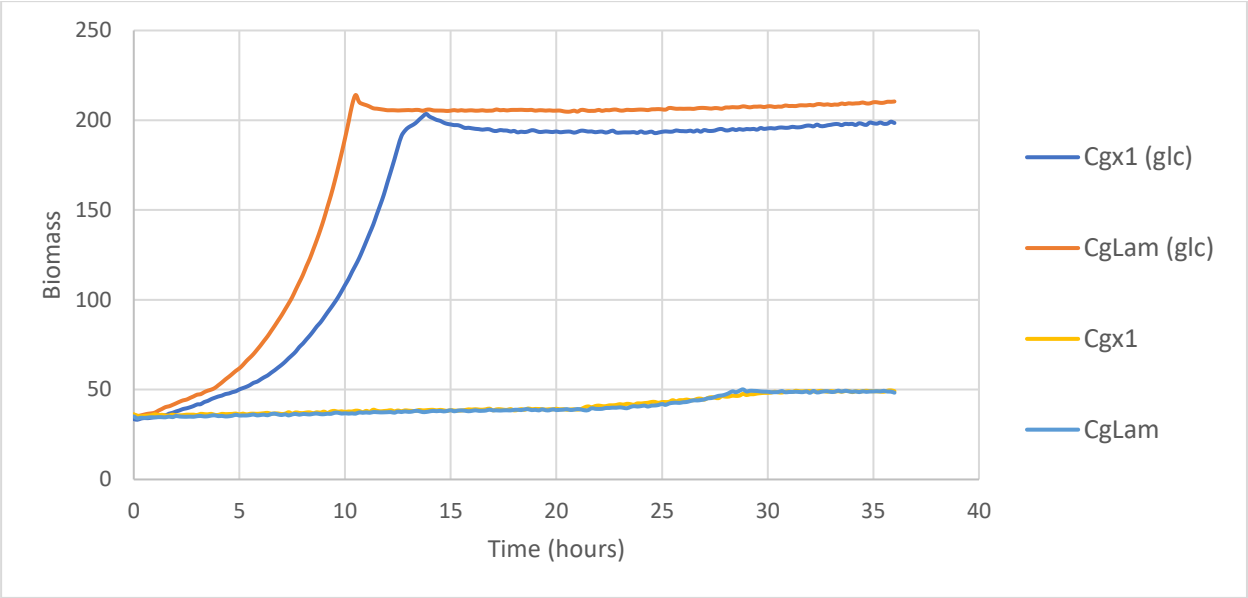

Figure 27: Average growth curves for Cgx1 and CgLam cultivated in CgXII minimal media with 1 % (w/v) glucose and 1 % (w/v) laminarin, respectively. 0.1 % (w/v) glucose was added to wells containing laminarin at 21 hours. Standard deviations are not shown. Glucose media are marked with (glc) (blue and orange), laminarin media are unmarked (yellow and light blue).

4 Discussion

Sustainable alternatives to glucose-based industry-scale microbial bioprocesses are being researched intensively, and include residual biomass or waste from agricultural crops, wood, or wastewater.[90] Seaweed has potential as an additional sustainable feedstock due to high concentrations of sugars and has already been exploited for the microbial production of lactic acid and lovastatin, a drug used for reducing cholesterol levels.[91, 92] The brown seaweed *L. hyperborea* contains high levels of laminarin, composed of glucose and mannitol, while red dulse contains high levels of galactose.[16, 17] These carbohydrates were exploited as non-native carbon sources for *C. glutamicum* in this work to enable efficient growth in seaweed-based media.

In this work the growth of *C. glutamicum* on galactose as sole carbon source was demonstrated. All strains containing the galactose utilizing operon *galMKTE* from *E. coli* grew and accumulated biomass, as shown in Table 5. Galactose utilization has been demonstrated before in *C. glutamicum* with genes from *L. cremoris,* but achieved lower biomass accumulation than in this work.[93] Unexpectedly, the strain CgG which contained only the *galMKTE* operon and no galactose importer grew at comparable rates to CgG-AG and CgG-TG in minimal medium with galactose. The control strain Cgx1 did not grow at all. These results indicate that the introduction of the operon *galMKTE* from *E. coli* enables *C. glutamicum* to metabolize galactose, and that there must be some native mechanism for galactose uptake.

Of all the galactose utilizing strains, CgG-TG was determined to be the best-performer with the highest growth rate at 0.34 ± 0.01 h^{-1} in minimal medium with 1 % (w/v) glucose. This growth rate was almost as high as for Cgx1 cultivated in minimal CgXII medium with 2 % (w/v) glucose, which in a publication by Pérez-García et al. yielded a growth rate of 0.37 ± 0.00 h^{-1}.[75] This demonstrates that galactose can be an efficient carbon source for the cultivation of *C. glutamicum*. The high growth rate for CgG-TG might indicate that low expression of the membrane protein GalP was advantageous for cultivation in medium containing galactose. This coincides with trends observed for the overexpression of membrane proteins in bacteria such as *E. coli*, which may have a negative impact on growth.[94] However, the strain CgG-AA had the second highest growth rate despite having the highest translational initiation rate for GalP, indicating that high expression levels of GalP did not severely affect growth in *C. glutamicum*.

In the proof-of-concept experiment for galactose utilization, 0.1 mM IPTG was used instead of the standard 1 mM used elsewhere in this project. A concentration of 0.1 mM IPTG provides sufficient induction of the vector pVWEx1 as seen in this experiment, and as previously demonstrated by Pérez-García et al.[75]

It has been demonstrated in this work that introduction of the *galMKTE* operon alone enables *C. glutamicum* to grow with galactose as the sole carbon source in CgXII minimal medium, as seen for CgGΔ in Table 7. This means that the symporter encoded by the *galP* gene was not necessary for galactose to enter the cells, and that there must be some uncharacterized native system in place to import galactose into *C.* glutamicum. As the only difference between the two strains CgGΔ and CgG was that the PTS systems for glucose and fructose were deleted in CgGΔ, either PTS^G or PTS^F must be the main pathway for

native galactose uptake in *C. glutamicum*. The two systems were investigated as candidates for native galactose import, with PTG^G being the most likely option. This is due to the structural similarity between glucose and galactose, as shown in Figure 3. Galactose is the C-4 epimer of glucose and their structures are consequently very similar. Fructose, on the other hand, is a ketohexose rather than an aldohexose and a larger shift in conformation of the transporter protein would be required for it to import both fructose and galactose. In other words, the PTS^F would have to be much less specific than the PTS^G for it to import galactose.

Two strains of CgGΔ with reintroduced PTS^G and PTS^F, respectively, were underway but were not finished in time to be included in this work due to time constraints. By cultivating these strains in minimal medium with galactose as the only carbon source, this line of investigation could be resolved and the PTS responsible for galactose import in *C. glutamicum* could finally be uncovered.

Minimal media utilized for the cultivation of galactose utilizing strains and deletion strains contained 1 % (w/v), or 10 g/L, of galactose. The HPLC method used detected only 3.8 g/L and 3.6 g/L of galactose in the media prior to inoculation, as seen in Table 6 and Table 8. However, strains CgG-AA, CgG-TG and CgG-TGΔ had a final biomass of 4-5 g/L, which was as expected for *C. glutamicum* cultivated in media with 1 % hexose according to results in this project and from a publication by Pérez-García et al. using the same growth conditions.[21] This indicates issues with the galactose standards rather than the media. Indeed, only three out of five galactose standards were used for quantification calculations in these experiments due to split peaks, see Figure A-1 in Appendix C. Despite these issues, the HPLC analysis did provide relative quantification of galactose, which in this case was sufficient to prove that galactose was utilized by CgG, CgG-AA, CgG-AG, CgG-TA and CgG-TG. The relative quantification was also sufficient to show that the concentration of galactose in the culture medium from CgG-TGΔ was too low to be detected, as shown in Figure A-3 in Appendix C, but was present at high levels in culture media for Cgx1Δ and CgGΔ, see Table 8. A more sensitive HPLC method was used for subsequent quantification of galactose in this project, see section 2.5.2.

Cultivation of the best-performing galactose utilizing strain, CgG-TG, in different concentrations of red seaweed hydrolysate established 50 % (v/v) RSWH as the superior condition in terms of growth rate, biomass and biomass yield, see Figure 13, Figure 14 and Figure 15. In addition, issues with detecting glucose or galactose in 100 % (v/v) RSWH, in combination with lower yield for CgG-TG in this concentration, might indicate that not all available carbon sources in the medium were utilized. As a result, 50 % RSWH medium was chosen for upscaling in fermenters. This conclusion is consistent with trends observed for *C. glutamicum* cultivated in brown seaweed based media in another publication, where 100 % (v/v) BSWH media provided lower or similar growth rates than 80 % (v/v) brown seaweed extract or hydrolysate, respectively.[21] The decrease in growth rates might be due to growth inhibitors such as furfural in the RSWH media due to the degradation of xylose, but concentrations of growth inhibitors were not measured in this work. Higher growth rates for CgG-TG in 10, 20 and 50 % RSWH compared to Cgx1, and higher biomass accumulation and biomass yield in all conditions, clearly show the advantage of galactose utilization for the cultivation of *C. glutamicum* in complex medium.

In this work, the strain CgG-Rib achieved riboflavin production in CgXII minimal medium with galactose as the only carbon source, at a concentration of 456.54 ± 13.83 mg/L. This was similar to the riboflavin titer achieved with mannitol as sole carbon source for a

mannitol utilizing *C. glutamicum* strain containing the same plasmid vector for riboflavin production, at 467.3 ± 45.7 mg/L.[21] This indicates that galactose is as efficient for riboflavin production as mannitol, another six-carbon non-native carbon source for *C. glutamicum*. These results also indicate that overexpressing *ribGCAH* yields more efficient riboflavin production than overexpressing the gene *sigH* which encodes a sigma factor usually involved in stress response to heat, pH and oxidative stress.[95, 96] In a publication by Taniguchi and Wendisch, overexpressing *sigH* yielded low titers of riboflavin.[95]

The riboflavin titer achieved in this work was higher than that of another *C. glutamicum* strain overproducing riboflavin by overexpression of *ribGCAH*, which achieved 238.5 mg/L in medium containing 10 % (w/v) glucose supplemented with soy bean extract and corn steep solids.[97] This strain also overproduced L-lysine, which depends on the NADPH produced from the pentose-phosphate pathway and thus may have shunted resources away from riboflavin production for this strain.[97, 98] A recombinant *B. subtilis* strain achieved a titer of 7.9 g/L of riboflavin when cultivated in medium containing glucose and yeast in flasks.[99] This titer was much higher than for CgG-Rib in galactose, but was achieved with native and less sustainable carbon sources. Further optimization is required to compete with industrial producers of riboflavin. However, in this work the viability and efficiency of galactose as a competitive carbon source for the overproduction of riboflavin in *C. glutamicum* was demonstrated.

Overproduction of riboflavin was also achieved for CgG-Rib cultivated in medium containing 50 % (v/v) RSWH as carbon source, with a titer of 388.65 ± 27.50 mg/L. This was lower than for CgG-Rib in glucose (1 % (w/v)) medium, in which a titer of 525.35 ± 34.33 mg/L was achieved. The titer achieved for CgG-Rib in flasks in RSWH based medium was 33 % lower than a *C. glutamicum* mannitol utilizing strain cultivated in BSWH (80 % (v/v)), which achieved 606.8 ± 69.7 mg/L.[21] Despite suboptimal titers of riboflavin compared to cultivation in another hexose-rich seaweed medium, the feasibility of using RSWH as carbon source for the overproduction of riboflavin in *C. glutamicum* was proven here. HPLC analysis showed that low concentrations glucose and galactose were detected in the 50 % RSWH medium, see Table 14. This may explain low riboflavin yield for CgG-Rib cultivated in this medium in the BioLector. In addition, no growth could be observed for CgG-Rib in 1 % (w/v) galactose in the BioLector, despite having been successfully cultivated in the exact same conditions in flasks. HPLC analysis confirmed the presence of 8-10 g/L of galactose in the medium prior to inoculation in the BioLector. This indicates that cultivation in the BioLector yields suboptimal conditions compared to flask experiments, making them difficult to compare.

Upscaling the production of riboflavin to lab-scale fermenters in media containing 50 % (v/v) RSWH yielded more promising results in terms of riboflavin production than experiments conducted in flasks or in a BioLector. Riboflavin production followed a linear trend in these processes, increasing at every time point. The final titer of 1,139.4 ± 58.6 mg/L was similar to the riboflavin titer achieved in brown seaweed hydrolysate medium by a mannitol utilizing *C. glutamicum* strain also overexpressing *ribGCAH*, at 1,108.9 mg/L.[21] Dynamic co-cultivation of two *C. glutamicum* strains overexpressing genes for xylose and enhanced mannose utilization, respectively, as well as overexpression of *sigH* for riboflavin production in both, yielded a titer of 27 mg/L.[100] These strains were cultivated in equal amounts of xylose, mannose and glucose, which are carbon sources commonly found in spent sulphite liquor from processing of lignocellulosic material.[100, 101] Although this was achieved in a sugar mixture found in sustainable feedstock, these results again indicate the advantage of overexpressing *ribGCAH* rather than *sigH* to achieve high titers of

riboflavin. Engineered strains of the common industrial producer of riboflavin, *B. subtilis*, can produce riboflavin in concentrations of 9.4 g/L when cultivated in 40 g/L glucose supplemented with yeast extract (5 g/L) for 48 hours.[102] This fermentations in this work proved the efficiency of RSWH as feed for lab-scale production of riboflavin by *C. glutamicum*, and its potential as feedstock in large-scale process, although optimization is needed to compete with industrial producers of riboflavin.

Figure 16 shows that both glucose and galactose were completely depleted in both fermenters as the exponential phase terminated at 14 hours. Galactose (red) was depleted more rapidly than glucose (blue), indicating that galactose was an efficient carbon source in this process. In addition, it confirms that glucose and galactose can be utilized simultaneously by *C. glutamicum* as was expected due to its lack of a complex catabolite repression system, see section 1.3. Riboflavin concentrations in samples taken after 26 hours in the fermentation processes were amended by using an experimentally devised conversion factor. This means that the titer, yield and volumetric productivity may deviate from reality. However, the values are similar to those achieved in BSWH by Pérez-García et al., indicating that they are within the range of the actual riboflavin levels in the fermenters at the end of the processes.[21]

For experiments conducted with strains that should have produced biliverdin, CgHO and CgG-HO, and phycocyanobilin, CgPCB and CgG-PCB, high growth rates were achieved compared to the controls Cgx3 and CgGx3, see Table 16 and Table 17. This was unexpected as the producer strains contain genes for the overproduction of biliverdin and PCB from heme, and as a result should have higher metabolic burdens. However, no green or blue colour could be observed in pellets or supernatants from culture media after cultivation of these strains with glucose or galactose as sole carbon source. In *C. glutamicum* there is a hypothetical protein which is orthologous to the heme oxygenase protein from *Synechocystis* sp. according to the Kyoto Encyclopedia of Genes and Genomes (KEGG) database.[103] Studies have shown that this gene, *hmuO,* is involved in heme utilization in *C. glutamicum* in iron-limiting conditions and converts heme to α-biliverdin.[104, 105] Overexpressing the gene encoding HmuO might lead to production of perceptible levels of biliverdin, and would circumvent the need for iron limiting conditions to achieve heme utilization. However, heme is strictly regulated in *C. glutamicum* and the intracellular concentration is continuously monitored due to the toxic effects of high intracellular concentrations of iron.[104] Above a certain threshold, a heme export system encoded by the operon *hrtBA* will be upregulated.[104] Induction of producer mutants with IPTG in precultures and supplementing the culture media with heme might increase biliverdin production, although a balance must be found to avoid excessive export of heme. Due to time constraints, further experiments could not be conducted for this thesis project. It is possible that further optimization can yield perceptible PCB production in *C. glutamicum*, as it has previously been achieved in *E. coli* using the same genes from *Synechococcus* sp., but it was not achieved in this work.[106]

The growth rates achieved for mannitol utilizing strains in 1 % (w/v) mannitol minimal medium in this work, at 0.25 ± 0.02 h^{-1} for CgM-AA, were twice as high as those of a strain containing the same genes cultivated in the same conditions published by Pérez-García et al.[21] The difference between these strains was that two expression vectors were used by Pérez-García et al. to express *mtlD* and *mtlAF,* respectively, rather than expressing both genes in one vector as was performed in this work.[21] Clearly, using only one expression vector provided an advantage in terms on growth rate and biomass accumulation, indicating that placing the genes *mtlDAF* under the control of the same promoter made the

pathway more efficient in *C. glutamicum*. This makes sense considering that the three genes are regulated by the same promoter natively in *B. subtilis,* where the expression of these genes is already optimally balanced.[107] However, the utilization of mannitol as sole carbon source has been demonstrated following utilization of arabitol by a restriction deficient *C. glutamicum* strain.[45] In the same publication, deletion of the regulator gene *atlR* in the same strain yielded a growth rate of 0.35 ± 0.04 h^{-1} with mannitol as sole carbon source.[45] Exploiting the native machinery for mannitol utilization in *C. glutamicum* seems to yield more efficient utilization of mannitol in minimal medium than using non-native genes. Regardless, the growth rates achieved in this work further supports the efficiency of mannitol as a carbon source for the cultivation of *C. glutamicum*.

Varying translational initiation rates for *mtlAF* gene products in mannitol utilizing strains yielded no difference in fitness when cultivated in minimal media with mannitol as sole carbon source. In addition, an optimal condition for upscaling could not be identified when strains were cultivated in four different concentrations of IPTG. Growth rates, biomass and biomass yields were similar between all strains in all conditions. In the BioLector experiments conducted with the mannitol utilizing strains in this work, a concentration of 0.2 % (w/v) mannitol was used. This is in the range of what has been tested before, as 0.25 % (w/v) mannitol has been shown to provide growth for several mannitol utilizing strains in previous publications.[21, 108] The IPTG concentrations varied from 0.1 mM to 0.7 mM, which have been shown to sufficiently induce the plasmid vector pVWEx1 in another publication.[21] However, the lack of observable differences in performance between mannitol utilizing strains in these concentrations might indicate that the differences in induction is small.

The two BioLector experiments conducted for the mannitol utilizing strains in varying concentrations of IPTG as described in section 3.3.1 yielded different growth rates despite identical conditions in each experiment. This indicates that cultivation in BioLector yields varying conditions, leading to discrepancies in growth rates in identical conditions, see Figure 19 for IPTG concentrations 0.2 and 0.4 mM, compared to 0.1 and 0.7 mM. When replicates were cultivated in the same plate, there was no such difference in growth rates, see Figure 22. On the other hand, HPLC analyses showed that all mannitol was utilized in the media, see Figure 21, which indicates that conditions were sufficiently optimized to allow efficient carbon source utilization and growth of *C. glutamicum*.

The strain CgM-AA, which achieved the highest growth rate in flask and BioLector experiments, was chosen for the flask experiment conducted to obtain a conversion factor. The IPTG concentration chosen for this experiment was 0.2 mM due to the highest growth rate being achieved in this condition in the BioLector experiment. However, the difference in strain performance between the four IPTG concentrations were so small that when CgM-AA was selected for cultivation in BSWH, no preference was taken and IPTG was added according to the standard recipe (1 mM).

For the cultivation of Cgx1 and CgM-AA in varying concentrations of BSWH, it could be observed that it was clearly an advantage in terms of biomass accumulation and yield for *C. glutamicum* to be able to consume non-native carbon sources, see Figure 24. However, the low growth rates observed for CgM-AA in 100 % (v/v) BSWH indicates that the strain struggled. This is also evident from the lack of mannitol utilization and the low amount of accumulated biomass in 100 % (v/v) BSWH for this strain, see Table 19 and Figure 25. This could be due to growth inhibitors such as furfural, which has been shown to be present in BSWH at a concentration of 0.42 ± 0.04 mM.[21] However, *C. glutamicum* should be able

to detoxify furfural up to concentrations as high as 20 mM.[25] Furfural might have a larger effect on CgM-AA in large concentrations such as in 100 % BSWH than on Cgx1 due to CgM-AA being under more metabolic stress initially, but the effect of growth inhibitors was not studied in this work. More investigation is required to ascertain what causes the decreased carbohydrate utilization for CgM-AA in 100 % BSWH.

A strain containing the same genes as CgM-AA, i.e. the PTS^M from *B. subtilis*, has been cultivated in the same BSWH in a publication by Pérez-García et al.[21] In this publication, all growth rates in a range of concentrations from 10 to 100 % (v/v) BSWH were below 0.10 h^{-1}.[21] Higher growth rates were achieved in this work by CgM-AA, which achieved growth rates surpassing 0.10 h^{-1} in all conditions, with the highest one achieved at 0.15 ± 0.00 h^{-1} in 50 % (v/v) BSWH, see Figure 24. This represented a marked improvement in mannitol utilization in complex media for *C. glutamicum* and reinforces mannitol as an efficient carbon source for the cultivation of this bacterium. The next step in this subproject would be coupling mannitol utilization with the production of added-value products, and up-scaling to cultivation in 50 % (v/v) BSWH in lab-scale fermenters.

The brown seaweed species used in this work, *L. hyperborea*, contains up to 65 % carbohydrates of the biomass dry weight, the major compounds being alginate, mannitol, cellulose and laminarin.[16] This is similar to the amount of carbohydrates in lignocellulosic biomass such as corn stover, at 67-90 % of dry weight, composed of cellulose, hemicellulose and lignin.[109] The red seaweed *P. palmata* contains around 47 % carbohydrates from dry weight, the major components being carrageenan and agar.[19] Breakdown of these carbohydrates by microbes represents a major advantage in the effort towards sustainability by enabling utilization of sustainable microbial feedstocks. In this regard there is added benefit from utilizing seaweed, which does not require any fresh water or arable land for cultivation.

Cultivation of CgLam in media with glucose and laminarin as sole carbon sources, respectively, indicated that while CgLam was fit, it did not grow in media with laminarin as sole carbon source. This indicates that the laminarase did not work as expected to break down laminarin into glucose that *C. glutamicum* could utilize, or that the laminarinase was not excreted as was predicted *in silico*. Either way, further investigation is required to enable laminarin utilization in *C. glutamicum*. Testing other laminarinase genes from other species, such as the flavobacterium *Formosa agariphila*, whose endo-β-1,3-glucanase has been demonstrated to successfully break down laminarin into glucose and oligomers, could be an alternative approach.[110] Adding excretion signals in the form of signal peptides native to *C. glutamicum*, as was attempted in this work, could also be a viable strategy despite its failure in this work at the stage of cloning. Optimization of the existing strain CgLam could also be feasible, although the addition of 0.1 % (w/v) glucose did not initiate laminarinase activity in this work, see Figure 27. This indicates that growth in another substrate prior or in parallel to growth in laminarin does not aid in optimization in this instance. As the brown seaweed *L. hyperborea* can consist of up to 25 % laminarin in dry weight in the summertime, utilization of laminarin by industrially important bacteria such as *C. glutamicum* remains an interesting topic of research to move towards more sustainable feedstock in this industry.[16]

It has been suggested that β-1,6-linkages have inhibitory effects towards binding of the *F. commune* laminarinase to β-1,3-linkages, which could explain a very low yield of glucose monomers.[52] On the other hand, this cannot explain the absence of growth at all in CgLam in minimal medium with laminarin as sole carbon source. The laminarin used in this work

was purchased from Thermo Scientific and the ratio of linkages were not known or not provided, and as a result no conclusion can be drawn about the potential efficiency of the laminarinase enzyme. On the other hand, a BioLector experiment conducted for CgG-Rib, see section 3.2.4, yielded no growth for this strain with galactose as sole carbon source despite galactose utilization being achieved in flask experiments using the same conditions. Suboptimal conditions in the BioLector could be a factor in this case, but due to the high price of pure laminarin upscaling to flasks was not desirable until a proof of concept could be achieved on a smaller scale. Evidently, more investigation is required to achieve laminarin utilization in *C. glutamicum*.

5 Summary

In this work *C. glutamicum* was successfully engineered to utilize the non-native, seaweed derived carbon sources mannitol and galactose, but utilization of laminarin was not achieved. Growth on laminarin requires further optimization, and in this work no conclusion could be drawn on the feasibility of laminarin degradation by laminarinase excretion in *C. glutamicum*. Mannitol and galactose utilizing strains were successfully cultivated in media with BSWH and RSWH, respectively. A native import system for galactose in *C. glutamicum* was investigated and given the similarity of glucose and galactose it is likely that PTS^G is responsible, but it has not been proven in this work. Production of riboflavin was achieved with galactose as sole carbon source and in medium with 50 % (v/v) RSWH. Riboflavin was produced in fermenters with RSWH-based media, with final titer, yield and volumetric productivity of 1139.4 ± 58.6 mg/L, 106.2 ± 5.5 mg/g and 25.3 ± 1.3 mg/L h, respectively. The production of PCB could not be achieved with glucose or galactose as sole carbon sources in this work, but it is possible that further optimization could yield perceptible PCB production in *C. glutamicum*. Overall, cultivation of *C. glutamicum* on seaweed derived hydrolysates, either red or brown, has potential for the future of industrial microbial processes and for production of added-value compounds such as riboflavin.

Literature

1. Zhang, C., et al., *Microbial Utilization of Next-Generation Feedstocks for the Biomanufacturing of Value-Added Chemicals and Food Ingredients.* Front Bioeng Biotechnol, 2022. **10**: p. 874612.
2. Zahoor, A., S.N. Lindner, and V.F. Wendisch, *Metabolic engineering of Corynebacterium glutamicum aimed at alternative carbon sources and new products.* Comput Struct Biotechnol J, 2012. **3**: p. e201210004.
3. Martínez-Gómez, K., et al., *New insights into Escherichia coli metabolism: carbon scavenging, acetate metabolism and carbon recycling responses during growth on glycerol.* Microbial Cell Factories, 2012. **11**(1): p. 46.
4. Meyer, F.M., et al., *Malate-mediated carbon catabolite repression in Bacillus subtilis involves the HPrK/CcpA pathway.* J Bacteriol, 2011. **193**(24): p. 6939-49.
5. Eggeling, L. and M. Bott, *Handbook of Corynebacterium glutamicum*. 2005: CRC press.
6. FAO, *State of World Fisheries and Aquaculture 2016 (russian)*. 2016: Food & Agriculture Org.
7. Eggertsen, M. and C. Halling, *Knowledge gaps and management recommendations for future paths of sustainable seaweed farming in the Western Indian Ocean.* Ambio, 2021. **50**(1): p. 60-73.
8. Buschmann, A.H., et al., *Seaweed production: overview of the global state of exploitation, farming and emerging research activity.* European Journal of Phycology, 2017. **52**(4): p. 391-406.
9. Kain, J.M., *Populations of Laminaria hyperborea at various latitudes.* Helgoländer Wissenschaftliche Meeresuntersuchungen, 1967. **15**(1): p. 489-499.
10. Rinde, E. and K. Sjøtun, *Demographic variation in the kelp Laminaria hyperborea along a latitudinal gradient.* Marine Biology, 2005. **146**(6): p. 1051-1062.
11. Vea, J. and E. Ask, *Creating a sustainable commercial harvest of Laminaria hyperborea, in Norway.* Journal of Applied Phycology, 2011. **23**: p. 489-494.
12. Grote, B., *Recent developments in aquaculture of Palmaria palmata (Linnaeus) (Weber & Mohr 1805): cultivation and uses.* Reviews in Aquaculture, 2019. **11**(1): p. 25-41.
13. Mouritsen, O.G., et al., *On the human consumption of the red seaweed dulse (Palmaria palmata (L.) Weber & Mohr).* Journal of Applied Phycology, 2013. **25**(6): p. 1777-1791.
14. Martínez, B., et al., *Open sea cultivation of Palmaria palmata (Rhodophyta) on the northern Spanish coast.* Aquaculture, 2006. **254**(1): p. 376-387.
15. Le Gall, L., S. Pien, and A.-M. Rusig, *Cultivation of Palmaria palmata (Palmariales, Rhodophyta) from isolated spores in semi-controlled conditions.* Aquaculture, 2004. **229**(1): p. 181-191.
16. Schiener, P., et al., *The seasonal variation in the chemical composition of the kelp species Laminaria digitata, Laminaria hyperborea, Saccharina latissima and Alaria esculenta.* Journal of Applied Phycology, 2015. **27**(1): p. 363-373.
17. Martínez, B. and J.M. Rico, *CHANGES IN NUTRIENT CONTENT OF PALMARIA PALMATA IN RESPONSE TO VARIABLE LIGHT AND UPWELLING IN NORTHERN SPAIN1.* Journal of Phycology, 2008. **44**(1): p. 50-59.
18. Simon-Colin, C., M.-A. Bessières, and E. Deslandes, *An alternative HPLC method for the quantification of floridoside in salt-stressed cultures of the red alga Grateloupia doryphora.* Journal of Applied Phycology, 2002. **14**(2): p. 123-127.
19. Mutripah, S., et al., *Bioethanol production from the hydrolysate of Palmaria palmata using sulfuric acid and fermentation with brewer's yeast.* Journal of Applied Phycology, 2014. **26**(1): p. 687-693.

20. Gallagher, J.A., et al., *Bio-processing of macroalgae Palmaria palmata: metabolite fractionation from pressed fresh material and ensiling considerations for long-term storage.* J Appl Phycol, 2021. **33**(1): p. 533-544.
21. Pérez-García, F., et al., *From Brown Seaweed to a Sustainable Microbial Feedstock for the Production of Riboflavin.* Front Bioeng Biotechnol, 2022. **10**: p. 863690.
22. Tongtummachat, T., A. Jaree, and N. Akkarawatkhoosith, *Continuous hydrothermal furfural production from xylose in a microreactor with dual-acid catalysts.* RSC Adv, 2022. **12**(36): p. 23366-23378.
23. Cheng, H., et al., *Xylitol production from xylose mother liquor: a novel strategy that combines the use of recombinant Bacillus subtilis and Candida maltosa.* Microb Cell Fact, 2011. **10**: p. 5.
24. Zaldivar, J., A. Martinez, and L.O. Ingram, *Effect of selected aldehydes on the growth and fermentation of ethanologenic Escherichia coli.* Biotechnology and Bioengineering, 1999. **65**(1): p. 24-33.
25. Tsuge, Y., et al., *Detoxification of furfural in Corynebacterium glutamicum under aerobic and anaerobic conditions.* Applied Microbiology and Biotechnology, 2014. **98**(20): p. 8675-8683.
26. Zhang, Q., X. Zhou, and Y. Xu, *Xylooligosaccharides Production from Xylan Hydrolysis Using Recyclable Strong Acidic Cationic Exchange Resin as Solid Acid Catalyst.* Applied Biochemistry and Biotechnology, 2022. **194**(8): p. 3609-3620.
27. Kinoshita, S., S. Udaka, and M. Shimono, *Studies on the amino acid fermentation. Part 1. Production of L-glutamic acid by various microorganisms.* J Gen Appl Microbiol, 2004. **50**(6): p. 331-43.
28. Collins, M., *Genus Corynebacterium.* Bergey's manual of systematic bacteriology, 1986. **2**: p. 1266-1276.
29. Lee, J.Y., et al., *The Actinobacterium Corynebacterium glutamicum, an Industrial Workhorse.* J Microbiol Biotechnol, 2016. **26**(5): p. 807-22.
30. Yukawa, H., et al., *Comparative analysis of the Corynebacterium glutamicum group and complete genome sequence of strain R.* Microbiology, 2007. **153**(4): p. 1042-1058.
31. Kalinowski, J., et al., *The complete Corynebacterium glutamicum ATCC 13032 genome sequence and its impact on the production of l-aspartate-derived amino acids and vitamins.* Journal of Biotechnology, 2003. **104**(1): p. 5-25.
32. Vallino, J.J. and G. Stephanopoulos, *Metabolic flux distributions in Corynebacterium glutamicum during growth and lysine overproduction.* Biotechnology and Bioengineering, 1993. **41**(6): p. 633-646.
33. Hirasawa, T. and M. Wachi, *Glutamate Fermentation-2: Mechanism of l-Glutamate Overproduction in Corynebacterium glutamicum*, in *Amino Acid Fermentation*, A. Yokota and M. Ikeda, Editors. 2017, Springer Japan: Tokyo. p. 57-72.
34. Blombach, B. and G.M. Seibold, *Carbohydrate metabolism in Corynebacterium glutamicum and applications for the metabolic engineering of l-lysine production strains.* Applied Microbiology and Biotechnology, 2010. **86**(5): p. 1313-1322.
35. Ruan, H., H. Yu, and J. Xu, *The glucose uptake systems in Corynebacterium glutamicum: a review.* World Journal of Microbiology and Biotechnology, 2020. **36**(9): p. 126.
36. Moon, M.W., et al., *The Phosphotransferase System of Corynebacterium glutamicum: Features of Sugar Transport and Carbon Regulation.* Microbial Physiology, 2007. **12**(1-2): p. 43-50.
37. Kanehisa, M., et al., *KEGG for taxonomy-based analysis of pathways and genomes.* Nucleic Acids Res, 2023. **51**(D1): p. D587-d592.
38. Kanehisa, M. and S. Goto, *KEGG: kyoto encyclopedia of genes and genomes.* Nucleic Acids Res, 2000. **28**(1): p. 27-30.
39. Moon, M.-W., et al., *Analyses of enzyme II gene mutants for sugar transport and heterologous expression of fructokinase gene in Corynebacterium glutamicum ATCC 13032.* FEMS Microbiology Letters, 2005. **244**(2): p. 259-266.

40. Brabetz, W., W. Liebl, and K.H. Schleifer, *Studies on the utilization of lactose by Corynebacterium glutamicum, bearing the lactose operon of Escherichia coli.* Archives of Microbiology, 1991. **155**(6): p. 607-612.
41. Weickert, M.J. and S. Adhya, *The galactose regulon of Escherichia coli.* Molecular Microbiology, 1993. **10**(2): p. 245-251.
42. Grossiord, B.P., et al., *Characterization, expression, and mutation of the Lactococcus lactis galPMKTE genes, involved in galactose utilization via the Leloir pathway.* J Bacteriol, 2003. **185**(3): p. 870-8.
43. Riley, M., et al., *Escherichia coli K-12: a cooperatively developed annotation snapshot--2005.* Nucleic Acids Res, 2006. **34**(1): p. 1-9.
44. Varzakas, T., *Sweeteners: Nutritional Aspects, Applications, and Production Technology*. 2012.
45. Laslo, T., et al., *Arabitol metabolism of Corynebacterium glutamicum and its regulation by AtlR.* J Bacteriol, 2012. **194**(5): p. 941-55.
46. Borriss, R., et al., *Bacillus subtilis, the model Gram-positive bacterium: 20 years of annotation refinement.* Microb Biotechnol, 2018. **11**(1): p. 3-17.
47. Dominguez, H. and N.D. Lindley, *Complete Sucrose Metabolism Requires Fructose Phosphotransferase Activity in Corynebacterium glutamicum To Ensure Phosphorylation of Liberated Fructose.* Appl Environ Microbiol, 1996. **62**(10): p. 3878-80.
48. Chen, J., et al., *Laminarin, a Major Polysaccharide in Stramenopiles.* Mar Drugs, 2021. **19**(10).
49. Klemm, D., et al., *Cellulose: Fascinating Biopolymer and Sustainable Raw Material.* Angewandte Chemie International Edition, 2005. **44**(22): p. 3358-3393.
50. Qin, F., et al., *Higher order structures of a bioactive, water-soluble (1→3)-β-d-glucan derived from Saccharomyces cerevisiae.* Carbohydrate Polymers, 2013. **92**(2): p. 1026-1032.
51. Graiff, A., et al., *Chemical characterization and quantification of the brown algal storage compound laminarin — A new methodological approach.* Journal of Applied Phycology, 2016. **28**(1): p. 533-543.
52. Qin, H.M., et al., *Laminarinase from Flavobacterium sp. reveals the structural basis of thermostability and substrate specificity.* Sci Rep, 2017. **7**(1): p. 11425.
53. Inoue, A., et al., *Characterization of an alginate lyase, FlAlyA, from Flavobacterium sp. strain UMI-01 and its expression in Escherichia coli.* Mar Drugs, 2014. **12**(8): p. 4693-712.
54. Bull, A.T. and C.G.C. Chesters, *The Biochemistry of Laminarin and the Nature of Laminarinase*, in *Advances in Enzymology and Related Areas of Molecular Biology*. 1966. p. 325-364.
55. Miao, D., et al., *Adapting photosynthesis to the near-infrared: non-covalent binding of phycocyanobilin provides an extreme spectral red-shift to phycobilisome core-membrane linker from Synechococcus sp. PCC7335.* Biochimica et Biophysica Acta (BBA) - Bioenergetics, 2016. **1857**(6): p. 688-694.
56. Newsome, A.G., C.A. Culver, and R.B. van Breemen, *Nature's Palette: The Search for Natural Blue Colorants.* Journal of Agricultural and Food Chemistry, 2014. **62**(28): p. 6498-6511.
57. Roda-Serrat, M.C., et al., *Fast cleavage of phycocyanobilin from phycocyanin for use in food colouring.* Food Chemistry, 2018. **240**: p. 655-661.
58. Koníčková, R., et al., *Anti-cancer effects of blue-green alga Spirulina platensis, a natural source of bilirubin-like tetrapyrrolic compounds.* Annals of Hepatology, 2014. **13**(2): p. 273-283.
59. Romay, C., et al., *Antioxidant and anti-inflammatory properties of C-phycocyanin from blue-green algae.* Inflammation Research, 1998. **47**(1): p. 36-41.
60. Li, Y., *The Bioactivities of Phycocyanobilin from Spirulina.* J Immunol Res, 2022. **2022**: p. 4008991.
61. Friedman, J., et al., *Structural Basis for Novel δ-Regioselective Heme Oxygenation in the Opportunistic Pathogen Pseudomonas aeruginosa.* Biochemistry, 2004. **43**(18): p. 5239-5245.

62. Frankenberg, N., et al., *Functional Genomic Analysis of the HY2 Family of Ferredoxin-Dependent Bilin Reductases from Oxygenic Photosynthetic Organisms.* The Plant Cell, 2001. **13**(4): p. 965-978.
63. Thakur, K., et al., *Riboflavin and health: A review of recent human research.* Critical Reviews in Food Science and Nutrition, 2017. **57**(17): p. 3650-3660.
64. Buehler, B.A., *Vitamin B2: Riboflavin.* Journal of Evidence-Based Complementary & Alternative Medicine, 2011. **16**(2): p. 88-90.
65. Pinto, J.T. and J. Zempleni, *Riboflavin.* Adv Nutr, 2016. **7**(5): p. 973-5.
66. Alam, M.M., S. Iqbal, and I. Naseem, *Ameliorative effect of riboflavin on hyperglycemia, oxidative stress and DNA damage in type-2 diabetic mice: Mechanistic and therapeutic strategies.* Archives of Biochemistry and Biophysics, 2015. **584**: p. 10-19.
67. Sheraz, M.A., et al., *Photo, thermal and chemical degradation of riboflavin.* Beilstein J Org Chem, 2014. **10**: p. 1999-2012.
68. Kanazawa, H., et al., *Symbiotic riboflavin degradation by Microbacterium and Nocardioides bacteria.* Bioscience, Biotechnology, and Biochemistry, 2020. **84**(5): p. 1056-1061.
69. Huang, R., H.J. Kim, and D.B. Min, *Photosensitizing Effect of Riboflavin, Lumiflavin, and Lumichrome on the Generation of Volatiles in Soy Milk.* Journal of Agricultural and Food Chemistry, 2006. **54**(6): p. 2359-2364.
70. Averianova, L.A., et al., *Production of Vitamin B2 (Riboflavin) by Microorganisms: An Overview.* Front Bioeng Biotechnol, 2020. **8**: p. 570828.
71. Schwechheimer, S.K., et al., *Biotechnology of riboflavin.* Applied Microbiology and Biotechnology, 2016. **100**(5): p. 2107-2119.
72. Hanahan, D., *Studies on transformation of Escherichia coli with plasmids.* J Mol Biol, 1983. **166**(4): p. 557-80.
73. Malumbres, M., J. Gil, and J.F. Martín, *Codon preference in Corynebacteria.* Gene, 1993. **134**(1): p. 15-24.
74. Peters-Wendisch, P.G., et al., *Pyruvate carboxylase is a major bottleneck for glutamate and lysine production by Corynebacterium glutamicum.* J Mol Microbiol Biotechnol, 2001. **3**(2): p. 295-300.
75. Pérez-García, F., P. Peters-Wendisch, and V.F. Wendisch, *Engineering Corynebacterium glutamicum for fast production of l-lysine and l-pipecolic acid.* Applied Microbiology and Biotechnology, 2016. **100**(18): p. 8075-8090.
76. Stansen, C., et al., *Characterization of a Corynebacterium glutamicum lactate utilization operon induced during temperature-triggered glutamate production.* Appl Environ Microbiol, 2005. **71**(10): p. 5920-8.
77. Henke, N.A., I. Krahn, and V.F. Wendisch, *Improved Plasmid-Based Inducible and Constitutive Gene Expression in Corynebacterium glutamicum.* Microorganisms, 2021. **9**(1): p. 204.
78. Abe, S., K.-I. Takayama, and S. Kinoshita, *TAXONOMICAL STUDIES ON GLUTAMIC ACID-PRODUCING BACTERIA.* The Journal of General and Applied Microbiology, 1967. **13**(3): p. 279-301.
79. Green, M.R. and J. Sambrook, *Polymerase Chain Reaction.* Cold Spring Harb Protoc, 2019. **2019**(6).
80. Inc., C.L. *CloneAmp™ HiFi PCR Premix Protocol-At-A-Glance*. Available from: https://www.takarabio.com/documents/User%20Manual/CloneAmp%20HiFi%20PCR%20Premix%20Protocol/CloneAmp%20HiFi%20PCR%20Premix%20Protocol-At-A-Glance_092612.pdf.
81. Lee, P.Y., et al., *Agarose gel electrophoresis for the separation of DNA fragments.* J Vis Exp, 2012(62).
82. QIAGEN. *QIAquick PCR Purification Kit and QIAquick PCR & Gel Cleanup Kit Quick-Start Protocol - (EN)*. Available from: https://www.qiagen.com/us/resources/resourcedetail?id=e0fab087-ea52-4c16-b79f-c224bf760c39&lang=en.
83. Gibson, D.G., et al., *Enzymatic assembly of DNA molecules up to several hundred kilobases.* Nature Methods, 2009. **6**(5): p. 343-345.

84. Hanahan, D. and D. Glover, *DNA cloning: a practical approach.* DNA cloning: a practical approach, 1985. **1**: p. 109-135.
85. Promega, *GoTaq G2 DNA Polymerase Product Information*. 2018: https://no.promega.com/-/media/files/resources/protocols/product-information-sheets/g/gotaq-g2-dna-polymerase-protocol.pdf?rev=898d6c55ba2b4af69deda726d7098996&sc_lang=en.
86. Whaley, D., et al., *Cryopreservation: An Overview of Principles and Cell-Specific Considerations.* Cell Transplant, 2021. **30**: p. 963689721999617.
87. Coskun, O., *Separation techniques: Chromatography.* North Clin Istanb, 2016. **3**(2): p. 156-160.
88. Petteys, B.J. and E.L. Frank, *Rapid determination of vitamin B2 (riboflavin) in plasma by HPLC.* Clinica Chimica Acta, 2011. **412**(1): p. 38-43.
89. Almagro Armenteros, J.J., et al., *SignalP 5.0 improves signal peptide predictions using deep neural networks.* Nature Biotechnology, 2019. **37**(4): p. 420-423.
90. Javourez, U., M. O'Donohue, and L. Hamelin, *Waste-to-nutrition: a review of current and emerging conversion pathways.* Biotechnology Advances, 2021. **53**: p. 107857.
91. Xiong, Z., et al., *An overview of the bioactivity of monacolin K / lovastatin.* Food and Chemical Toxicology, 2019. **131**: p. 110585.
92. Suraiya, S., et al., *Influences of fermentation parameters on lovastatin production by Monascus purpureus using Saccharina japonica as solid fermented substrate.* LWT, 2018. **92**: p. 1-9.
93. Barrett, E., et al., *Heterologous expression of lactose- and galactose-utilizing pathways from lactic acid bacteria in Corynebacterium glutamicum for production of lysine in whey.* Appl Environ Microbiol, 2004. **70**(5): p. 2861-6.
94. Wagner, S., et al., *Consequences of Membrane Protein Overexpression in Escherichia coli*.* Molecular & Cellular Proteomics, 2007. **6**(9): p. 1527-1550.
95. Taniguchi, H. and V.F. Wendisch, *Exploring the role of sigma factor gene expression on production by Corynebacterium glutamicum: sigma factor H and FMN as example.* Front Microbiol, 2015. **6**: p. 740.
96. Kim, T.-H., et al., *Functional analysis of sigH expression in Corynebacterium glutamicum.* Biochemical and Biophysical Research Communications, 2005. **331**(4): p. 1542-1547.
97. Park, S.H., et al., *Microorganism for simultaneously producing L-amino acid and riboflavin, and method for producing L-amino acid and riboflavin using same*. 2020, Google Patents.
98. Ikeda, M., *Lysine Fermentation: History and Genome Breeding*, in *Amino Acid Fermentation*, A. Yokota and M. Ikeda, Editors. 2017, Springer Japan: Tokyo. p. 73-102.
99. Li, Z.X., G.M. Yin, and T. Chen, *Optimization of Riboflavin Production by Recombinant Bacillus Subtilis X42 Using Statistical Designs.* Advanced Materials Research, 2013. **634-638**: p. 1031-1036.
100. Pérez-García, F., et al., *Dynamic Co-Cultivation Process of Corynebacterium glutamicum Strains for the Fermentative Production of Riboflavin.* Fermentation, 2021. **7**(1): p. 11.
101. Rueda, C., et al., *Biorefinery options to valorize the spent liquor from sulfite pulping.* Journal of Chemical Technology & Biotechnology, 2015. **90**(12): p. 2218-2226.
102. Man, Z.-w., et al., *Enhanced riboflavin production by recombinant Bacillus subtilis RF1 through the optimization of agitation speed.* World Journal of Microbiology and Biotechnology, 2014. **30**(2): p. 661-667.
103. Ikeda, M. and S. Nakagawa, *The Corynebacterium glutamicum genome: features and impacts on biotechnological processes.* Applied Microbiology and Biotechnology, 2003. **62**(2): p. 99-109.
104. Heyer, A., et al., *The two-component system ChrSA is crucial for haem tolerance and interferes with HrrSA in haem-dependent gene regulation in Corynebacterium glutamicum.* Microbiology, 2012. **158**(12): p. 3020-3031.

105. Frunzke, J., et al., *Control of heme homeostasis in Corynebacterium glutamicum by the two-component system HrrSA.* J Bacteriol, 2011. **193**(5): p. 1212-21.
106. Zhao, X., et al., *Efficient Synthesis of Phycocyanobilin by Combinatorial Metabolic Engineering in Escherichia coli.* ACS Synthetic Biology, 2022. **11**(6): p. 2089-2097.
107. Heravi, K.M., M. Wenzel, and J. Altenbuchner, *Regulation of mtl operon promoter of Bacillus subtilis: requirements of its use in expression vectors.* Microb Cell Fact, 2011. **10**: p. 83.
108. Peng, X., et al., *Characterization of the mannitol catabolic operon of Corynebacterium glutamicum.* Applied Microbiology and Biotechnology, 2011. **91**(5): p. 1375-1387.
109. Tröger, N., D. Richter, and R. Stahl, *Effect of feedstock composition on product yields and energy recovery rates of fast pyrolysis products from different straw types.* Journal of Analytical and Applied Pyrolysis, 2013. **100**: p. 158-165.
110. Becker, S., et al., *Accurate Quantification of Laminarin in Marine Organic Matter with Enzymes from Marine Microbes.* Appl Environ Microbiol, 2017. **83**(9).

Appendix A

In this appendix all sequencing primers used in this work can be found in Table A-1. It should be noted that Ex1Fw and Ex1Rv, or the primers used for cloning of their associated genes (see Table 3), were used to sequence all plasmid vectors created in this work, see Table 4. Only where genetic inserts exceeded 1000 bp were additional sequencing primers used, as shown here. Sequencing primers were purchased from Sigma-Aldrich or Invitrogen.

Table A-1: A list of sequencing primers with name and primer sequence in the (5′ - 3′) direction, as well as the vectors that were sequenced with these primers. All plasmid vectors created in this work were sequenced using Ex1Fw and Ex1Rv (Table 3), and additional sequencing primers were only used where inserts exceeded 1000 bp. (AA, AG, TA, TG) indicates that all base change variants of the associated plasmid, see section 2.2.2 and Table 4, were sequenced using the primer. All primers presented here are forward primers. Primers were purchased from Sigma-Aldrich or Invitrogen.

Plasmid vector	**Primer name**	**Primer sequence (5′ - 3′)**
pVWEx1-*galMKTE* pVWEx1-*galMKTE-galP* (AA, AG, TA, TG)	galEc_seq1	ATTGCCCTGCTGCGCTACTTCAAC
pVWEx1-*galMKTE* pVWEx1-*galMKTE-galP* (AA, AG, TA, TG)	galEc_seq2	CGCACGATCCAGATTGCTTC
pVWEx1-*galMKTE* pVWEx1-*galMKTE-galP* (AA, AG, TA, TG)	galEc_seq3	AAAGCTGACCAGTCGTTATG
pVWEx1-*galMKTE* pVWEx1-*galMKTE-galP* (AA, AG, TA, TG)	galEc_seq4	CCGGGTTAAGTTCTTCCGCTTC
pVWEx1-*galMKTE* pVWEx1-*galMKTE-galP* (AA, AG, TA, TG)	galEc_seq5	GTACAGCAAGCTGTCGCTGAAC
pVWEx1-*mtlD-mtlAF* (AA, AG, TA, TG)	mtlDAFBs-seq1	CAAAGAAGCAATTGATCATC
pVWEx1-*mtlD-mtlAF* (AA, AG, TA, TG)	mtlDAFBs-seq2	CGCCATCATTTTAAAGAAAC
pVWEx1-*mtlD-mtlAF* (AA, AG, TA, TG)	mtlDAFBs-seq3	GCAGCCATTGCCGGCGGAGC
pEKEx3-*ho1-pcyA*	pcyA_seq	ACATGAAGATGTTCAACGAACTGG

Appendix B

Conversion factor calculations

Due to only having two replicates for each condition, conversion factors were calculated for the BioLector experiment in 0.2 % (w/v) mannitol and IPTG concentrations of 0.1, 0.2, 0.4 and 0.7 mM IPTG for the strains Cgx1, CgM-AA, CgM-AG, CgM-TA and CgM-TG as presented in section 3.3.1. An additional flask experiment was conducted with the best-performing strain in the best condition that could be observed in terms of growth rate, see Figure 22. CgM-AA and the control Cgx1 were grown in minimal medium with 0.2 % mannitol and 0.2 mM IPTG with three replicates each. Conversion factors were calculated based on the average growth rate and biomass achieved by CgM-AA in this experiment, at 0.11 ± 0.01 h^{-1} and 0.72 ± 0.03 g/L, respectively. These values were used to calculate a conversion factor for the growth rates and biomass values in the two-replicate BioLector experiment.

The average growth rate for CgM-AA from the flask experiment (0.1099 h^{-1}) was divided by the average growth rate of CgM-AA in 0.2 mM IPTG in the BioLector experiment (0.2412 h^{-1}) to give the conversion factor 0.4556. All growth rates and their standard deviations in the two-replicate BioLector experiment in section 3.3.1 were multiplied by this conversion factor.

The average biomass accumulation for CgM-AA from the flask experiment (0.72 g/L) was divided by the average biomass accumulation for CgM-AA in 0.2 mM in the BioLector experiment (0.96 g/L) to give the conversion factor 0.7495. All biomass values and their standard deviations from the two-replicate BioLector experiment in section 3.3.1 were multiplied by this conversion factor.

Appendix C

HPLC chromatograms

In this appendix you will find images from HPLC analyses conducted to detect either glucose, mannitol or galactose. Standards are only shown here as examples of good vs. suboptimal chromatograms. Standards that are not shown have clear peaks and from these only the expected retention time for the molecule may be given. In some chromatograms, the desired peak could not be distinguished from other peaks and an example will be shown in each case. Replicates in the same conditions follow the same trends unless otherwise stated.

Figure A-1 shows chromatograms of three galactose standards following HPLC analysis of the flask experiment in 1 % (w/v) galactose presented in section 3.2.1, with initial galactose concentrations of 0.0625 (top), 0.25 (middle) and 0.5 % (w/v) (bottom) respectively. For galactose concentrations of 0.0625 % and 0.25 % galactose, there is one single clear peak but a shoulder on the right side of each peak. In the chromatogram for the standard with 0.5 % galactose, there is a dual peak in which the two peaks cannot be distinguished from one another. The standard containing 1 % galactose had a chromatogram with a similar dual peak. The standards containing 0.5 % and 1 % galactose were not used for calculations.

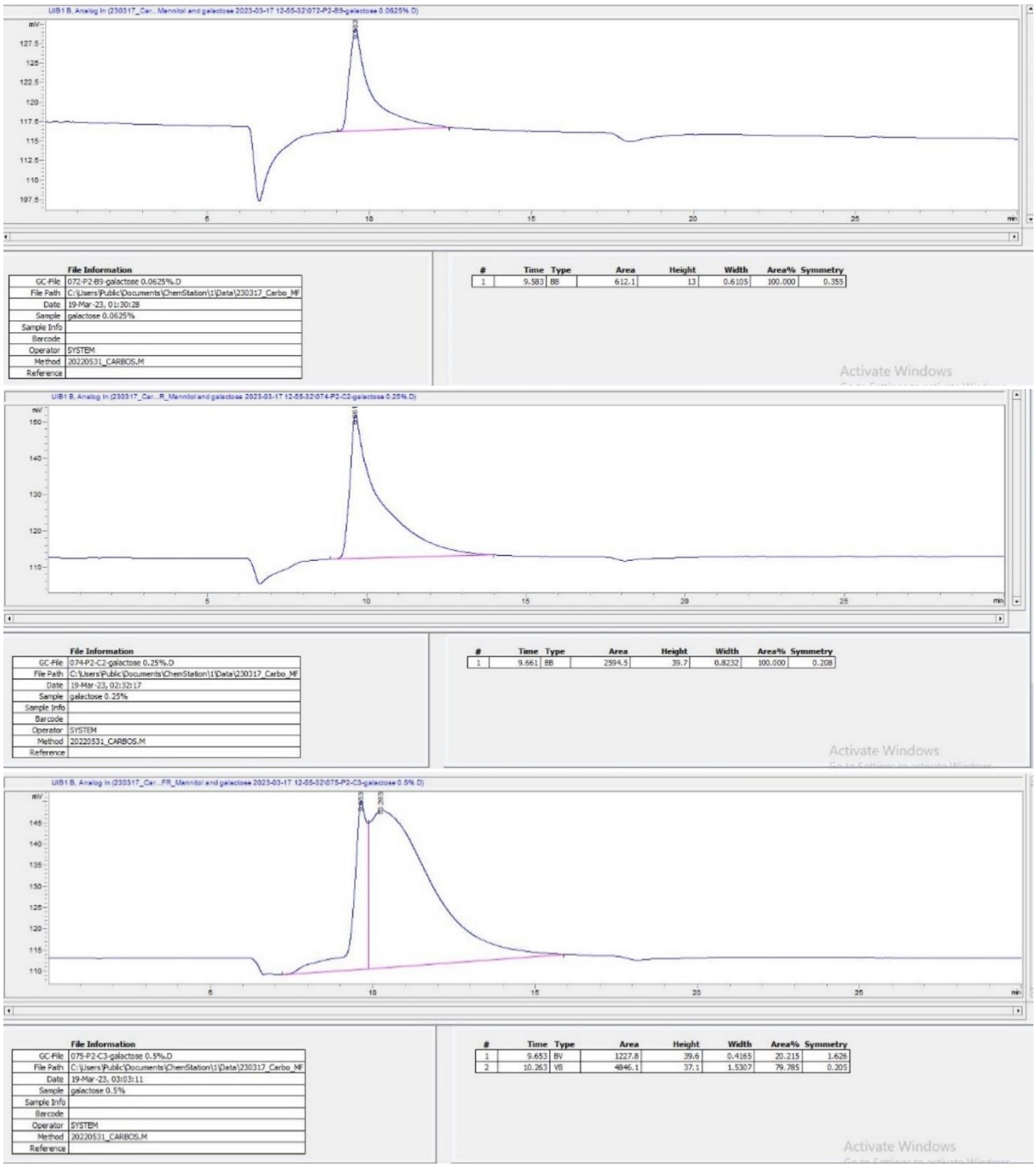

Figure A-1: HPLC chromatograms for galactose standards with concentrations of 0.0625 % (top), 0.25 % (middle) and 0.5 % (w/v) (bottom) galactose from a flask experiment described in section 3.2.1. Retention time, area and height for each peak is shown in the bottom right area of each image. The retention time for galactose in this case was 9.6 minutes.

Figure A-2 shows the chromatogram of a replicate of CgG-AA following HPLC analysis from the proof-of-concept flask experiment in 1 % (w/v) galactose that is presented in section 3.2.1. This is an example of a sample where there was no distinguishable peak at the expected retention time for galactose (9.6 minutes), but rather a peak at 7 minutes which obscures the area at 9.6 minutes so that galactose could not be detected. All chromatograms in this experiment that were not used in calculations for Table 6 looked like the one presented in Figure A-2.

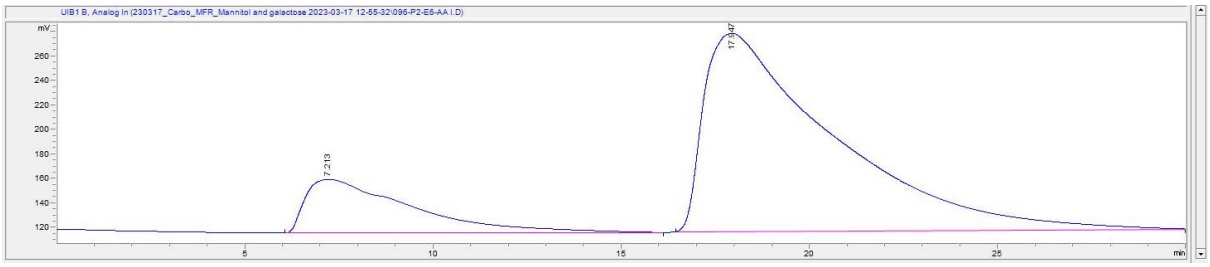

Figure A-2: Chromatogram from HPLC analysis for one replicate of CgG-AA from the flask experiment described in section 3.2.1. The expected retention time for galactose was 9.6 minutes.

Figure A-3 shows the chromatogram of a replicate of CgG-TGΔ following HPLC analysis from the flask experiment in 1 % galactose that is presented in section 3.2.2. This is an example of a sample where there was no distinguishable peak at the expected retention time for galactose, which was at around 9.6 minutes according to the standards in Figure A-1.

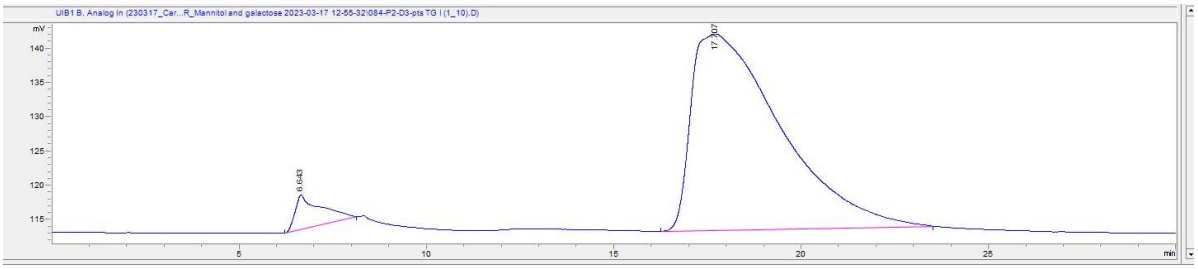

Figure A-3: Chromatogram from HPLC analysis for one replicate of CgG-TGΔ from the flask experiment described in section 3.2.2. The expected retention time for galactose was 9.6 minutes according to the standards in this round of HPLC.

Figure A-4 shows the HPLC chromatogram for CgG-TG cultivated in 100 % (v/v) RSWH as described in section 3.2.3. The marked peak in the chromatogram clearly spans the area where glucose would appear, at 17.6 minutes for this run (not shown), making it impossible to determine whether glucose was present in the medium or not. The same peak also made it impossible to detect glucose for Cgx1 in 100 % RSWH. The peak at 20.45 minutes could be obstructing the presence of galactose, which had a retention time of 20.1 in this run (not shown), and galactose could for this reason not be detected in samples from 100 % RSWH.

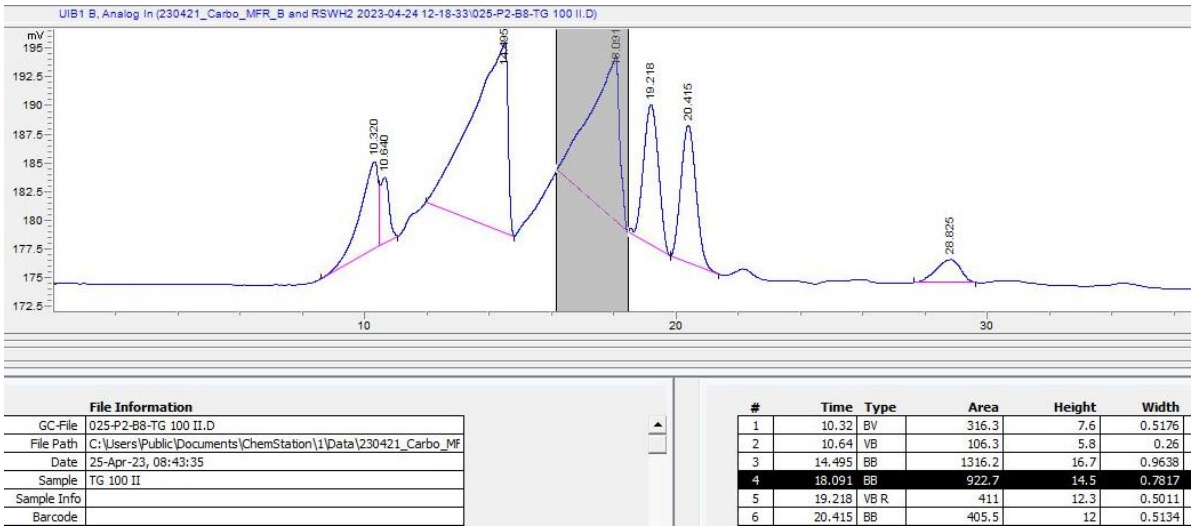

Figure A-4: Chromatogram from HPLC analysis for one replicate of CgG-TG cultivated in 100 % (v/v) RSWH in the experiment described in section 3.2.3. The marked peak has a retention time of 18 minutes, and the peak spans the expected retention time for glucose, which in this run was 17.6 minutes. The peak with retention time 20.415 minutes could be obstructing the peak for galactose, which had a retention time of 20.1 minutes in this run.

Figure A-5 shows chromatograms of standards with concentrations of 0.0625 % (top) and 0.5 % (w/v) (bottom) mannitol and the retention time for mannitol at 9.9 minutes. The mannitol standards with concentrations of 0.5 and 1 % (w/v) were not used for calculations. Figure A-6 shows the chromatogram for CgM-AG following HPLC analysis of the supernatant after growth in 0.2 % mannitol and 0.1 mM IPTG as described in section 3.3.1. No peak can be observed at the expected retention time of mannitol at 9.9 minutes.

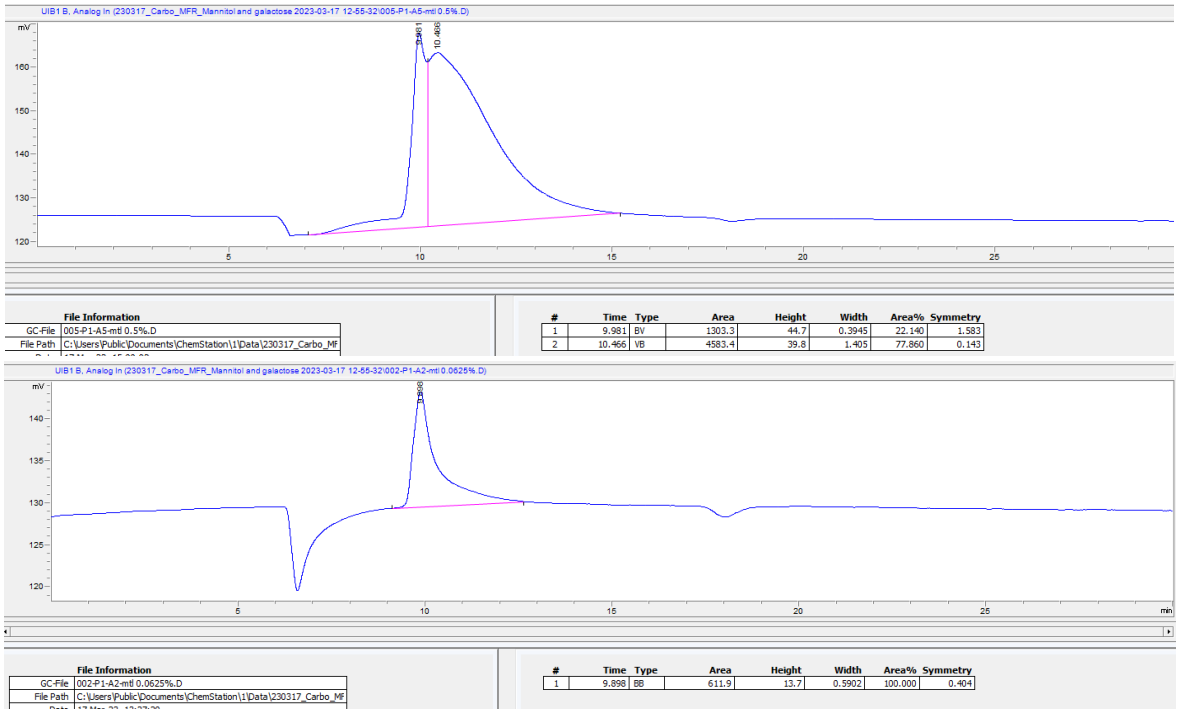

Figure A-5: HPLC chromatograms for mannitol standards with concentrations of 0.0625 % (top) and 0.5 % (w/v) (bottom) mannitol. Retention time, area and height for each peak is shown in the bottom right area of each image. The retention time for mannitol is around 9.9 minutes.

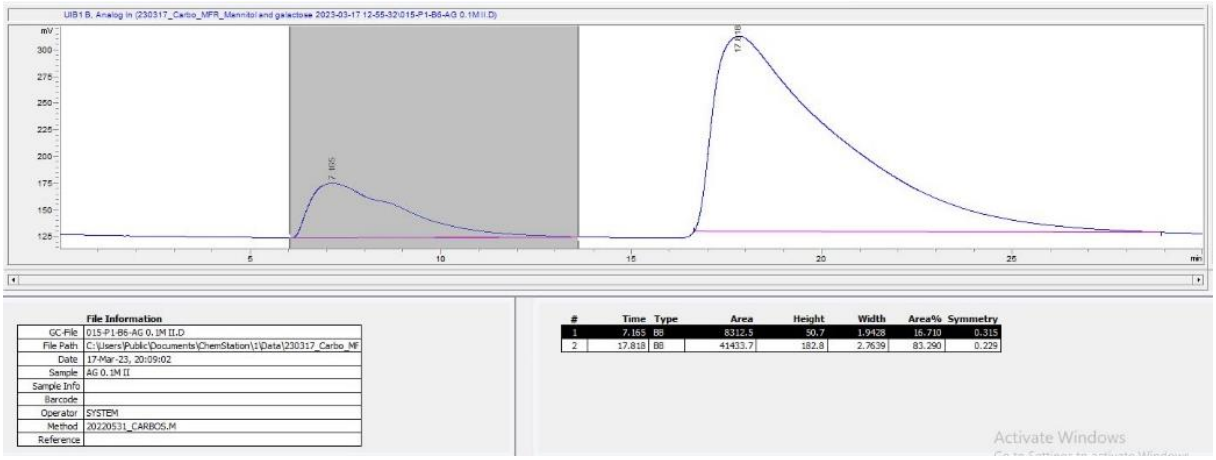

Figure A-6: Chromatogram from HPLC analysis for a replicate of CgM-AG after growth in 0.2 % (w/v) mannitol and 0.1 mM IPTG described in section 3.3.1. The dark gray area marks where the mannitol peak would be, with an expected retention time of 9.9 minutes in this case.

Figure A-7 shows examples of HPLC chromatograms from culture media samples of Cgx1 (top) and CgM-AA (bottom) in 50 % (v/v) BSWH, an experiment described in section 3.3.2. The expected retention time for glucose and mannitol in this run was 17.6 minutes and 40.5 minutes, respectively (not shown). A peak can be observed at 17.8 minutes which obscures any surrounding peaks, meaning glucose could not be detected in these samples. Figure A-8 shows chromatograms from Cgx1 (top) and CgM-AA (bottom) from the same experiment in 100 % (v/v) BSWH. In the sample from Cgx1 glucose could not be detected due to connecting peaks at 15.3 minutes and 18.3 minutes obscuring any peaks between them. This was the case for all three replicates of Cgx1 in 100 % BSWH. For one replicate of CgM-AA, a large peak at 17.6 minutes was detected. For the remaining two replicates, the peak was connected to another peak as shown for Cgx1, and glucose could not be distinguished from other compounds in this range.

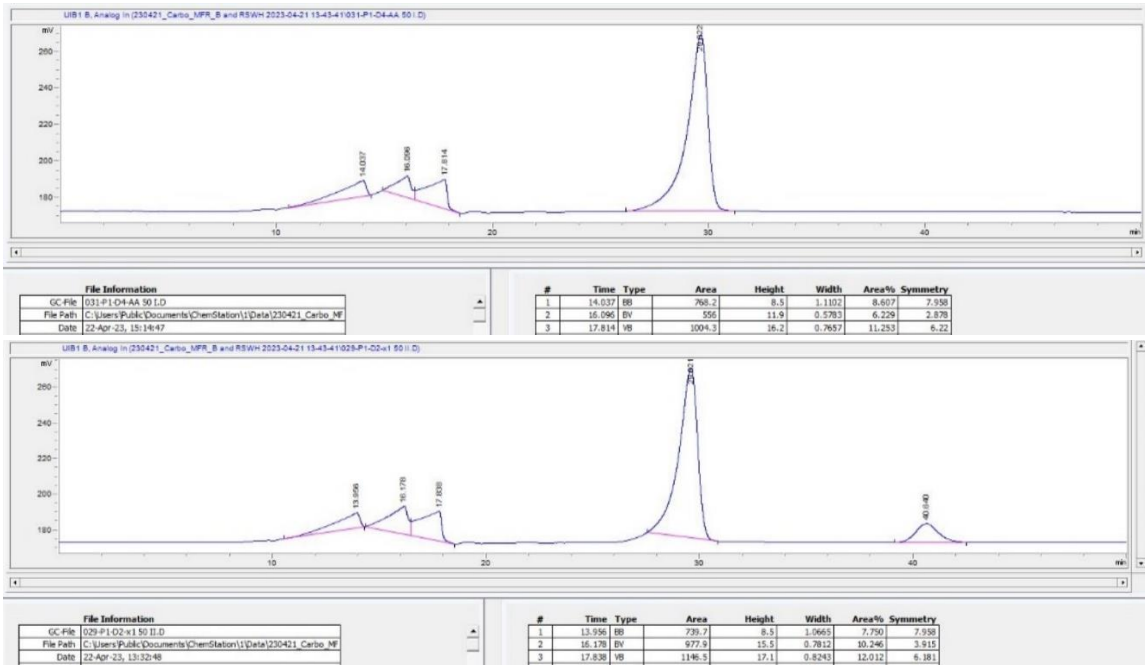

Figure A-7: HPLC chromatograms of Cgx1 (top) and CgM-AA (bottom) cultivated in 50 % BSWH as described in section 3.3.2. Expected retention time for glucose was 17.6 minutes in this case.

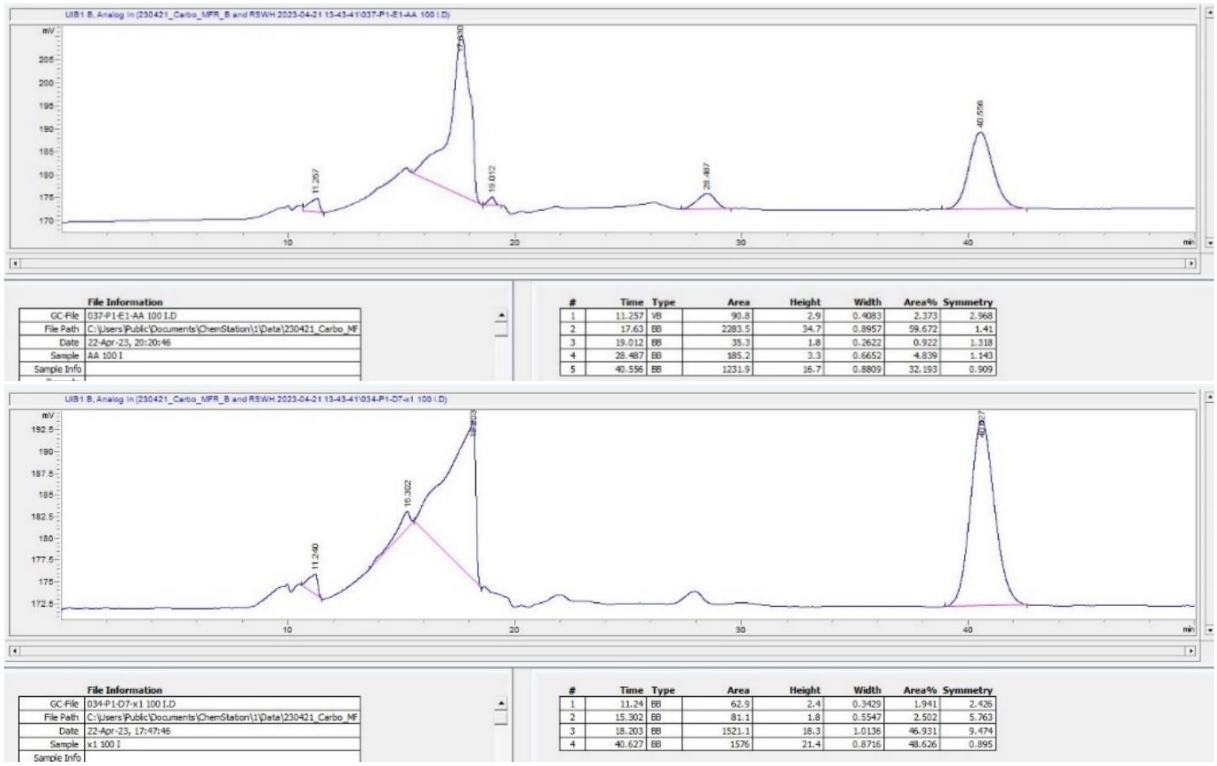

Figure A-8: HPLC chromatograms of Cgx1 (top) and CgM-AA (bottom) cultivated in 100 % BSWH as described in section 3.3.2. Expected retention time for glucose was 17.6 minutes in this case.

Appendix D

A calculation example for riboflavin precipitation

A precipitation factor was calculated to account for riboflavin precipitation in two lab-scale fermenters where CgG-Ribo was cultivated in RSWH, see section 3.2.5. The standard deviation is omitted in the example calculation. A precipitation factor was calculated (0.0715 mg/L h) as described in section 2.5.2.1. The method and equation (1-2) from section 2.5.2.1 was used here to calculate the total amount of riboflavin precipitation in samples collected after 26 hours.

A sample was collected at 30 hours, for which the HPLC detected an average of 527 mg/L for two fermenters. According to equation (1-2), the calculation becomes:

$$700\frac{mg}{L} \times (4 \times 0.0715) = 200\, mg/L$$

A total of 200 mg/L of riboflavin is estimated to have precipitated in the sample taken at 30 hours. To calculate the total amount of riboflavin present in the sample, 200 mg/L is added to the 527 mg/L detected by the HPLC to yield a total of 727 mg/L riboflavin in this sample.

Appendix E

Identification of a secretory signal in *lamFc*

Analysis of the laminarin gene (*lamFc)* from *F. commune* in SignalP yielded the image in Figure A-9, as well as a probability of a secretory signal of 0.86 (86%)[89]. Prior to the search, organism group was set to "Gram-positive" and the output format was set to "long output".

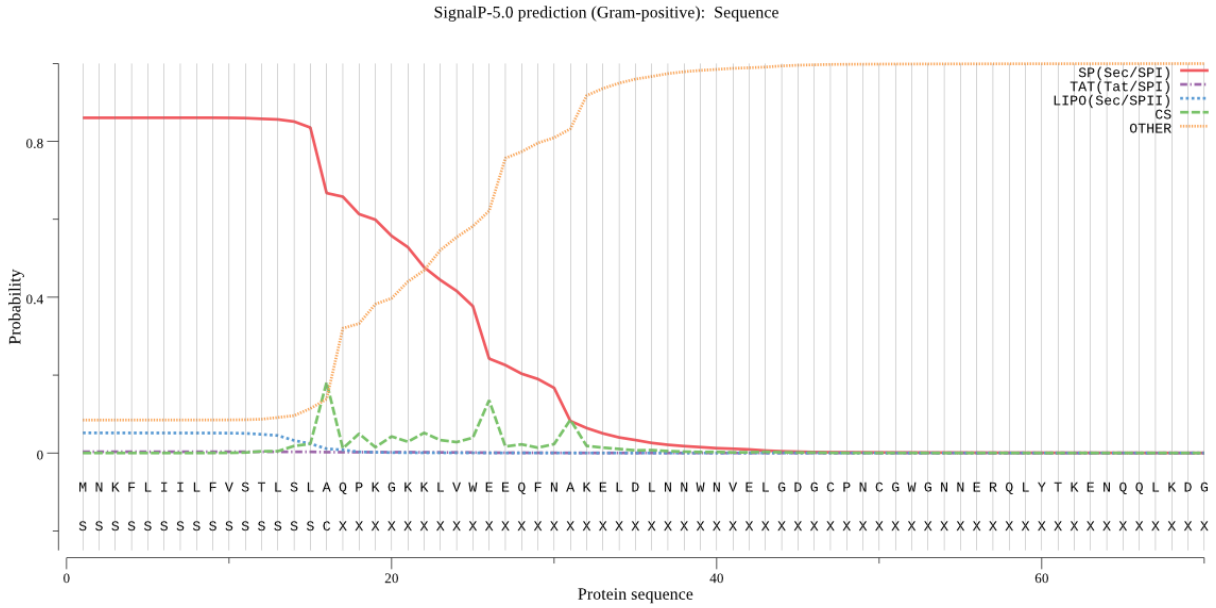

Figure A-9: Analysis of the amino acid sequence of the laminarin gene, *lamFc*, from *F. commune* in SignalP 5.0[89]. Prior to the search, organism group was set to "Gram-positive" and the output format was set to "long output". The given probability of a "Sec" or secretory signal being present in this amino acid sequence was 0.86 (86%).

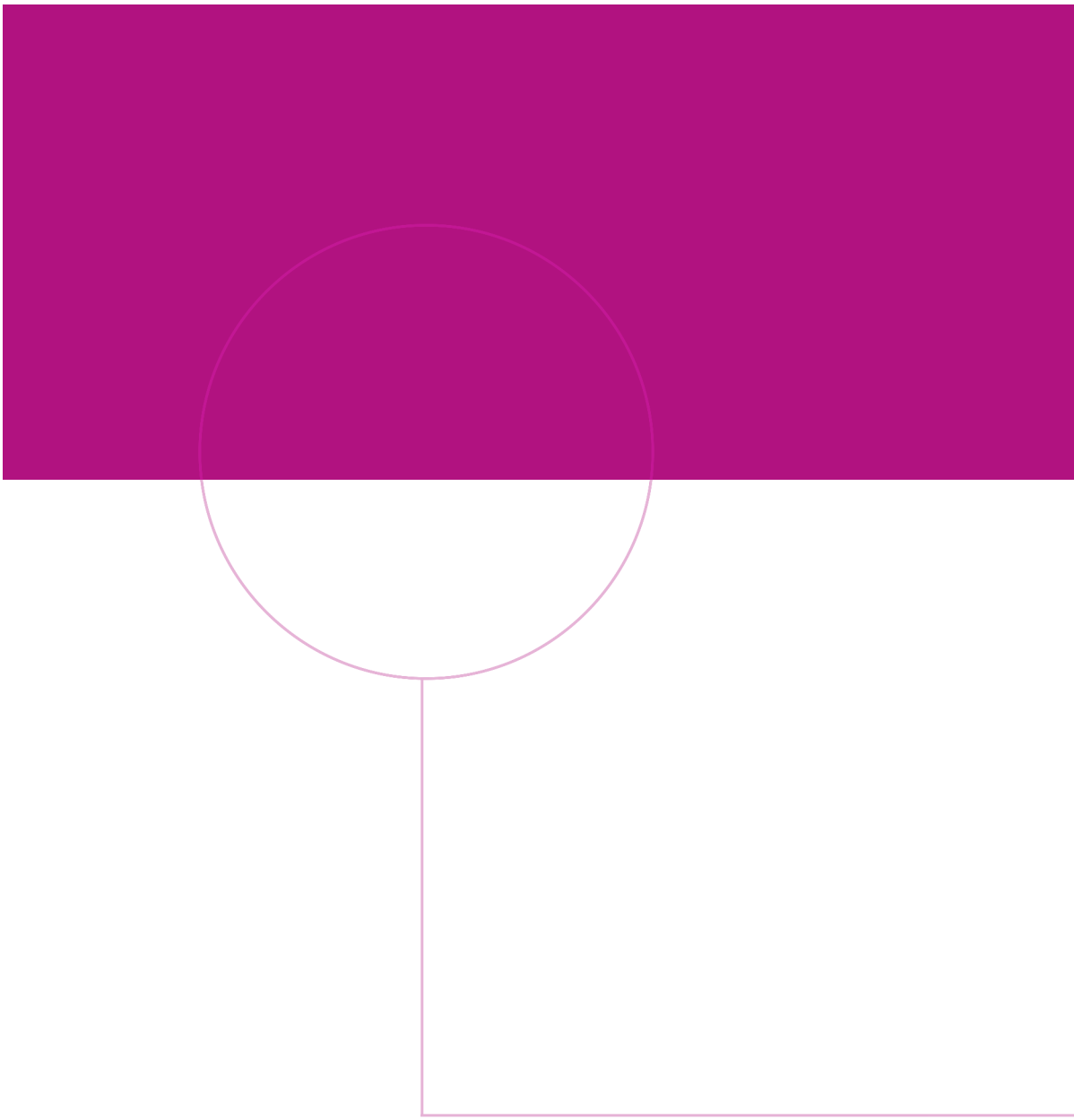

NTNU

Norwegian University of
Science and Technology